



THE HONG KONG
POLYTECHNIC UNIVERSITY

香港理工大學

Pao Yue-kong Library

包玉剛圖書館

Copyright Undertaking

This thesis is protected by copyright, with all rights reserved.

By reading and using the thesis, the reader understands and agrees to the following terms:

1. The reader will abide by the rules and legal ordinances governing copyright regarding the use of the thesis.
2. The reader will use the thesis for the purpose of research or private study only and not for distribution or further reproduction or any other purpose.
3. The reader agrees to indemnify and hold the University harmless from and against any loss, damage, cost, liability or expenses arising from copyright infringement or unauthorized usage.

IMPORTANT

If you have reasons to believe that any materials in this thesis are deemed not suitable to be distributed in this form, or a copyright owner having difficulty with the material being included in our database, please contact lbsys@polyu.edu.hk providing details. The Library will look into your claim and consider taking remedial action upon receipt of the written requests.

DESIGN OF TEXTILE-FABRICATED DIABETIC INSOLE FOR
ENHANCING FOOT THERMAL COMFORT

NING SEN

MPhil

The Hong Kong Polytechnic University

2024

The Hong Kong Polytechnic University

School of Fashion and Textiles

Design of Textile-Fabricated Diabetic Insole for Enhancing Foot Thermal
Comfort

Ning Sen

A thesis submitted in partial fulfilment of the requirements for the degree of

Master of Philosophy

June 2023

CERTIFICATE OF ORIGINALITY

I hereby declare that this thesis is my own work and that, to the best of my knowledge and belief, it reproduces no material previously published or written, nor material that has been accepted for the award of any other degree or diploma, except where due acknowledgement has been made in the text.

_____ (Signed)

NING SEN (Name of student)

ABSTRACT

Diabetes is a global public health issue in the 21st century that cause accelerated atherosclerosis and leads to an increase in elastic shear stiffness and a reduction in wound healing ability and sensitivity of the foot. This arises the risk of diabetic patients developing diabetic foot ulcers (DFUs). The use of diabetic footwear and orthosis is the most essential approach to preventing foot ulceration. However, due to the limitation of material choice, the diabetic insoles are mostly made of traditional foam with satisfactory pressure off-loading but poor permeability. Skin temperature and humidity have already been recognized as two risk factors for DFUs, the absence of a proper management approach means that the in-shoe high temperature and excessive moisture might cause deformation of the plantar foot tissues. Some novel approach of fabricate new materials for cushioning application have been investigated such as three-dimensional (3D) knitting and 3D printing technologies. Even so, their performance as an insole material during daily activities and locomotion is still unclear.

The ultimate goal of this research is to develop a diabetic insole orthosis with the use of both a novel knitted textile and 3D printed materials to optimize the wear comfort in terms of the in-shoe environment and even distribution of plantar pressure with reference to experimental analysis.

To understand the footwear and insole needs and preferences of the diabetic patient, a foot care program is conducted with a questionnaire for each participant. A total of 30 diabetic elderly between the ages of 55 to 75 years old comprised of 16 women and 14 men (mean: 64.9; standard deviation (SD): 6.27) were invited to answer the questionnaire about the problem or foot pain they are suffering using their current footwear in daily activities. A total of 30 diabetic patients are recruited. Their problem or foot pain using current footwear, as well as their

footwear and insole preference were collected. Also, their practical use of footwear in daily activities was investigated. The foot pain of the diabetic patient was found mainly at the heel, forefoot, and medial side of the foot. Textile materials are found as the most common 1st layer of the insole currently used by the participants. The cushioning pad at the high-pressure region and arch pad is their preferred features on the insole. The findings provide useful references in the design of diabetic insoles.

To investigate the thermal performance of different insole materials including traditional foam materials, novel textiles materials, and 3D printed materials, a wear trial has been conducted regarding the effect of the insole materials on the change of foot skin temperature and humidity during fast walking. Traditional insole materials which trap heat and moisture inside footwear cause discomfort to the wearer. Here, a novel textile-fabricated insole material with a 3D structure that offers good porosity and breathability for improving the footwear microclimate is proposed. Changes in foot skin temperature and humidity when wearing the textile-fabricated insole throughout treadmill walking are collected from 21 female subjects (age: 25.5 ± 4.5) and compared with traditional and 3D printed insoles. A subjective assessment of their perceived thermal comfort with various insole conditions is also conducted. In comparison to polyurethane, 3D printed thermoplastic polyurethane, and leather insoles, textile-fabricated insoles show no significant changes in foot skin temperature. Nevertheless, a significant reduction of the relative humidity of the skin of the sole (3.21%) and heel (24.41%) is found. The findings are a valuable reference for the fabrication of insoles with higher wear comfort. To design and develop an insole prototype that can effectively improve the thermal comfort of the insole with desirable plantar pressure distribution to reduce the rate of foot ulcers, a novel weft-knitted spacer fabric with foam inlays and a 3D printed insole with arch pad and auxetic heel pad was developed. Weft-knitted spacer fabric was fabricated with six knitting conditions

with a combination of different inlay densities and spacer course densities. The effect of inlay density and spacer course densities on the performance of weft-knitted spacer fabrics regarding their thermal conductivity, evaporative resistance, compression behaviour, and impact force reduction was investigated. It was found that fabric with higher inlay density and /or spacer density tends to perform better in force reduction and compressive resistance. With the same inlay density, higher spacer density reduces air permeability. Also, the high density of inlay materials tends to increase evaporate resistance. A fabric shows the best overall performance with thermal conductivity of 0.071W/mK, a maximum compressive stress of 323.43 kPa, and force reduction of 70.07%, and air permeability of 35.96 ml/s/cm², has been applied as the upper layer of the novel insole prototype. As for the 3D printed materials for insole application, a total of eight 3D prints with different structures using four different soft materials are demonstrated and evaluated by material test and wear trial. It was observed that the 3D printed materials in the auxetic structure show an excellent force reduction, a rapid reduction of compression force when removing the force from the materials, and outstanding water vapor permeability. The 3D printed re-entrance auxetic structural resin (80A hardness) exhibits an average of 12.7% pressure reduction at the rearfoot as a heel pad.

A half-insole consisting of a heel pad in auxetic re-entrance structure, and an 3D arch pad was designed and printed by using resin to provide the required conforming foot shape, fit, support, as well as cushioning effect on the heel. The proposed orthotic insole is therefore comprised of the 3D half-insole and the novel spacer inlaid weft-knitted fabric. In laboratory wear trial, a total of 8 female participants were invited. Its offloading performance was measured. Compared to the commercial diabetic insoles, the insole developed in this research shows lower mean peak pressure (MPP) at the toes and rearfoot which is also able to maintain the most evenly distributed plantar pressure with all the regions <202 kPa. It also has the highest

perceived comfort in all the foot regions. The offloading performance of the proposed insole prototype was verified by means of wear trial that a total of 23 diabetic elderly participants was invited. A reduction of plantar mean peak pressure up to 30.7% has been observed, while the plantar peak pressure was lower than 201 kPa in all foot regions. Aligned with the results from young participants, higher perceived comfort was reported when the textile insoles are worn in comparison to the market-available diabetic insoles.

The weft-knitted spacer fabric with inlay and the 3D printed auxetic material structure proposed in this study provide an alternative material choice to advance the design and development of footwear insoles that improve wear comfort. The insole prototype fabricated by using 3D knitting and 3D printing technologies not only effectively improve in-shoe humidity and perceived comfort, but also offer desirable cushioning and offloading performance. The output of the study could extend to the development of customized insole orthosis to prevent the development of diabetic foot ulcers.

PUBLICATIONS ARISING FROM THE THESIS

Journal Research articles:

Ning, K., Yick, K. L., Yu, A., & Yip, J. (2022). Effects of textile-fabricated insole on foot skin temperature and humidity for enhancing footwear thermal comfort [Article]. *Applied Ergonomics*, 104, Article 103803. <https://doi.org/10.1016/j.apergo.2022.103803>

Li, N. W., Yick, K. L., Yu, A., & Ning, S. (2022). Mechanical and Thermal Behaviours of Weft-Knitted Spacer Fabric Structure with Inlays for Insole Applications [Article]. *Polymers*, 14(3), Article 619. <https://doi.org/10.3390/polym14030619>

Chow, L., Yick, K. L., Wong, K. H., Leung, M. S. H., Sun, Y., Kwan, M. Y., Ning, K., Yu, A., Yip, J., Chan, Y. F., & Ng, S. P. (2022). 3D Printing Auxetic Architectures for Hypertrophic Scar Therapy [Article]. *Macromolecular Materials and Engineering*, 307(5), Article 2100866. <https://doi.org/10.1002/mame.202100866>

Conference presentation:

Ning, K., Yick, K. L., Yu, A., & Yip, J. (2022). Thermal Comfort of 3D Spacer Fabric for Footwear Insole Application. The 15th Textile Bioengineering and Informatics Symposium. <https://tbisociety.org/index.php?thispage=publications&c=publications&s=TBIS2022>

(Outstanding Presentation Award)

ACKNOWLEDGMENTS

I would like to express my deepest gratitude to my Chief Supervisor, Prof. Kit-Lun YICK, Associate Professor of the School of Fashion and Textiles at The Hong Kong Polytechnic University for her continuous support of my MPhil study and related research. Her guidance with motivation, skills, rigorous research manners and critical insights helped me throughout the time of research and writing of this thesis. Without her insightful advice, encouragement, and support, this study would hardly have been completed smoothly.

Similarly, I would like to express my warmest gratitude to my co-supervisors, Prof. Joanne Yip, Associate Dean and Associate Professor of the School of Fashion and Textiles at The Hong Kong Polytechnic University, and Dr. Annie YU, Assistant Professor of the Department of Advanced Fibro Science at Kyoto Institute of Technology in Japan for their insightful and valuable comments and encouragement.

Besides, I am very grateful to Mr. Calvin Tiu, technician of the Knitting Laboratory of the School of Fashion and Textiles at The Hong Kong Polytechnic University. His technical support and knitting expertise have contributed significantly to this research. I would also like to extend my thanks to Mr. Choi Kwan-on, a technician at the Physical Testing Laboratory for his technical support for the experimental work.

I would also like to thank my research teammates, especially Mr. Lung Chow, Dr. Nga Wun Li, Ms. Hiu Ying Lee, Mr. Kam Ho Wong, Mr. Sin Hang Matthew Leung, Ms. Mei Ying Kwan, Ms. Liying Zhang for their immeasurable help, continuous encouragement and support.

Finally, I wish to thank my family for their unconditional love and support throughout the study.

TABLE OF CONTENTS

CERTIFICATE OF ORIGINALITY	I
ABSTRACT	II
PUBLICATIONS ARISING FROM THE THESIS	VI
ACKNOWLEDGMENTS	VII
LIST OF TABLES	XVI
Chapter 1 Introduction	1
1.1 Background	1
1.2 Problem Statement	2
1.3 Aims and Objectives	3
1.4 Significance of the Study	4
1.5 Outline of Thesis	6
Chapter 2 Literature Review	8
2.1 Introduction	8
2.2 Diabetes	8
2.3 Formation of Diabetic Foot Ulcers	9
2.4 Risk Factors of Diabetic Foot Ulcers	10
2.4.1 Abnormal Plantar Pressure Distribution	10
2.4.2 Reduction of Sensitivity	11
2.4.3 Gait Impairment	12
2.4.4 Increase of Plantar Soft Tissue Stiffness	12
2.4.5 Foot Skin Thermal Conditions	13
2.5 Diabetic Footwear and Insoles	14
2.5.1 Diabetic Footwear	14
2.5.2 Diabetic Insoles	15
2.6 Novel 3D Weft Knitted Spacer Fabric for Force Reduction	18
2.6.1 Structure and Fabrication Parameters	18
2.6.2 Compression Properties and Energy Absorption	19
2.6.3 Thermal Properties	22
2.6.4 Knitted Spacer Fabric with Inlay	23
2.6.5 Use of Spacer Fabric on Insoles	24
2.7 Material Structure and 3D Printing Technology for Energy Absorption under Compression Force	25
2.7.1 3D Auxetic Structure	25
2.7.2 3D Printing Techniques and Materials	28

2.7.3 3D Printed Insole for Pressure Offloading	32
2.8 Evaluation of In-shoe Thermal Conditions and Plantar Pressure	35
2.8.1 Evaluation Methods of In-shoe Thermal Conditions.....	35
2.8.2 Evaluation Methods of Plantar Pressure	36
2.9 Summary.....	38
Chapter 3 A Foot Care Program to Understand the Footwear Preference of Diabetic Patient ..	41
3.1 Introduction.....	41
3.2 Methods.....	41
3.3 Results and Discussion.....	43
3.3.1 Foot Discomfort Wearing Footwear.....	43
3.3.2 Preference of Insole Materials and Element.....	45
3.3.3 The Needs on Daily Activity.....	47
3.3.4 Price Preference of the Footwear Product.....	49
3.3.5 Summary.....	50
Chapter 4 Analysis of the In-shoes Microclimate under Different Insole Materials to Enhance Orthotic Shoes Design in Thermal Comfort	51
4.1 Introduction.....	51
4.2 Methods.....	52
4.2.1 Participants.....	52
4.2.2 Insole Sample.....	52
4.2.3 In-shoe Temperature and Relative Humidity.....	54
4.2.4 Experimental Protocols	55
4.2.5 Subjective Sensation Rating.....	56
4.2.6 Statistical Analysis	57
4.3 Results.....	58
4.3.1 Changes in Foot Skin Relative Humidity.....	58
4.3.2 Change in Foot Skin Temperature	62
4.3.3 Distribution of Foot Skin Relative Humidity and Temperature.....	64
4.3.4 Subjective Sensation Rating.....	65
4.4 Discussion.....	66
4.4.1 Foot Skin Moisture.....	67
4.4.2 Foot Skin Temperature	70
4.4.3 Distribution of Foot Skin Humidity and Temperature.....	70
4.4.4 Thermal and Comfort Sensations.....	71
4.5 Summary.....	72

Chapter 5 Development of Novel Weft-knitted Spacer Fabric with Foam Inlays for Diabetic Insole Design.....	73
5.1 Introduction.....	73
5.2 Methods.....	74
5.2.1 Stage I – Material Preparation	74
5.2.2 Stage II – Knitting and Evaluation.....	77
5.3 Results and Discussion.....	82
5.3.1 Yarn Selection for Outer Layer	82
5.3.2 Thermal Properties of Fabric Samples	84
5.3.3 Mechanical Properties of Fabric Samples	88
5.3.4 Fabric Selection for Diabetic Insole Design	92
5.4 Summary.....	93
Chapter 6 Design and Development of Insole with Novel Weft-knitted Spacer Fabric and 3D Printed Arch and Heel Pad	95
6.1 Introduction.....	95
6.2 Methods.....	96
6.2.1 Stage I – Development of Auxetic Heel Pad.....	96
6.2.2 Stage II – Insole Prototyping and Pilot Trial.....	102
6.2.3 Stage III – Evaluation of Insole Prototype.....	108
6.3 Results and Discussion.....	109
6.3.1 Stage I – Development of Auxetic Heel Pad.....	109
6.3.2 Stage II – Insole Prototyping and Pilot Trial.....	122
6.3.3 Stage III – Evaluation of Insole Prototypes	129
6.4 Summary.....	135
Chapter 7 Conclusions and Suggestions for Future Research.....	138
7.1 Conclusions.....	138
7.2 Limitations of the Study	141
7.3 Suggestions for Future Research	142
References.....	145

LIST OF FIGURES

Figure 2. 1 Development of diabetic foot ulcer (Schaper et al., 2016).....	10
Figure 2. 2 Commercially available diabetic footwear.	15
Figure 2. 3 Examples of market ready-made diabetic insoles.	16
Figure 2. 4 Plantar pressure distribution of diabetic patient when (a) barefoot, and with the use of a (b) flat cushioning insole, and (c) customised insole (Cavanagh & Bus, 2011). The red and purple colours represent the areas with the highest measured pressure.....	17
Figure 2. 5 The PU (Poron®), EVA (Nora® Lunalastik EVA), EVA (Nora® Lunalight A), and PE (Pe-Lite®) insole used in the walking trial (Shi et al., 2022).....	18
Figure 2. 6 Typical structure of spacer fabric (Hamedi et al., 2020).....	19
Figure 2. 7 Typical compression stress-strain curve of a spacer fabric (Liu et al., 2012).....	20
Figure 2. 8 Spacer yarn patterns: (a) 1-needle spacing; (b) 2-needle spacing; (c) 3-needle spacing; and (d) 4-needle spacing (Zhao et al., 2018).	22
Figure 2. 9 (a) Image, and (b) design pattern of inserted silicon inlay (Yu et al., 2020a).....	24
Figure 2. 10 (a) Structure, and (b) appearance of 3-layer insole with spacer fabric and (3) vertical cross section of spacer fabric (Lo et al., 2016).	25
Figure 2. 11 The deformation of a.) non-auxetic material and b.) auxetic material during tensile and compressive loading (dashed lines – undeformed geometry) (Novak et al., 2016).	26
Figure 2. 12 Deformation of auxetic pads under compression: (a) combined, (b) honeycomb, (c) re-entrant hexagon, (d) and arrowhead (Yang et al., 2018).....	27
Figure 2. 13 (a) Classical 3D re-entrant lattice structure and (b) new 3D re-entrant lattice structures (Shen et al., 2021).....	28
Figure 2. 14 3D porous lattice structures printing effects of resin on (a) structure 1, (b) structure 2, and (c) structure 3 (Xiaogang et al., 2022).	30

Figure 2. 15 60mm³ gyroid printed sample: (a) 0.6 mm wall, 10 mm cell; b) 0.6 mm wall, 15 mm cell; c) 0.6 mm wall, 20 mm cell; d) 1.2 mm wall, 10 mm cell; e) 1.2 mm wall, 15 mm cell; f) 1.2 mm wall 20 mm cell (Holmes et al., 2022).31

Figure 2. 16 3D printed insole infill pattern for different densities (10% to 20%) (Chatzistergos et al., 2020).33

Figure 2. 17 3D printed customized Foot Orthoses (FO) glued with neutral insoles (Tarrade et al., 2019).34

Figure 2. 18 Internal structure of heel pads: (A), (B), and (C) internal angle, and (D), (E), and (F) internal structure (Leung et al., 2022).34

Figure 2. 19 Centre of pressure with two different insoles based on the entire foot during walking (Nouman et al., 2019).37

Figure 2. 20 Test set-up to investigate effect of loading on ability of cushioning materials to uniformly distribute plantar load with 3D printed heel model (Chatzistergos et al., 2017). ...38

Figure 3. 1 The number of patients with foot discomfort in certain foot region.44

Figure 3. 2 the material of (a) the patient currently used insole, (b) the contact surface of the insole to plantar; (c) the preferred feature of the insole.46

Figure 3. 3 (a) the sport that the patient used to do and (b) the time they spend on the sport weekly.48

Figure 3. 4 The price the patient willing to spend on a pair of daily outdoor footwear.49

Figure 4. 1 Insole samples: (a) PU; (b) TPU; (c) textile-fabricated; (d) leather, and their microscopic longitudinal cross-sectional view.53

Figure 4. 2 Measured locations of skin temperature and humidity on dorsal and plantar of foot.55

Figure 4. 3 (a) Mesh shoes used in wear trial, and (b) checking foot temperature with FLIR camera.	56
Figure 4. 4 Perceived (a) heat sensation; (b) wetness; and (c) thermal comfort scales.	57
Figure 4. 5 Change in mean RH after 30 mins of walking at (a) Point 2, and (b) Point 4. Error bars show the standard error.	59
Figure 4. 6 The skin RH during 30 mins of walking at Points (a) 1 (neck of big toes); (b) 2 (sole); (c) 3 (middle sole); (d) 4 (heel); and (e) 5 (dorsal).	61
Figure 4. 7 Foot skin temperature during 30 mins of walking at Points (a) 2, and (b) 4.	63
Figure 4. 8 Mean of change in (a) RH and (b) temperature of all the measurement points. Error bars show the standard deviation.	65
Figure 4. 9 Subjective rating of heat and moisture sensations, and thermal comfort of insole conditions. Error bars show the standard deviation.	66
Figure 4. 10 The (a) thermal conductivity (W/mK), (b) Water Vapour Permeability (g/m ² /day), and (c) moisture regain of the insole materials. Error! Bookmark not defined.	
Figure 5. 1 Air resistance (kPa.s/m) and thermal conductivity (W/mK) of fabric samples.	84
Figure 5. 2 Thermal conductivity (W/mk) of the fabric samples.	85
Figure 5. 3 Evaporative resistance (m ² ·Pa/W) of the fabric samples.	86
Figure 5. 4 Air permeability (ml/s/cm ²) of spacer fabric samples.	88
Figure 5. 5 Maximum compressive stress (kPa) of spacer fabric samples.	90
Figure 5. 6 Force reduction (%) of spacer fabric samples.	91
Figure 5. 7 Overall performance of spacer fabric samples.	93
Figure 6. 1 3D view of material samples: (A) Resin (Flexible 80A), (B) Resin (Elastic 50A), (C) TPU (Flexa Bright), (D) TPU (FS 1092A), (E) TPU (FS 1092A) (Non-auxetic), (F) TPU	

(FS 1092A) (large beam size), (G) TPU (FS 1092A) (Non-auxetic) (large beam size), (H) Double-layered EVA foam (Inocep®), (I) EVA foam (nora® Lunalastik), and (J) PU (Poron®).	98
Figure 6. 2 (a) Insertion method of specimens onto EVA insole, and (b) the 4 regions for comparison of MPP.....	101
Figure 6. 3 (a) Top, (b) medial side, (c) front, and (d) 3D view of the 3D half-insole model.	103
Figure 6. 4 Scale of the 3D model of the half-insole for foot size 38-40.	104
Figure 6. 5 The 3D, top, and medial side views of (a) 3D knitted and printed insole prototype (Insole X), and (b) commercially available diabetic insole with a heel cup and arch pad (Insole Y), and (c) commercially available diabetic insole (Insole Z) with a heel cup.	105
Figure 6. 6 The foot region for comfort perception.	107
Figure 6. 7 Perceived scale of wear comfort.....	107
Figure 6. 8 Impact force reduction of the 3D printed materials (A to G) and commercially available insole materials (H to J).....	110
Figure 6. 9 Force-time curves of the 3D printed materials (A to G) and commercially available insole materials (H to J).....	111
Figure 6. 10 Hysteresis energy loss of the 3D printed materials (A to G) and commercially available insole materials (H to J) during compression with 800N of force.	112
Figure 6. 11 Stress-strain curves the 3D printed materials (A to G) and commercially available insole materials (H to J) during compression with 800N of force.	113
Figure 6. 12 Water vapour permeability of the 3D printed materials (A to G) and commercially available insole materials (H to J).....	115
Figure 6. 13 Moisture regain of the 3D printed materials (A to G) and commercially available insole materials (H to J).....	116

Figure 6. 14 Mean peak pressure during standing with heel pad samples.....	119
Figure 6. 15 Mean peak pressure during walking with heel pad samples.	120
Figure 6. 16 Mean peak pressure changes (%) at the rearfoot during standing and walking.	121
Figure 6. 17 (a) Top, and (b) bottom views of the 3D half-insole model printed with resin.	122
Figure 6. 18 Mean peak pressure during standing with use of insole samples and without insole.	123
Figure 6. 19 Mean peak pressure during walking with insole samples.	125
Figure 6. 20 Subjective rating of perceived comfort with the insoles at the toes, forefoot, medial midfoot, lateral midfoot, and rearfoot.	128
Figure 6. 21 Mean peak pressure during walking with use of insole samples and without insole (diabetic elderly participants). Error bars show the standard error.	130
Figure 6. 22 Mean reduction of peak pressure during walking with use of insole samples (diabetic elderly participants). Error bars show the standard error.....	132
Figure 6. 23 Mean contact area during walking with use of insole samples and without insole (diabetic elderly participants). Error bars show the standard error.....	133
Figure 6. 24 Mean change of contact area during walking with use of insole samples (diabetic elderly participants). Error bars show the standard error.....	134
Figure 6. 25 Subjective rating of perceived comfort with the insoles at the toes, forefoot, medial midfoot, lateral midfoot, and rearfoot samples (diabetic ealderly participants).	135

LIST OF TABLES

Table 3. 1 Subject profiles.....	42
Table 4. 1 Material specification of the four insoles.....	53
Table 4. 2 Comparison between textile-fabricated and other 3 insole conditions based on skin RH during 30 mins of walking.....	59
Table 5. 1 Yarn specifications.....	75
Table 5. 2 Specifications of the knitted fabric samples.....	75
Table 5. 3 Materials of weft-knitted spacer fabrics.....	77
Table 5. 4 Specifications of inlaid spacer fabrics.....	77
Table 5. 5 Knitting notations and images of fabrics with different spacer patterns.....	78
Table 5. 6 Thermal test results of fabric samples.....	82
Table 5. 7 Physical properties of the inlaid spacer fabric samples.	89
Table 5. 8 Performance score of fabric samples.	92
Table 6. 1 Material specifications.	97
Table 6. 2 Material specifications of insole samples.	106
Table 6. 3 Material properties of the insole samples.....	117

Chapter 1 Introduction

1.1 Background

Diabetes-related peripheral neuropathy is one of the most serious complications of diabetes mellitus (DM) (Schaper et al., 2016). With reduced sensitivity and flexibility, diabetic patients face the high risk of diabetic foot ulcers (DFUs) (Nurse & Nigg, 2001; Schaper et al., 2016). This not only adds to the inconvenience in movement but could also result in nerve damage or even amputation. The risk factors of ulceration have been extensively investigated in the literature, including but not limited to gait impairment, foot morphology, high peak pressure, poor relaxation of shear stress, temperature, etc. (Bagavathiappan et al., 2010; Guiotto et al., 2013; Pai & Ledoux, 2012; Waaijman et al., 2014). One of the most essential means of preventing ulceration in the diabetic foot is to use diabetic footwear (Bus et al., 2020; Healy et al., 2012; van Netten et al., 2018). Research has proven that customised diabetic insoles can reduce and redistribute plantar pressure (Bus et al., 2004; Cavanagh & Bus, 2011).

However, the material options for diabetic insoles are still limited. Conventional materials commonly used for insoles are polyurethane (PU), ethyl vinyl acetate (EVA), and polyethylene (PE) foam which can offer pressure off-loading and can be used in customised insoles, and leather (Ahmed et al., 2020; Bus et al., 2004; Bus et al., 2013; Martinez-Santos et al., 2019; Nouman et al., 2019). Yet the performance of these traditionally used materials in terms of the in-shoe microenvironment has rarely been investigated.

Aside from conventional materials, the use of knitting technology for diabetic insoles has also not been fully explored yet. While the three-dimensional (3D) configuration of spacer fabrics, for example, exhibits superior compressibility and breathability, as well as a wide range of

thickness and energy absorption performance, this type of fabric has not been considered for insoles commercially. When paired with 3D printing (additive manufacturing) technologies, the use of 3D textile-fabricated structures not only facilitates resistance to pressure induced by body weight, but also acts as a buffer to prevent moisture build-up in the in-shoe microclimate that surrounds the skin when humans intermittently perspire (Rajan et al., 2016). Nevertheless, the practical use of 3D printed and textile-fabricated insoles and their impacts on foot skin temperature and humidity have not been fully investigated. In this study, a scientific approach is developed to demonstrate the use of both a novel knitted textile and 3D printed materials for diabetic insoles to optimise the wear comfort in terms of the in-shoe environment and plantar pressure.

1.2 Problem Statement

1) Lack of research on improving in-shoe environment of diabetics

Over the past decades, much of the work on footwear insoles has aimed to reduce the stresses that act on the feet for force reduction and cushioning, particularly in clinical practices. Studies on diabetic insoles have rarely examined and considered improving the in-shoe environment. While skin temperature and humidity have already been recognised as two risk factors for DFUs, the absence of a proper management approach means that the in-shoe high temperature and excessive moisture might cause deformation of the plantar foot tissues. Traditional footwear insoles constructed with a structure of multiple cushioning materials, such as PU, EVA, and PE, will inevitably hamper the free flow of heat and humidity, thus adversely affecting the thermal regulating performance of the foot at higher foot skin temperatures and rates of perspiration. They offer poor breathability and heat retaining properties, which result

in a high level of foot discomfort from heat and perspiration. Therefore, more information is needed about the effect of these insole materials on foot skin conditions.

2) Lack of novel materials for insoles

Traditional diabetic footwear and insoles made of soft foam materials can effectively reduce the peak plantar pressure by 25% to 41%, whilst the in-shoe pressure can be reduced to 300 kPa or less. Nevertheless, the likelihood of foot ulceration occurrence and re-occurrence is still high. As foot temperature may increase readily in response to repetitive stress during walking, the relationship between the changes in foot temperature and diabetic foot ulceration has been of particular interest lately. A suitable footwear material that could facilitate heat dissipation together with reduction of plantar skin temperature, humidity from sweating and shear stress may be able to prevent moisture build-up inside the footwear, thus reducing the risk of ulcers. With advances in materials sciences in recent years, 3D printing technology has been adopted for flexible selection of shape and hardness to cater to personal needs and conditions of the individual patient. Also, novel 3D knitted spacer fabrics with inlays have demonstrated a satisfactory performance in force reduction which is a desirable property for the diabetic insole. However, the level of durability and wear comfort of these new insole materials during daily activities and locomotion is still unclear. Further research is needed to evaluate the application of 3D printing and knitting on insole design.

1.3 Aims and Objectives

The specific research objectives of this project are as follows:

1. To establish a thorough scientific basis to understand the foot conditions and footwear needs of diabetic patients, as well as the current designs and materials of diabetic footwear insoles.
2. To examine the properties of footwear materials, and investigate the potential use of 3D spacer knitting techniques and 3D printing technologies in footwear applications which can enhance the in-shoe thermal environment and comfort. The dynamic compression, resilience, and stress-strain behaviour of the insole materials upon repeated use will also be considered.
3. To design and develop an optimally fitting insole prototype that can effectively enhance the in-shoe micro-climate and reliably alleviate plantar pressure, thus reducing the risk of diabetic foot ulcerations.
4. To undertake laboratory wear trials so that the foot skin temperature, humidity, plantar pressure distribution, and the perceived wear comfort of the newly designed insoles can be systematically evaluated.

1.4 Significance of the Study

Diabetes is a rising global health challenge in the 21st century that affects a large population. The IDF Diabetes Atlas (*Diabetes around the world in 2021*, 2021) shows that there is a 316% increase in diabetes diagnoses with 537 million adults who suffer from the disease worldwide in 2021. The various complications caused by diabetes result in high medical expenses, poor quality of life, mental stress of patients and their family, and premature mortality. In different regions around the world, 3-15% of diabetic patients develop a foot ulcer sometime during their lifetime (Ahmed et al., 2020; Boulton, 2004). The amputation rate of the limb and foot of diabetic patients is as high as 1.4% and 5.9%, respectively (Karimi, 2018), which is 15 times higher than that of non-diabetic individuals (Papanas & Maltezos, 2009). In the US, around

US\$1.38 billion are spent on wound care for DFUs annually which accounts for more than 80% of all amputations (Hicks et al., 2016).

Diabetic footwear and insoles are the most common first-line means of preventing DFUs. Many researchers have also recommended diabetic footwear for individuals who suffer from diabetic feet to prevent the occurrence of wounds (van Netten et al., 2018). Changes in the diabetic plantar soft tissues which are known as accelerated atherosclerosis have been found, which leads to an increase in elastic shear stiffness and reduction in wound healing ability (Gefen et al., 2001; Pai & Ledoux, 2012; Schaper et al., 2016). Therefore, the means to reduce the probability of incurring minor injuries are urgently needed to prevent foot ulcers right from the beginning of diagnosis. As the direct media of contact with the foot, the use of diabetic shoes is critical in ulcer prevention. However, improper fit limits the effectiveness of the ability of diabetic shoes to prevent ulcers in terms of plantar pressure reduction (Jones et al., 2019). Also, neglect of in-shoe microclimate management increases the risk of foot skin deformation (Bagavathiappan et al., 2010; Moulaei et al., 2021).

Given the limited research on the design of diabetic footwear and insoles, a scientific approach is used here to develop an in-shoe orthosis for diabetic patients based on novel 3D knitting technology, and 3D printing technology to enhance the in-shoe microclimate and provide suitable properties for pressure off-loading and optimise the fit even during walking. A knitted spacer fabric structure will be designed and evaluated to provide suitable properties including thermal and mechanical aspects. The information collected by the motion scanning and pressure measuring system is used to optimise the 3D insole design so as to enhance the pressure off-loading. The results of this study will provide valuable information for the design of diabetic insoles and the use of novel knitting materials for orthoses.

1.5 Outline of Thesis

There are a total of 7 chapters in this thesis. Chapter 1 provides background information on the research work, the problems to be solved, the objectives, and the values of this study. Chapter 2 is the literature review which includes a review of the formation of DFUs, available prevention approaches, and their limitations. Also, the novel materials for the insole were reviewed including 3D knitted spacer fabric with inlaid and 3D printed materials, and they will be applied to the insole development in this study. The evaluation of insole performance was also reported in this chapter.

Chapter 3 examines the common foot problem or discomfort, and daily use of orthotic footwear and insole of diabetic patients. Their daily activity level and preferences of footwear and insole were also investigated. This provides a useful reference to improve the design of the diabetic insole.

Chapter 4 explores the potential use of 3D printing technology and the 3D spacer knitted structure for footwear insole applications to improve in-shoe thermal environment. The effect of different insole materials on foot skin temperature and humidity was investigated. This chapter provides a reference for material selection for the design and development of diabetic insole regarding the enhancement of maintaining an appropriate skin condition for comfort.

Chapter 5 demonstrates the design of the 3D knitted spacer fabric with foam rods inlay for insole application. The choice of yarn and the 3D spacer structure were firstly compared. The

effects of different knitting parameters (inlay density and spacer course density) on the fabric properties (thermal conductivity, evaporative resistance, air permeability, compression stress, and impact force reduction) were investigated. The most desirable fabric material for foot support and in-shoe thermal environment was identified.

Chapter 6 describes the insole prototype design that auxetic structure material by using 3D printing technology as well as 3D knitted spacer fabric are adopted. The auxetic structure heel pad not only alleviates excessive plantar pressure, but also reduces the weight of insole. The use of 3D knitted spacer fabric on the top could enhance cushioning and thermal comfort of the insole. The influence of 3D printing materials and printing approach on the mechanical properties of the heel pad, and the overall offloading performance of insole are investigated. Objective tests on insole materials and laboratory wear trials are conducted. The findings provide a new dimension in the potential use of 3D printing technology and textile-fabricated insoles so as to enhance the effectiveness of orthotic treatment for diabetic patients.

Chapter 7 conclude the observations, findings, and limitations of this study and offers recommendations for future work related to 3D knitted and 3D printed materials for insole application. plantar pressure distribution

Chapter 2 Literature Review

2.1 Introduction

DFUs are a costly complication of diabetes that reduces the quality of life, and increases morbidity, mortality, and healthcare expenditures (Hicks et al., 2016; van Netten et al., 2018). Aside from frequent screenings of the feet to determine the risk of diabetic neuropathy (DN), a number of foot orthoses have been used to prevent injuries and excessive plantar pressure. Although foot orthoses are commonly used, scientific information on footwear material options and their corresponding mechanical and thermal properties is somewhat limited. In this chapter, current knowledge of the risk factors of DFUs, the principles of diabetic footwear insoles, properties of novel textile cushioning materials, as well as evaluations of in-shoe thermal conditions and plantar pressure in relation to various footwear insole designs and materials are given an overview as the academic basis of this study based on different studies and research done by various scholars.

2.2 Diabetes

Insulin is a peptide hormone that helps body cells absorb glucose which is converted into energy. For diabetics, the pancreas cannot produce enough insulin, or the cells of the body do not respond properly to the insulin produced. Thus, there is an increase in blood glucose. There are three main types of diabetes: Types I and II, and gestational diabetes, among which Type II is the most common (Kaul et al., 2013). Type I diabetes could occur at any age and most frequently in children and adolescents. Their body produces very little or no insulin so they require daily insulin injections to maintain blood glucose levels. Type II diabetes is the most common type of diabetes, which is found in 85-90% of all cases and 90% of adults whose body

is not able to make use of insulin (*Diabetes around the world in 2021*, 2021; Kaul et al., 2013). Gestational diabetes occurs in women during pregnancy who do not have a previous history of diabetes. However, both mother and baby have a higher risk of Type II diabetes afterward. Diabetes among older adults causes many complications such as a decrease in physical ability of the lower limbs and diabetic foot which lead to the increased need for medical care, and reduces their quality of life.

2.3 Formation of Diabetic Foot Ulcers

Diabetic peripheral neuropathy is a shared factor for foot ulceration in around 90% of diabetic patients (Alexiadou & Doupis, 2012). The reduced sensitivity of the feet reduces the ability of patients to feel any minor injuries that can precipitate ulceration. Changes in the diabetic plantar soft tissues known as accelerated atherosclerosis have been found, which leads to an increase in elastic shear stiffness and reduction in wound healing ability (Gefen et al., 2001; Pai & Ledoux, 2012; Schaper et al., 2016). The reduction in wound healing ability greatly exacerbates the severity of impact forces or abrasion on the skin of the foot, which holds true even for those that easily and commonly happen on a daily basis. Unfortunately, a slight occurrence of excessive force or abrasion builds up calluses on non-diabetic feet but enough to cause an ulcer in diabetic feet. Also, there is a reduction in joint mobility which affects the gait, thus increasing plantar loading in some areas of the feet (Schaper et al., 2016). Calluses then develop in those areas, which further affect the loading on the soft tissues of the feet. As a result, a small wound or harden tissues develop which then increase in size and depth; see Figure. 2.1.



Figure 2.1 Development of diabetic foot ulcer (Schaper et al., 2016).

2.4 Risk Factors of Diabetic Foot Ulcers

To reduce the burden of medical treatment and health threats on health systems, research is being carried out to understand the risk factors for ulcerations in attempts to prevent them. The main risk factors currently being studied included foot sensitivity, gait impairment, soft tissue stiffness, and foot skin temperature.

2.4.1 Abnormal Plantar Pressure Distribution

Changes in plantar pressure and increase in pressure-time integrals (used to evaluate plantar loading) have been observed in diabetic patients with neuropathy in comparison to non-diabetic subjects (Abri et al., 2019). Sacco et al. (2014) also determined that plantar pressure is increased with severity of DN. DN is more aggravative in patients with moderate and severe neuropathy which results in significantly higher peak pressure and time-pressure integrals in

the forefoot than those without neuropathy. Moreover, increments of plantar pressure have been observed on the heel of patients in the later stages of diabetes compared to that of patients in the early stages. In addition, patients with more advanced diabetes also show higher pressure-time integrals (Sacco et al., 2014). Therefore, the advancement of diabetes has a negative effect on plantar pressure distribution and the rollover process during walking.

2.4.2 Reduction of Sensitivity

Diabetics may also experience reduced sensitivity of the feet (Schaper et al., 2016). The central nervous system (CNS) receives sensory input from the muscles and skin of the lower limbs to control the balance of the body both consciously and subconsciously. The received information determines both posture and locomotion control and the body seeks information input of these are inadequate (Nurse & Nigg, 2001). Nurse and Nigg (2001) showed that the sensation inhibition with diabetic peripheral neuropathy causes changes in the load-bearing distribution of the foot. The human body tends to reduce loading in the less sensitive areas by shifting them to the more sensitive areas to ensure sufficient information input. The centre of pressure is then adjusted for better balance of the body. When there is larger less sensitive region, the sensitive region in the foot needs to accommodate a higher degree of pressure. Indeed, more pressure and longer induced forces mean that the skin can more easily break down (Guiotto et al., 2013). Besides the need for balance control, sensitivity is essential for intuitive protection of the feet and to ensure healthy feet. For diabetic patients with neuropathy, their sensitivity and response to peak pressure and stress increment are reduced. The CNS can no longer provide a suitable motion response through feedback of discomfort (Nurse & Nigg, 2001). As a result, they are less able to prevent calluses and ulcers simply by adjusting their movement pattern. Functional shoes for adjusting plantar pressure distribution and releasing load then become critical to protecting the plantar skin.

2.4.3 Gait Impairment

Chronic hyperglycaemia is one of the complications of DM which contributes to the reduction of flexibility and sensation in the lower limb and then alters the ability of the patient to control his/her movement. Raspovic (2013) showed that the loss in control of the lower limbs significantly reduces the range of motion of the hips and knees during gait where the patient tended to walk 0.17 m/s slower than a non-diabetic person. Besides the hips and knees, the ankle dorsiflexor and plantiflexor strength is reduced which limits the stride length of the patient (Martinelli et al., 2013). In a gait cycle, DM patients with peripheral neuropathy show early flattening of their feet because of ankle dorsiflexion reduction. This then reduces the dorsiflexion balance phase and contributes to a shorter stride length (Martinelli et al., 2013). With a shorter step and different gait cycles, the ankle power, plantar-flexion, and ground reaction forces are therefore reduced (Raspovic, 2013). This means that the pressure pattern of the patient with a rigid foot is no longer the same as non-diabetics (Rao et al., 2010). Thus, this requires further awareness of the pressure release of the plantar foot to prevent ulcerations.

2.4.4 Increase of Plantar Soft Tissue Stiffness

The changes in soft tissue stiffness caused by diabetes might be associated with foot ulcers. The plantar tissue loading of diabetic patients is found to be much higher than that of non-diabetics due to the increase in soft tissue stiffness (Gefen, 2003). (Gefen, 2003) conducted computer simulations and found that there is concentration of tension stress that ranges from 90-150 kPa in the diabetic forefoot which is at four times the maximum stress of non-diabetics under the first metatarsal head and nearly eight times the maximum stress under the second

metatarsal head. This increases the risk of injury in the diabetic feet which is initiated in the deeper tissue rather than on the surface of the skin.

The increase in plantar soft tissue stiffness not only erodes load-bearing ability but also reduces stress softening. Stress softening by the plantar soft tissues helps to relax stress at a certain strain level during movement. The plantar skin deforms which releases the stress, for example, the stress given by the uneven surface that comes into contact with the foot. However, compared to non-diabetic feet, the plantar soft tissues of diabetics are stiffer, and higher in shear and elastic modulus (Gefen et al., 2001; Pai & Ledoux, 2012). This means that the feet have less ability to strain and relax the shear stress. This results in a 52% higher peak shear stress and 47% higher final shear modulus as opposed to the plantar tissues of non-diabetics (Pai & Ledoux, 2012). The first metatarsal head shows the highest increment of local stiffness in comparison to another part of the plantar in a diabetic foot where ulceration is more likely to occur (Gefen et al., 2001). As a result, the shearing stress generated during daily movement could be harmful to these patients, which would result in ulceration. Therefore, the relaxation of shear properties should be considered in diabetic shoe designs, especially for the insole.

2.4.5 Foot Skin Thermal Conditions

There are few scientific studies that have concluded on the importance of foot skin conditions, including skin temperature and humidity, which play an important role in foot ulcer prevention. As diabetic patients need to don diabetic shoes most of the time, and even indoors, the in-shoe environment becomes critical in maintaining good foot skin condition. For patients with diabetic feet, a high skin temperature has been recognised as a risk factor of skin deformation (Bagavathiappan et al., 2010). Schario et al. (2017) also pointed out that the degree of humidity

of the body skin has an influence on skin vulnerability. The moisture on the foot surface causes foot tissue damage and the spread of infection (Moulaei et al., 2021). If a high in-shoe temperature and humidity persist for long periods of time, the organic substance contained in sweat would be decomposed causing more alkaline pH of the foot skin followed by developing pathogenic bacteria and fungi (Irzmańska et al., 2014). Thus, the temperature increase, and the excessive moisture together contribute to the discomfort and deformation of plantar foot tissues (Bagavathiappan et al., 2010; Moulaei et al., 2021). As footwear is mostly impermeable, the sweat absorbed and trapped by the insole materials could release heat through evaporation and result in increased local skin temperatures.

2.5 Diabetic Footwear and Insoles

Custom-fabricated footwear and insoles that offer proper arch support can be worn to reduce the magnitude of induced pressure and redistribute the plantar weight forces which act on the metatarsal heads, distal tips of the digits, and other bony prominences that tend to build excessive hyperkeratotic tissues and eventually lead to ulcerations. There is a wide range of footwear and insole designs and materials available in the commercial market.

2.5.1 Diabetic Footwear

People with diabetes who face the risk of foot ulceration are recommended to wear diabetic footwear according to their risk level which can protect their feet (Bus et al., 2020). Custom-made footwear can reduce the peak plantar pressure up to 53% more than regular shoes (Zwaferink et al., 2020). The considerations in selecting diabetic shoes should include, but are not limited to fit, protection, shear and friction reduction, pressure relief, offloading, and adherence to wearing the shoes (Bus et al., 2013; van Netten et al., 2018). A suitable fit allows

the feet to move freely with adequate space to reduce friction while the feet are being protected. However, manufactured diabetic shoes might not provide the best fit due to different needs and conditions of patients (Uccioli et al., 1995). Thus, those who have a higher risk of plantar foot ulcers are always advised to purchase medical-grade footwear such as customised diabetic shoes (van Netten et al., 2018). For instance, custom-made insoles and insoles for diabetic shoes have been found to enhance the ability of pressure release and reduce peak pressure. Apart from customisation, various diabetic insoles are available in the market but there is largely an absence of information on their performance.



Figure 2.2 Commercially available diabetic footwear.

2.5.2 Diabetic Insoles

The primary function of diabetic insoles is to redistribute pressure via the principle of increasing the contact area between the foot and the insole and adding corrective elements to the insole (Bus et al., 2004; van Netten et al., 2018). Currently available diabetic insoles basically fall into two types: prefabricated and custom-made. There are also many ready-made insoles in the market that are fabricated with a diversity of materials, see Figure 2.3. However, information on their performance in terms of pressure offloading and thermal regulation during

actual wear is limited and differ from individual to individual. Patients with a moderate and high risk of foot ulcers are recommended to wear custom-made diabetic insoles (Schaper et al., 2016). It is suggested that diabetic insoles should be able to achieve <200 kPa plantar peak pressure and facilitate $>80\%$ adherence with the wear treatment (Waaajman et al., 2014).



Figure 2. 3 Examples of market ready-made diabetic insoles.

The effect of customised diabetic insoles on plantar pressure distribution has also been widely investigated and compared to flat insoles. For example, Figure. 2.4 shows the plantar pressure distribution of diabetic patients when they are (a) barefoot, and using (b) flat cushioning insole, and (c) customised insole (Cavanagh & Bus, 2011). The plantar peak pressure is largely reduced when using a diabetic insole. Compared to a flat cushioning insole, the customised insole is more able to redistribute the plantar pressure and further reduce the peak pressure (Bus et al., 2004; Cavanagh & Bus, 2011). A plantar peak pressure reduction of 35-39% could be achieved in a custom-made insole with a plantar peak pressure less than 200 kPa (Bus et al., 2011; Guldemond et al., 2007; Zwaferink et al., 2020).

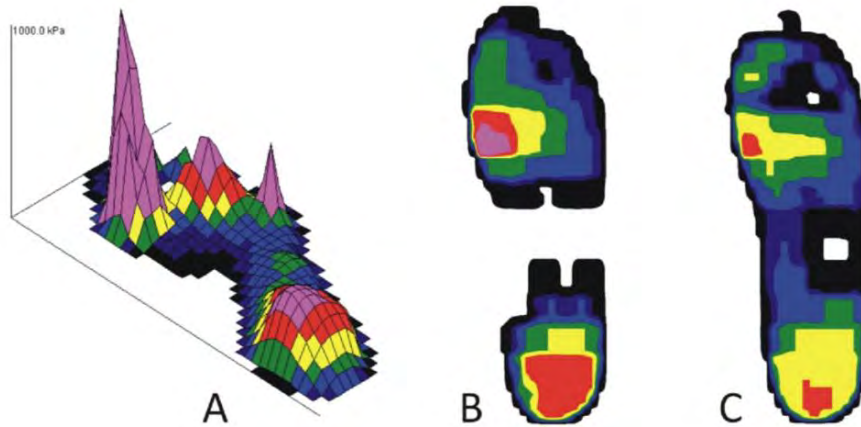


Figure 2. 4 Plantar pressure distribution of diabetic patient when (a) barefoot, and with the use of a (b) flat cushioning insole, and (c) customised insole (Cavanagh & Bus, 2011). The red and purple colours represent the areas with the highest measured pressure.

The materials commonly used for prefabricated and customised diabetic insoles are foam materials (e.g. EVA, PORON®, PPT®, Plastazote®, NORA®) with a cushioning effect (Bus et al., 2004; Guldemon et al., 2007; Martinez-Santos et al., 2019; Yu et al., 2016). The offloading performance of contoured insoles made of different foam materials, including PU (Poron®), EVA (Nora® Lunalastik EVA), EVA (Nora® Lunalight A), and PE (Pe-Lite®), were compared, Figure 2.5. Results show that PU (Poron®) can effectively reduce plantar pressure in toes, forefoot, midfoot, and rearfoot during walking (Shi et al., 2022). Metatarsal pads made of EVA has superior offloading and cushioning performance (Martinez-Santos et al., 2019).

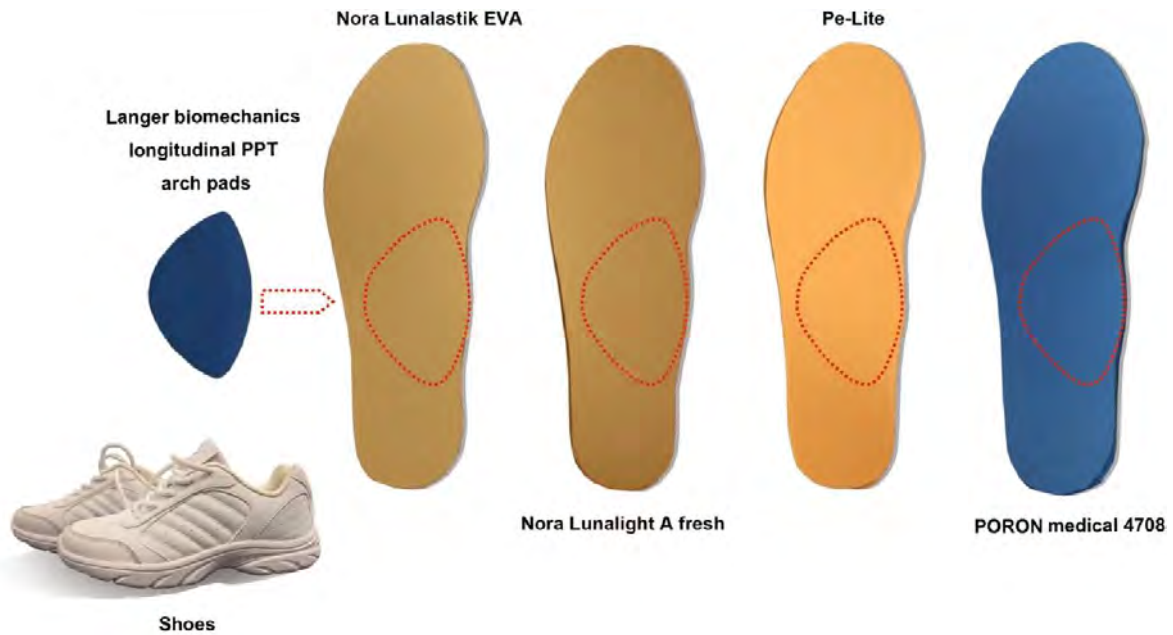


Figure 2.5 The PU (Poron®), EVA (Nora® Lunalastik EVA), EVA (Nora® Lunalight A), and PE (Pe-Lite®) insole used in the walking trial (Shi et al., 2022).

2.6 Novel 3D Weft Knitted Spacer Fabric for Force Reduction

With the rapid development of advanced textile materials, 3D spacer fabrics are increasingly being adopted for various medical purposes. Inherent to their special sandwiched structure, spacer fabrics not only well absorb impact forces with good compressive strain, but also have excellent planar elasticity for cushioning and breathability (Lo et al., 2016, 2018; Rajan et al., 2016; Yick et al., 2019).

2.6.1 Structure and Fabrication Parameters

The basic element of the knitted spacer fabric consists of the top and bottom layers, with spacer monofilaments between the two layers (Figure. 2.6). The outer layers are connected with the monofilaments to form a sandwich structure. The spacer monofilaments are usually polymeric

fiber, which helps to withstand the external force and maintain space between the two outer layers (Hamedi et al., 2020).

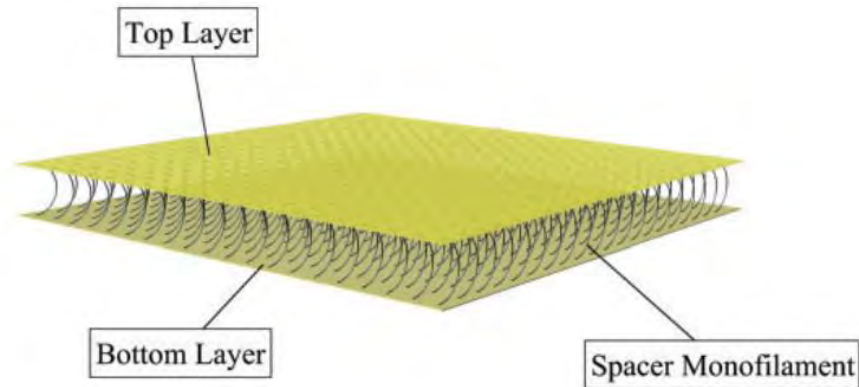


Figure 2. 6 Typical structure of spacer fabric (Hamedi et al., 2020).

Previous studies have also examined the different combinations of insole structure, materials and fabrication methods (Anderson et al., 2020; Lo et al., 2016; Melia et al., 2021; Nouman et al., 2019). Both warp-knitted and weft-knitted spacer fabrics are studied where the parameters that affect the fabric performance include but are not limited to the type, diameter, slope, and thickness of the spacer yarn, knitting pattern, etc. (Liu & Hu, 2011; Liu et al., 2012; Yip & Ng, 2008; Zhao et al., 2018). Unfortunately, due to limitations of knitting machines, adjusting parameters and combining different parameters may not be practicable (Hamedi et al., 2020). Further research should be done to explore the possibility of developing a new structure or increasing specific parameters with the available knitting techniques.

2.6.2 Compression Properties and Energy Absorption

Knitted spacer fabric has a good cushioning effect. Figure. 2.7 shows the typical behaviours of 3D spacer fabrics under compression which can be classified into four stages (Liu et al., 2012).

Stage I is the initial stage with a lower slope which results from the compression of the loose outer layers and the free post-buckling of the monofilaments. In Stage II, when the fabric is further compressed, the yarn in the outer layers becomes more compact. This enhances the tightness of the constraint of the spacer monofilaments and increases the buckling of the monofilaments. As a result, there is a rapid increase in compressive stress in the second stage. In Stage III, the compression stress becomes nearly constant with the deformation of the spacer fabric. With excessive force, there could be buckling, rotating and shearing, contact of the monofilaments with the outer layers, etc. Stage IV shows another rapid increase in the compression stress with the swift densification of the overall fabric. All of the materials including the outer layers and the monofilaments come into contact with each other to form a compact layer with a high degree of stiffness.

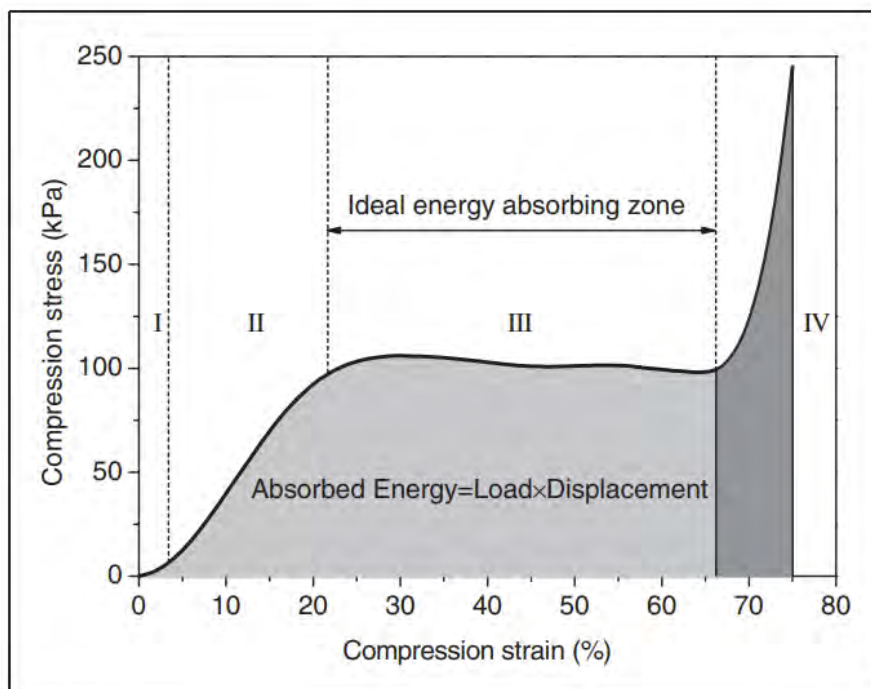


Figure 2. 7 Typical compression stress-strain curve of a spacer fabric (Liu et al., 2012).

Liu et al. (2012) observed a displacement of 47.9% with constant stress during Stage III. This shows the good cushioning effect and energy absorption of the spacer fabric. Hamed et al. (2020) proposed a weft-knitted spacer fabric with shape memory alloy monofilaments as the spacer yarn for use as a cushioning pad. Their study showed an energy absorption that is 2.4 times higher than that of commercial polyamide pads.

There are various parameters that affect the mechanical properties of spacer fabric. The type of spacer yarn has a large effect on the compression properties of spacer fabrics (Yip & Ng, 2008). Monofilaments with a larger diameter provide better compression resistance and facilitates better recovery (Liu & Hu, 2011). In addition, spacer fabric with more widely spaced spacer yarn exhibits better compression recovery. Figure. 2.8 shows the difference in inclination angle with different spacing between the spacer yarns. On the other hand, spacer fabric which have more closely spaced yarn and a higher density of monofilaments has a higher compression resistance but less capable of recovering from deformation (Zhao et al., 2018). Furthermore, the density of the outer fabric layer increases the compression resistance but reduces the ability to recover from compression (Liu & Hu, 2011).

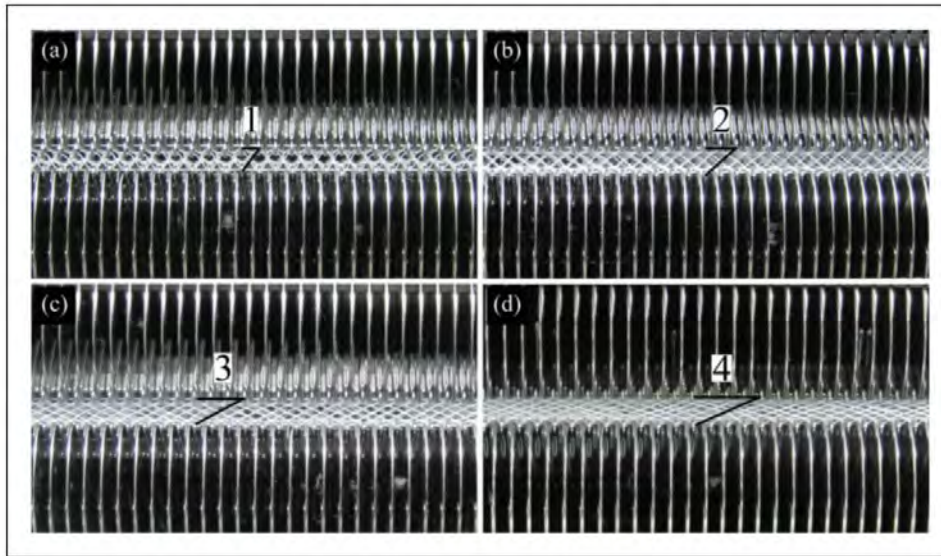


Figure 2. 8 Spacer yarn patterns: (a) 1-needle spacing; (b) 2-needle spacing; (c) 3-needle spacing; and (d) 4-needle spacing (Zhao et al., 2018).

2.6.3 Thermal Properties

Knitted spacer fabric has exceptional ability to transfer heat and moisture. Spacer fabric used as cushioning material is found to provide a more suitable microclimate in hot environments where the user perspires, as opposed to the use of PU foam (Muthu Kumar et al., 2020). Yu et al. (2016) compared spacer fabric with a thermoplastic material (Plastazote® foam) and showed that the former has a much lower air resistance (0.05–0.12 kPa s/m) and higher water vapor transmission (34.35–102.39 g/h·m²) rate.

The thermal properties of spacer fabric can be manipulated based on the structural design. The air permeability and thermal conductivity of spacer fabric are found to be related to the fabric density (Yip & Ng, 2008). Liu and Hu (2011) showed that using monofilaments of the same diameter, the air resistance of spacer fabric increases with the spacer yarn connecting distance (the monofilament inclination angle). Also, higher loop density in the outer layer reduces the

air permeability of the fabric. On the other hand, higher density enhances thermal conductivity (Liu & Hu, 2011). Rajan et al. (2016) further demonstrated that the porosity of spacer fabric is the key factor that influences the air and water vapor permeabilities. The porosity of spacer fabric is determined by the vertical gap between the two outer layers, and the thickness of the outer layers. A smaller vertical gap means a smaller void space for airflow but better thermal conductivity, and vice versa. The pore size of the outer layers also determines the permeability and thermal conductivity of spacer fabrics in which a higher porosity of the outer layer contributes to higher air and water vapor permeabilities (Rajan et al., 2016). Thus, to achieve a specific degree of breathability and conductivity of the fabric, the optimal combination of outer layer and monofilament structures (which affect the vertical gap) should be found.

2.6.4 Knitted Spacer Fabric with Inlay

Yu et al. (2020a) proposed a novel weft-knitted spacer fabric with a silicone tube inlay to enhance the durability of knitted spacer fabric under repeated compression. Silicon tubes of 1 mm in diameter was inserted into every 4th row by miss stitches during the knitting process, see Figure. 2.9. It was held by a monofilament inlay with tuck stitches. With the insertion of the silicone inlay, the fabric thickness and weight, and stitch density are all increased. The compression resistance and energy absorption are also largely increased. Thus, the inlay enhances the effectiveness of impact force absorption and reduction (Yu et al., 2020a). Compared to spacer fabric without an inlay, the air permeability is slightly inhibited by the silicon tubes in the fabric even though the air permeability is still higher than that of other cushioning materials. The key properties of spacer fabrics, together with inlays, support their use in the construction of footwear insoles.

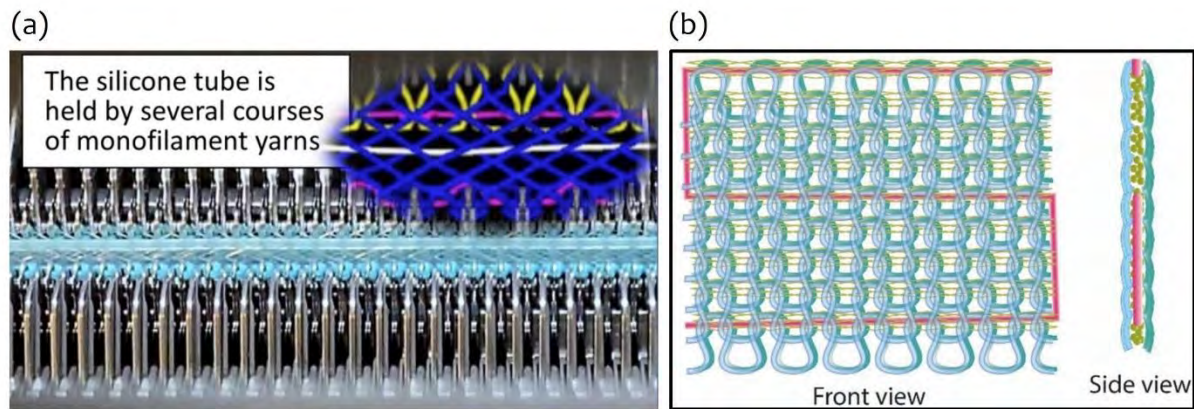


Figure 2.9 (a) Image, and (b) design pattern of inserted silicon inlay (Yu et al., 2020a).

2.6.5 Use of Spacer Fabric on Insoles

With an outstanding performance in force reduction, energy absorption, and breathability, spacer fabric has the potential to be used for protective or compressive garments. Indeed, spacer fabric has already been used for load-bearing purposes, such as in chairs and sofas. However, only a few research studies have investigated the relevance of using spacer fabric on insoles. The application of spacer fabrics for shoe insoles is to improve wear comfort by normalising the transfer of heat and moisture (Rajan et al., 2016). Lo et al. (2016) developed two 3-layer insoles by using 3D spacer fabric and compared them with an insole fabricated by using EVA (Figure. 2.10). A walking trial was conducted to observe their performance on plantar pressure distribution. The first insole with spacer fabric as the top layer reduces more than 12% of the plantar peak pressure and 13% of the pressure-time integral compared with the traditional EVA insole, and the pressure in the different regions could also be reduced. Another insole was developed by using spacer fabric as the top two layers which showed a plantar peak pressure that is more than 18% lower than the EVA insole. The performance of the spacer fabric in Lo et al. (2016) shows the potential use of textile-fabricated insoles and increases material options in orthosis designs.

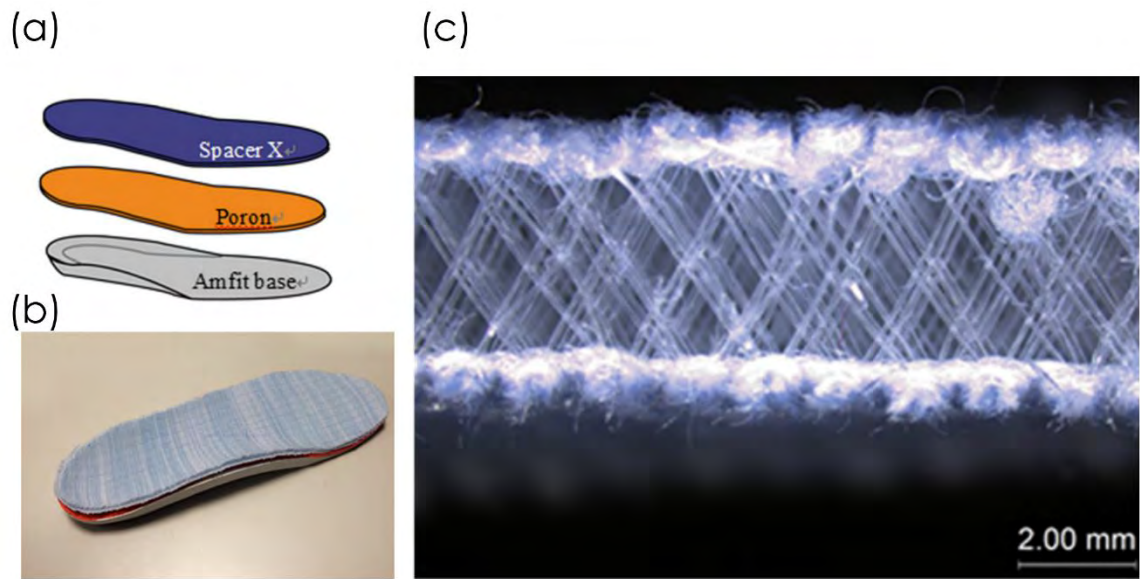


Figure 2.10 (a) Structure, and (b) appearance of 3-layer insole with spacer fabric and (c) vertical cross section of spacer fabric (Lo et al., 2016).

2.7 Material Structure and 3D Printing Technology for Energy Absorption under Compression Force

The 3D printing technology provides a flexible choice in material dimension, structure, hardness, and mass. Different material structures could therefore be produced for specific purposes.

2.7.1 3D Auxetic Structure

The auxetic materials are the material with a negative Poisson's ratio which contracts when uniaxially compressed and expand when uniaxially stretched (Ren et al., 2018). Auxetic material is a type of mechanical metamaterial with unique properties compared with most natural materials (Ren et al., 2018; X. Yu et al., 2018). In contrast to conventional materials,

the properties of mechanical metamaterials are not obtained from their material composition but mainly their microstructural geometry (X. Yu et al., 2018). The unique properties of auxetic materials included: high force adsorption, shear resistance, fracture toughness, etc. These unique properties provide wide application possibilities as the protective garment, daily clothing for better fitting, and shoes for force absorption.

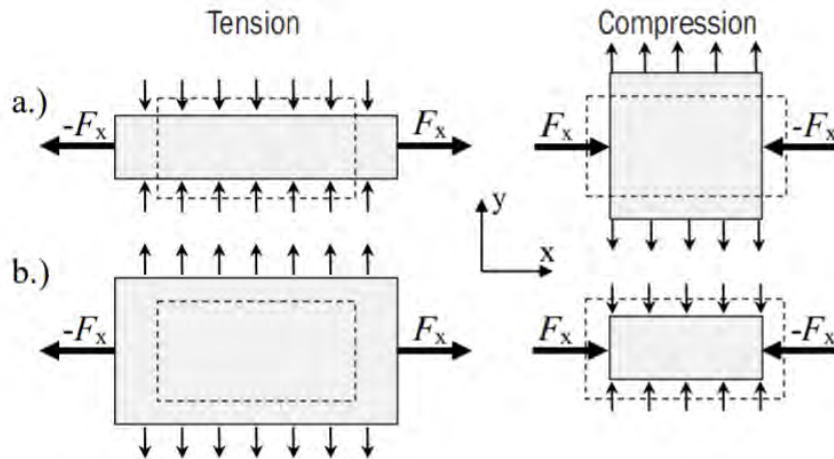


Figure 2.11 The deformation of a.) non-auxetic material and b.) auxetic material during tensile and compressive loading (dashed lines – undeformed geometry) (Novak et al., 2016).

2.7.1.2 Mechanical Properties of Auxetic Structure in Related to Insole Application

The ability in energy absorption is one of the outstanding properties of auxetic materials. Research demonstrated the superior compression and force absorption behaviour of auxetic materials (Li et al., 2020; Wang et al., 2021; Yang et al., 2018). Scarpa et al. (2006) also found that the auxetic foam has a damping capacity 10 times higher than the conventional one in cyclic compression test (Scarpa et al., 2006). The auxetic material not only performs excellent energy absorption and compression, but also crashworthiness (shock absorption). Yang et al. (2018) analysed the compression and force absorption behaviour of auxetic materials by using

3D models, see Figure. 2.12. Auxetic structures showed better shock absorption performance than non-auxetic structure, especially the re-entrant hexagon and arrowhead structures.

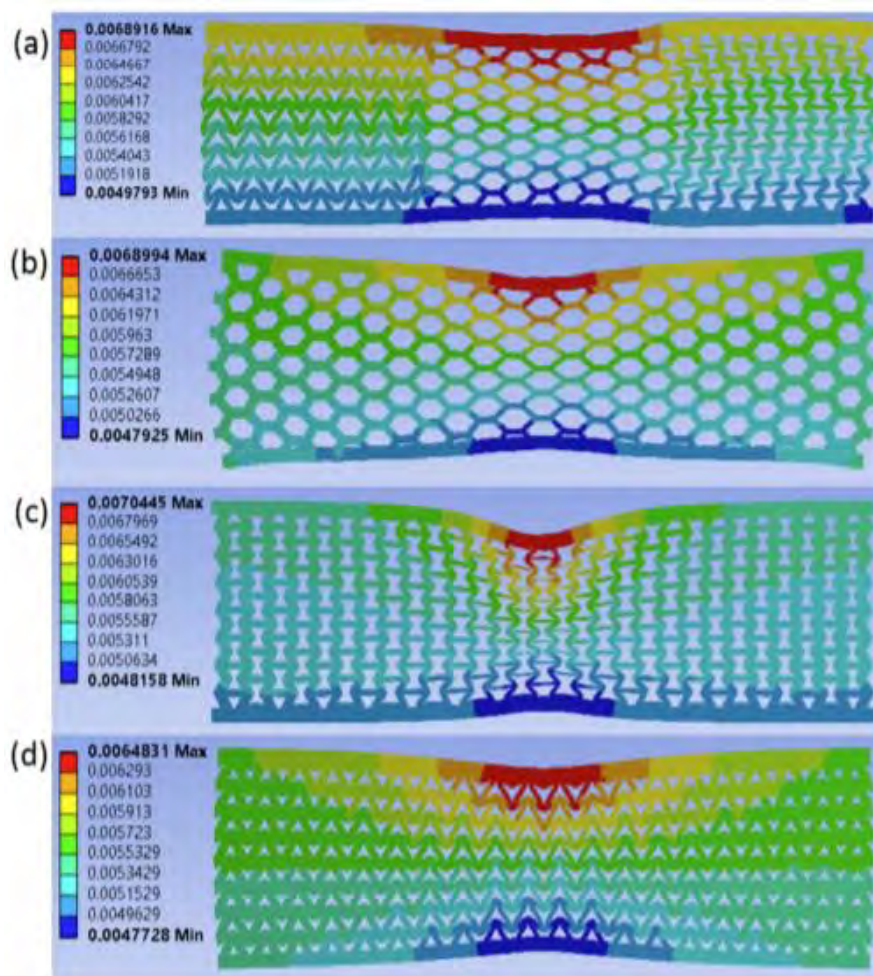


Figure 2. 12 Deformation of auxetic pads under compression: (a) combined, (b) honeycomb, (c) re-entrant hexagon, (d) and arrowhead (Yang et al., 2018).

As compared to conventional material, the loads distributed over a larger surface area in auxetic structures, thus resulting in reduced peak force (Yang et al., 2018). It is anticipated that materials in auxetic structure may improve redistribution of plantar pressure for fabrication of orthotic insoles for diabetic patients.

2.7.1.2 3D Auxetic Re-entrant Structure

3D auxetic structure is formed by combining two 2D auxetic components for enhancing the negative Poisson's ratio in traditional auxetic structure (Wang et al., 2022). Shen et al. (2021) has evaluated the compression behaviour of a new 3D re-entrant auxetic structure and compared it with the classical 3D re-entrance structure (Figure 2.13). Results show that the specific strength and stiffness of the new lattice structure are higher than the classical structure with outstanding energy absorption properties (Shen et al., 2021). Compared to the traditional 2D auxetic re-entrant component, 3D auxetic has huge improvement in air permeability with porosity.

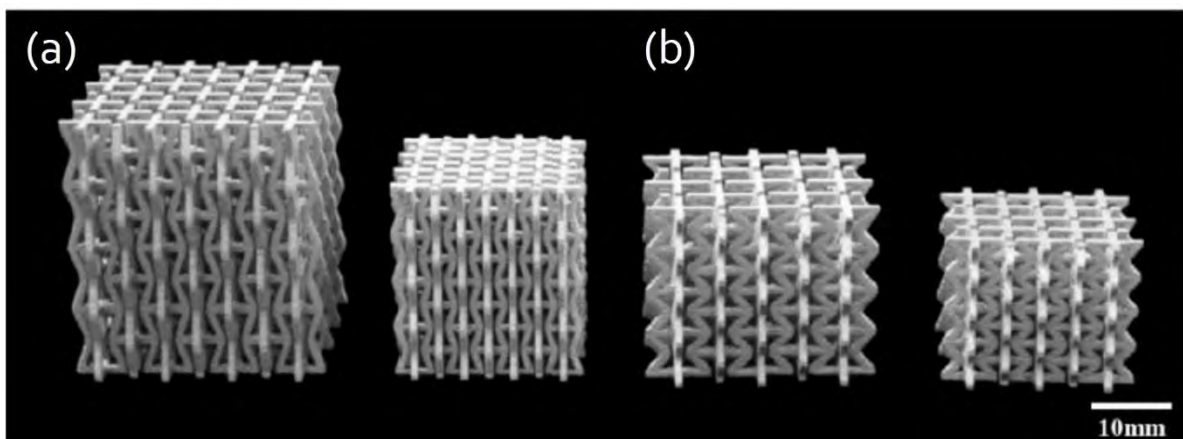


Figure 2. 13 (a) Classical 3D re-entrant lattice structure and (b) new 3D re-entrant lattice structures (Shen et al., 2021).

2.7.2 3D Printing Techniques and Materials

3D printing techniques and materials have been studied to achieve the desirable compression and energy absorption properties. According to different needs, such as accuracy, structure,

dimension, desired mechanical properties and end-uses, unlimited material designs and models can be printed by using different 3D printing methods and flexible materials.

2.7.2.1 Flexible Material for 3D Printing - Resin

Stereolithography (SLA) known as resin 3D printing, harden the liquid resin layer by layer through light polymerization which can fabricate finely printed parts with high accuracy and flexible hardness (Ma, 2013). The study by Dave et al. (2022) investigated the effect of different process parameters in SLA 3D printing on compressive properties. It was found that the compression energy absorption can be increased by using flexible polyurethane (FPU) than rigid acrylonitrile butadiene styrene (ABS) (Dave et al., 2022). Also, printing by YXZ orientation enhances energy absorption more than XYZ for both kinds of material.

The accuracy of SLA using resins allows the development of different structures with high porosity. Xiaogang et al. (2022) developed the novel flexible 3D porous lattice structures using this method (Figure 2.14). Different shapes of single components and diameters of rods can be printed with high resolution. The materials showed their potential to be applied to flexible materials that require energy absorption.

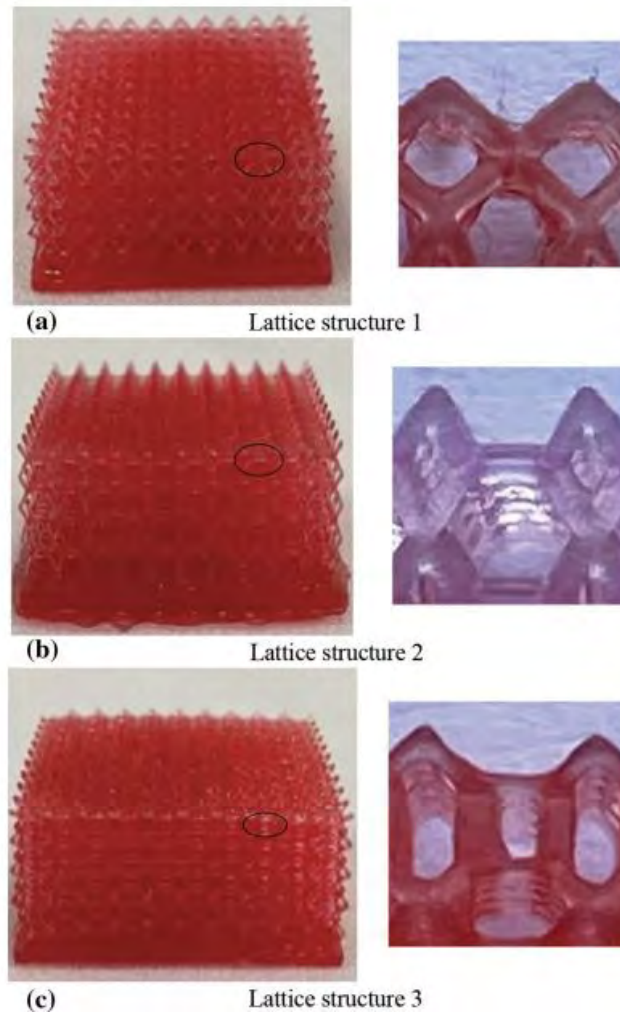


Figure 2.14 3D porous lattice structures printing effects of resin on (a) structure 1, (b) structure 2, and (c) structure 3 (Xiaogang et al., 2022).

2.7.2.2 Flexible Material for 3D Printing - Thermoplastic Polyurethane (TPU)

Apart from flexible resin, TPU is another common flexible material for 3D printing by fused deposition modelling (FDM) and selective laser sintering (SLS). FDM 3D printing, also known as fused filament fabrication (FFF), can fuse the thermoplastic filament and extrude it by the nozzle to form the shape of the designed model. Holmes et al. (2022) demonstrated the development of 3D-printed flexible gyroid structures printed by FDM using flexible TPU 3D printing filaments to obtain a similar cushioning effect as soft polyurethane foams. A total of

6 gyroid printed samples were printed with different wall and cell thicknesses (Figure 2.15). Minimal strength degradation has been achieved by 3D-printed flexible gyroid structures. These samples exhibit comparable resistance to damage during the repeating cycle of compression to that of the rehab foam. Xiaogang et al. (2022) also demonstrated the development of auxetic components by using TPU materials and FMD printing method to provide high energy absorption performance.

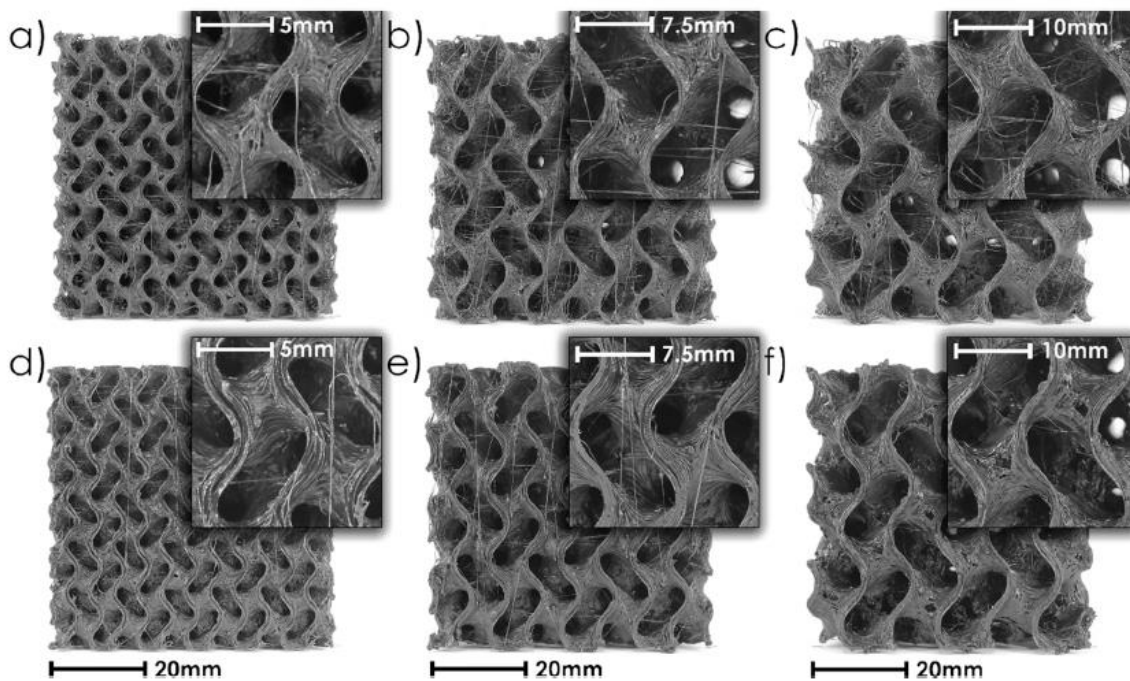


Figure 2. 15 60mm³ gyroid printed sample: (a) 0.6 mm wall, 10 mm cell; b) 0.6 mm wall, 15 mm cell; c) 0.6 mm wall, 20 mm cell; d) 1.2 mm wall, 10 mm cell; e) 1.2 mm wall, 15 mm cell; f) 1.2 mm wall 20 mm cell (Holmes et al., 2022).

SLS is a powder-based 3D printing technology that uses a laser to fuse the thermoplastic material layers into a final part (Ma, 2013). It can be used to print TPU models with complex structures without supporting material. This printing method was applied to develop the lattice

structures which also provide outstanding energy absorption performance (Bian et al., 2021). However, research study on energy absorption performance of 3D printing methods and materials are largely absent. In consideration of the cushioning requirements of orthotic insoles in this study, the effect of 3D printed method and materials on energy absorption properties are investigated.

2.7.3 3D Printed Insole for Pressure Offloading

With advances in materials sciences in recent years, three-dimensional (3D) printing technology has been adopted to create objects with different shapes and degrees of hardness with flexibility which cater to the personal needs and conditions of individual patients. However, studies on the design and evaluation of 3D printed insoles have been minimal.

Xu et al. (2019) conducted 8 weeks wear trial to compare the performance of 3D printed customised insole and conventional insoles regarding the reduction of plantar pressure and subjective pain level. Results indicated that 3D printed customised insole could reduce the plantar pain level by shifting the load from the metatarsals to the midfoot. Chatzistergos et al. (2020) applied 3D printing technology (using thermoplastic polyurethane (TPU) material) to achieve different stiffnesses of insoles by adjusting their structural density to optimise cushioning (Figure. 2.16). The result showed that the difference in optimal stiffness is individual specific. When an insole with the same density was used by all of the participants, 37% of the plantar peak pressure could be reduced. To further reduce the peak pressure, the optimum stiffness had to be found for each subject, and the plantar peak pressure reduction was then increased to 46%. This shows the potential application of 3D printing for customising orthoses, not only to customise the shape, but also the stiffness of the insole materials by modifying the structure.

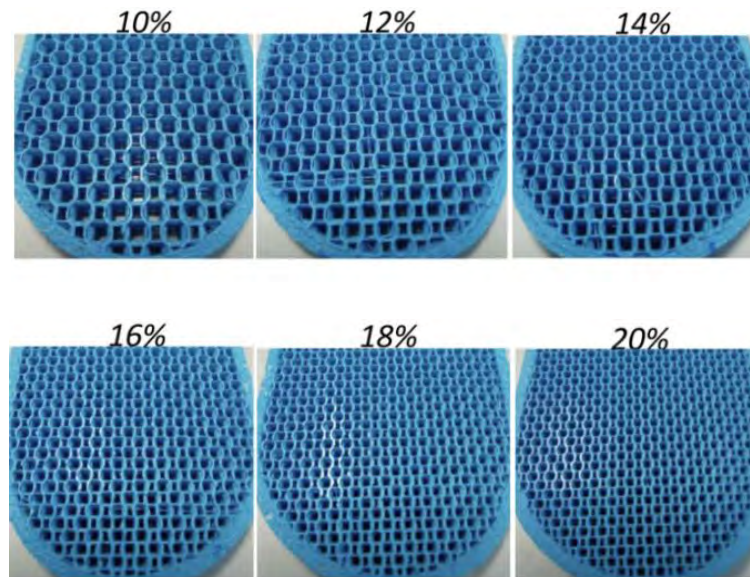


Figure 2. 16 3D printed insole infill pattern for different densities (10% to 20%) (Chatzistergos et al., 2020).

The study by Tarrade et al. (2019) demonstrated the use of custom-made 3D-printed insole orthoses and conducted a wear trial with 34 standing workers. Figure 2.17 shows the 3D printed customized Foot Orthoses (FO) glued with neutral insoles. The static and dynamic plantar pressures were measured, and the subjective feelings of foot pain and comfort was collected by a questionnaire. Results found that the foot pain and discomfort were significantly reduced after wearing 3D-printed orthoses. There is a significant reduction in the mean peak pressure due to the redistribution of plantar pressure, and improvement in standing balance. Leung et al. (2022) developed a heel pad with auxetic structure by SLA 3D printing for diabetic insole application (Figure 2.18). The heel pad with auxetic angle 80° exhibit optimal heel pressure reduction. It increases the heel contact area by 32.77% than the PU foam which helps to reduce 16.71% more plantar pressure on heel.

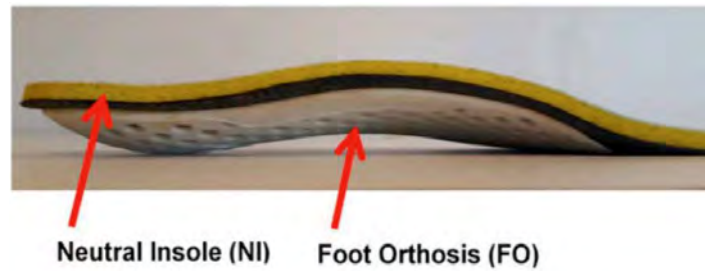


Figure 2.17 3D printed customized Foot Orthoses (FO) glued with neutral insoles (Tarrade et al., 2019).

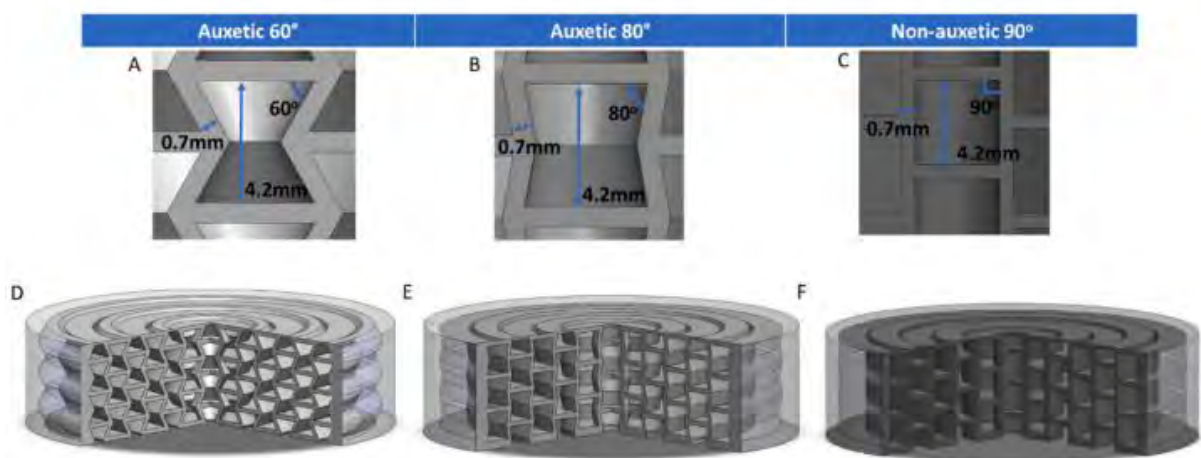


Figure 2.18 Internal structure of heel pads: (A), (B), and (C) internal angle, and (D), (E), and (F) internal structure (Leung et al., 2022).

Although these studies provide the knowledge on the performance of 3D printed orthosis in plantar peak pressure and pain reduction, the practical use of the 3D printed insoles and their thermal performance during both static and dynamic activities are largely neglected. Therefore, more research is needed to investigate the applicability of 3D printing of diabetic orthoses with different printed structures (Ma et al., 2019).

2.8 Evaluation of In-shoe Thermal Conditions and Plantar Pressure

An overview of the evaluation methods of in-shoe thermal conditions and plantar pressure in relation to various footwear insole designs and materials is given in this section.

2.8.1 Evaluation Methods of In-shoe Thermal Conditions

Examination of the thermal properties of foot orthoses has been comparatively limited, especially for diabetic footwear and insoles. Only a few studies have evaluated the in-shoe thermal conditions. Measurements of in-shoe thermal conditions normally require human participants. Shimazaki et al. (2016) evaluated the thermal formation and air ventilation in footwear during gait by conducting a trial with human subjects. During the experiment, foot skin temperatures were measured at seven points during gait at 1-min intervals by using thermocouples. West, Schönfisch, et al. (2019) investigated the changes in the in-shoe microclimate with different footwear donned during a trial that involved running. The foot temperature and humidity were also measured by using thermocouples.

Apart from objective measurements, subjective questionnaires have also been used to examine the perceived wear comfort of the participants. The result can be used to observe the performance of footwear or insoles with regard to different wear comfort factors which could be difficult to address solely through measurements done manually, including but not limited to the fit, convenience of activities (e.g., walking, running), dampness, air permeability, softness, and thermal feeling (Anderson et al., 2020; Irzmańska, 2015; Lo et al., 2018; West, Schönfisch, et al., 2019).

However, there is still the lack of evaluation of the thermal properties especially for diabetic footwear and insoles. Although some physical tests could be conducted to determine the air-

permeability, moisture regain, and water vapor permeability of footwear and insole materials, information of their performance in actual wear with respect to in-shoe microclimate is still limited.

2.8.2 Evaluation Methods of Plantar Pressure

As plantar pressure is one of the risk factors for DFUs, the compression and pressure off-loading properties of the materials or entire footwear/insole have been the mostly investigated. The plantar pressure distribution could be observed by using a pressure measurement system. For instance, the Novel Pedar-X system is a pressure distribution measurement system used to monitor local loads between the foot and the shoe. The size of the Pedar insole corresponds to the foot size with 85-99 sensors. The device could be applied in human trials to examine the changes in plantar pressure pattern and centre of pressure during different activities such as standing, walking, and running (Anderson et al., 2020; Bus et al., 2013; Martinez-Santos et al., 2019; Owings et al., 2008). The F-scan sensor (F-scan®, Tekscan, Boston, MA, US) is also a similar sensor as the Pedar that is used to record the plantar pressure (Chatzistergos et al., 2020; Chatzistergos et al., 2017; Healy et al., 2012). By looking at the data collected with different footwear or insole used, the total load and peak pressure in plantar could be found and compared which is the pressure off-loading performance, see Figure. 2.18.

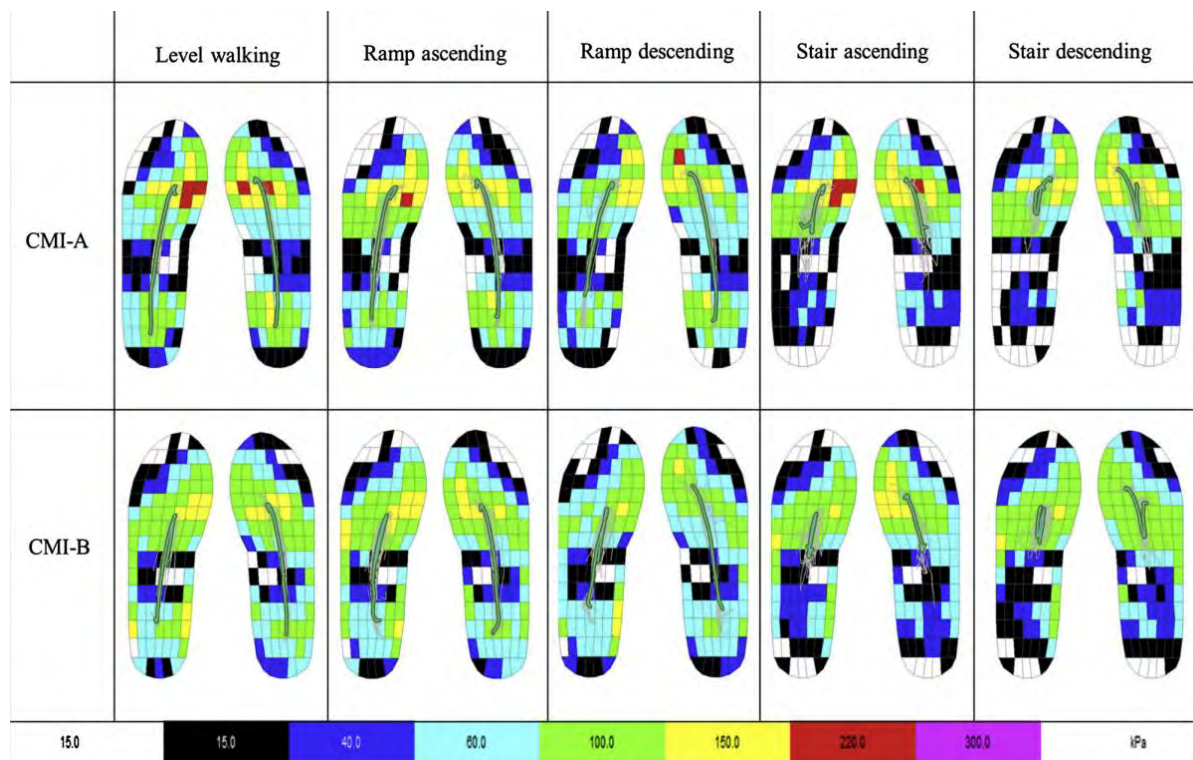


Figure 2.19 Centre of pressure with two different insoles based on the entire foot during walking (Nouman et al., 2019).

Besides human trials, traditional physical tests could be conducted to determine the material properties due to the difficulties in measuring some of the properties in human trials and the need for preliminary data on the materials. Indeed, some advanced evaluation methods are also designed to only simulate the actual wear conditions and predict the actual performance. Chatzistergos et al. (2017) combined a plantar pressure sensor with 3D-printed heel and an INSTRON ElectroPuls™ E3000 load frame to investigate the optimal stiffness of the insole for maximum plantar pressure reduction, see Figure. 2.20.

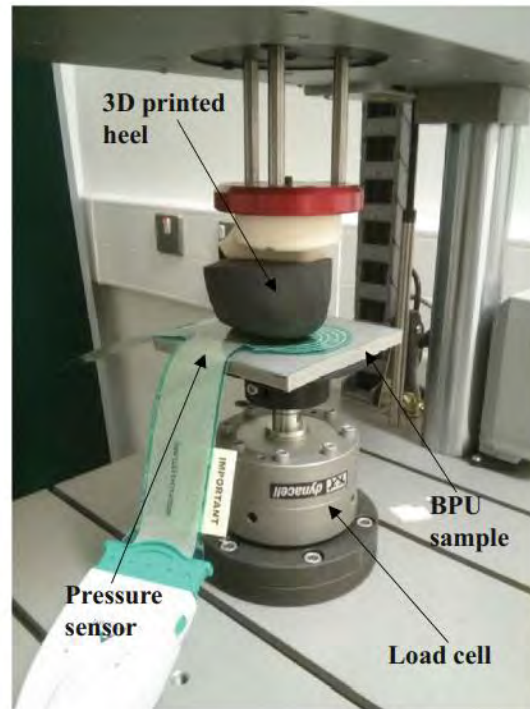


Figure 2. 20 Test set-up to investigate effect of loading on ability of cushioning materials to uniformly distribute plantar load with 3D printed heel model (Chatzistergos et al., 2017).

Also, Lo et al. (2014) demonstrated a novel method for measuring the dynamic coefficient of friction and shearing angle to simulate the contact conditions between the plantar and the insole. The human plantar was simulated by using pigskin for contact with the insole materials. This method can be used to evaluate the foot skin discomfort brings by the material surface and whether it is suitable to be applied as a contact material to diabetic foot.

2.9 Summary

Diabetic Foot Ulcers (DFUs) are foot problems found among diabetic patients, which affect the sensitivity, stiffness of skin tissue, and wound healing ability of their feet. As a result, small wounds or calluses can develop into large and deep ulcers, increasing the risk of amputation. To prevent foot ulcers, various scholars have investigated the risk factors associated with them.

Numerous studies have recommended the use of diabetic insoles to prevent diabetic foot ulcers by reducing plantar peak pressure. The research on diabetic insoles has focused on redistributing plantar pressure evenly through insole geometry and cushioning materials to offload forces. Literature proposes that the use of insoles significantly reduces plantar peak pressure.

However, the approach of preventing diabetic foot ulcers by improving the in-shoe environment has been underexplored. Despite skin temperature and humidity being recognized as risk factors for DFUs, studies on diabetic footwear and insoles have rarely examined or considered improving the in-shoe environment. High skin temperature is a risk factor for skin deformation, while high humidity increases skin vulnerability and the likelihood of foot tissue damage. The materials commonly used for diabetic insoles, such as PU, EVA, and PE, are non-permeable foam materials. These materials have limited breathability and tend to retain heat, causing discomfort due to heat and moisture. Thus, there is a need for new materials to improve foot skin temperature and humidity and prevent foot ulcers.

To achieve satisfactory plantar offloading and reduce plantar skin temperature and humidity caused by sweating, novel materials need to be explored. Researchers have recently proposed the use of 3D knitted spacer fabrics with inlays for protective garments, as these textile materials offer permeability and water absorbency, enhancing thermal comfort when applied to the skin. The satisfactory compression resistance and energy absorption of 3D knitted spacer fabrics with inlays show their potential for application as insole materials. Furthermore, while auxetic 3D printed materials have been investigated for their high force absorption, shear resistance, and fracture toughness, their application in insoles has not yet been explored. The

flexibility in insole geometry and material stiffness also benefits the application of auxetic materials in diabetic insoles.

While these novel materials exhibit desirable properties for diabetic insole applications, their performance and combination as insole materials have been rarely investigated. Therefore, further research is needed to demonstrate the application of 3D printing and knitting in insole design and evaluate their performance in terms of thermal comfort and reduction of plantar pressure to facilitate the prevention of diabetic foot ulcers.

Chapter 3 A Foot Care Program to Understand the Footwear

Preference of Diabetic Patient

3.1 Introduction

The diabetic patients are suggested to wear diabetic foot orthoses. The proper selection of diabetic footwear and insole are very important which affect the effectiveness of foot protection. To understand the footwear and insole preference of the diabetic patient, a foot care programme is conducted with a questionnaire for each participant. A total of 30 diabetic patients are recruited. Their foot care routine, as well as their footwear and insole preference and practical use in daily activities were collected, hence providing useful references in design of diabetic insoles.

The purposes of the questionnaire survey are: 1) to examine the common foot problem or discomfort, and daily use of orthotic footwear and/or insole of diabetic patients, and 2) to understand their preferences of footwear and insole.

3.2 Methods

To accomplish the purposes, a foot care program was conducted from March to May 2021 to collect the information of diabetic patients about their foot problem and their needs of diabetic foot orthoses by foot measurement and questionnaire. A total of 30 subjects with Type 1 or 2 diabetes between the ages of 55 to 75 years old who comprised 16 women and 14 men (mean: 65.0 years old; SD: ± 5.8) are recruited from Institute of Active Ageing. Their foot sizes range from EU 37 to 43.5. The inclusion criteria are people who are 50 or older, and able to walk independently across a distance of at least 6 m with or without the use of a walking aid. Their

body mass index (BMI) ranges from 18.2 to 28.7 kg/m² (mean: 23.9 kg/m²; SD: ± 2.8). Foot size range, etc. The questionnaire is presented in Appendix I. The experiment was approved by the Human Subjects Ethics Sub-Committee of the Hong Kong Polytechnic University (reference number: HSEARS20200128001). All the participants provided informed written consent before participation in the study. A table of subject profile is also mandatory (Table 3.1).

Table 3.1 Subject profiles.

Subject No.	Sex	Age	Weight(kg)	Body height(cm)	BMI (kg/m ²)	Foot Size (EU)	Years from diagnosis
S01	F	63	59	164	21.9	40	63
S02	M	68	70.5	163	26.5	38	28
S03	F	75	56	154.5	23.5	38.5	8
S04	M	62	69	164.5	25.5	39.5	4
S05	F	57	64	151.5	27.9	37.5	18
S06	F	65	73.5	160	28.7	38	13
S07	M	70	54	157	21.9	38.5	5
S08	M	60	65	166	23.6	42	11
S09	F	66	52	151	22.8	39	2
S10	M	66	67	170	23.2	40.5	5.5
S11	M	72	71.5	167	25.6	42	31
S12	M	65	65	158.5	25.9	39.5	8
S13	F	65	42	152	18.2	37	5
S14	F	57	49.5	165	18.2	37.5	20
S15	M	68	58.5	169	20.5	41	1
S16	F	66	58.5	160	22.9	40	1
S17	F	64	52	154.5	21.8	38	31
S18	F	71	65	157	26.4	38	1
S19	M	55	70	166	25.4	43	2
S20	F	71	52	155.5	21.5	38.5	1
S21	F	61	50	158	20.0	38.5	10
S22	F	62	62	157	25.2	38	8
S23	F	71	60	155	25.0	39.5	27
S24	M	54	66.5	170	23.0	40.5	5
S25	M	74	79	175	25.8	43.5	21

S26	M	55	85	173.5	28.2	41	1
S27	M	71	70	162	26.7	41	23
S28	M	62	67	168	23.7	43.5	1
S29	F	62	54	163	20.3	39	7
S30	F	73	64	157	26.0	39	10

The questionnaire is designed with three major focuses: 1) foot pain wearing indoor footwear; 2) preference of footwear design elements and materials, and the details about the most often used insole; and 3) their daily activity level. The first part of the questionnaire aims to assess the discomfort of diabetic patients wearing indoor footwear without orthoses element. The foot is divided into six regions: toes, dorsal, forefoot, heel, medial side, and lateral side of the foot. Without proper protection in terms of pressure and thermal environment by proper footwear, there could be discomfort in various foot regions. This could be considered during the design of the insole. The second focus includes the preference of insole regarding the arch support on insole, shape, contact materials, and cushioning materials. The participants are required to wear their most used insole and a photo was being taken on the insole as a record. The materials of their insole were also recorded in the questionnaire. This information is used to understand the common material used on the insole for daily use and the preferred material and design element of the diabetic patient. The third focus is the activity level of the diabetic patient for an insole design that could satisfy their need for daily activity, such as some low intensity sport.

3.3 Results and Discussion

3.3.1 Foot Discomfort Wearing Footwear

Problem of wearing the footwear with insufficient protection and improper materials cause foot discomfort especially for the elderly. A question of self-assessment of foot discomfort (uncomfortable/ hot/ sweaty) wearing indoor footwear was included in the questionnaire.

Figure 3.1 shows the percentage of patients with foot discomfort in six-foot regions: toes, dorsal, forefoot, medial side of foot, lateral side of foot, and heel. Only 33.3% of patients do not have foot pain wearing indoor footwear at home. For the patients with foot pain, heel is the most common foot region reported to have foot pain (23.3%), followed by the forefoot and the metatarsal head of the foot (20%). The toes (10%), dorsal (6.67%), and lateral side of foot (6.67%) was the less common region suffer from foot pain wearing indoor footwear.

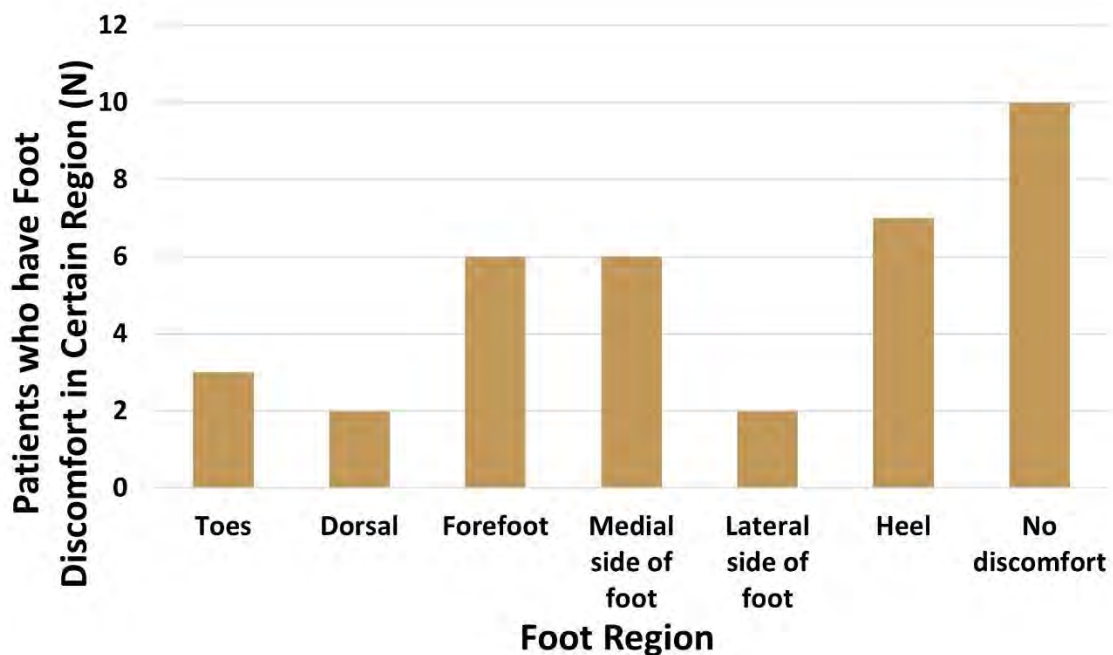


Figure 3. 1 The number of patients with foot discomfort in certain foot region.

The investigation on the common foot discomfort of the participant reflects the needs of the concern on the comfort of certain foot region. As mentioned in the results, the heel is the most common region where the participants feel uncomfortable which should be considered during the design of the foot product to reduce the pressure and enhance the thermal environment. As the sole of the indoor footwear are mostly single material only for the reduction of slippery,

the function on force reduction is limited. Similarly, the forefoot is also a common foot discomfort region for the participant which caused by the excessive plantar pressure. As investigated by the previous research, both the heel and metatarsal head is the region having plantar pressure relatively higher than other foot region (Bennetts et al., 2013; Bus, 2016). Therefore, the results are aligned with the previous studies. Thus, the reduction of plantar pressure on these two regions are needed to improve the plantar comfort. In addition, the medial side of the foot is also a region which needs the concern for comfort enhancement. For some footwear without arch support, there are less contact area between the medial side of the foot and the sole/insole. The insufficient support on the arch might increase the abrasion and force beard by the remaining area that have contact with the footwear. This could be the reason tends to cause the foot pain on the medial side of the foot. This indicated that the support on the arch is essential to reduce the foot discomfort. The reduction of plantar pressure in forefoot and heel, and the increase of support on the arch would be consider in the later design of diabetic insole.

3.3.2 Preference of Insole Materials and Element

The insole wearing habits of elderly with diabetes included what materials of insole they usually wear and the design feature of the insole that they tend to choose. Figure 3.2 (a) shows the materials of the participants' most used insole. Results indicate that the foam has the highest rate of application (93.33%) on the insole worn by the participants. The fabric materials are also commonly used insole materials with the application on 80% of participants' insole. In contrast, less rate of application was observed on the leather (6.67%) and rubber materials (20%).

For the contact materials to the foot, 77% of the insole use fabric materials as the surface layer to contact with the foot skin, see Figure 3.2(b). Also, there are 13% of the insole directly contact

the foot with foam, 7% with leather, and only 3% with rubber. It can be observed that the foam material is mostly applied as the second layer under the fabric as a cushioning material.

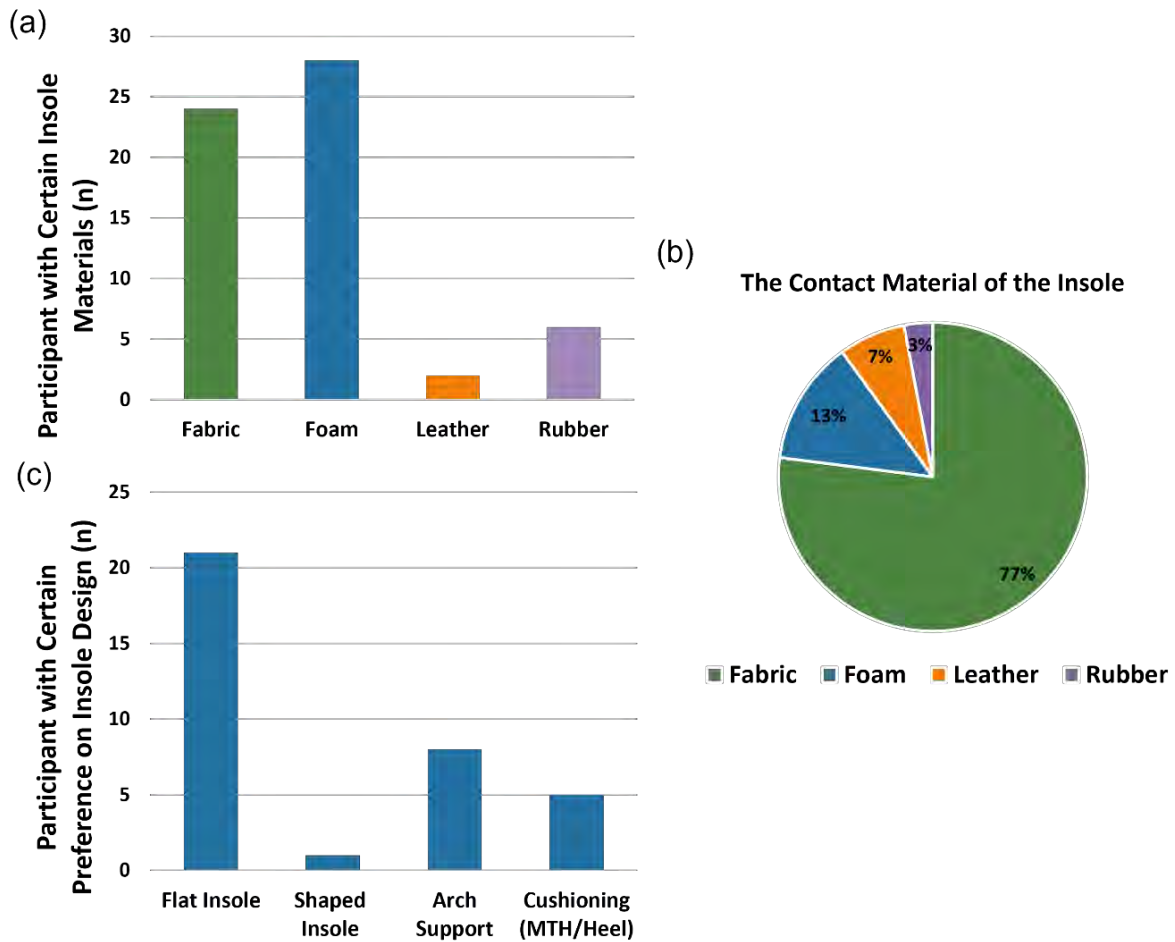


Figure 3. 2 the material of (a) the patient currently used insole, (b) the contact surface of the insole to plantar; (c) the preferred feature of the insole.

The results confirm that fabric is a material that is commonly used on the insoles worn by diabetes elderly participants in this program. Although foam is a common insole material, foam is used as the second layer of the insole for cushioning that helps to reduce the pressure on plantar. Most of the insole use fabric as the first layer to contact with the foot because textile material is favourable for sweat absorption to reduce the slipperiness of the insole surface and reduce the moisture level on the foot. The common application and wide acceptance of the

textile materials on the insole confirms that it is a suitable material for insole and an acceptable material by the users.

Moreover, the insole preference of the participants could be observed that 70% of subjects prefer a flat insole while only 3% of them prefer a shaped insole with be shaping according to their foot. For other features, 26.67% of the participant prefer arch support on the insole and 16.67% of them prefer having cushioning materials on the high-pressure region such as the metatarsal head (MTH) and the heel.

The results show that the customers prefer a flat insole they are using instead of an insole that exactly fits the shape of their foot (i.e., customized insole). Indeed, as indicated by other researchers, the customized insole with perfect fitting reduces and redistributes the plantar pressure more ideally than the flat insole (Bus et al., 2004; Cavanagh & Bus, 2011). However, as most of the midsole and outsole of the shoes already have a designed shape for comfort, especially for sports shoes. With the well-shaped midsole and outsole of the footwear, the contact area between the footwear and the plantar increases, enhancing the plantar pressure redistribution. Therefore, sufficient comfort could be provided by only inserting flat insoles. Besides, the results show again the importance of arch support and the cushioning on the high-pressure area on the plantar which is preferred by some of the diabetes elderly participants.

3.3.3 The Needs on Daily Activity

The daily activity level of the participants was mainly assessed by their sport behavior and the time they used to spend on the sports activities. Around 50% of the participants used to have a walk frequently. As shown in Figure 3.3(a), a total of 86.67% of the participants need to wear footwear for the activity. Figure 3.3(b) shows the times the participants spend on the activities

per week. It can be observed that 73% of the participants spend over 2 hours on the activities every week and half of them spend at least 3 hours. For the need of having daily activity and sport, footwear that can offer comfort and protection is important.

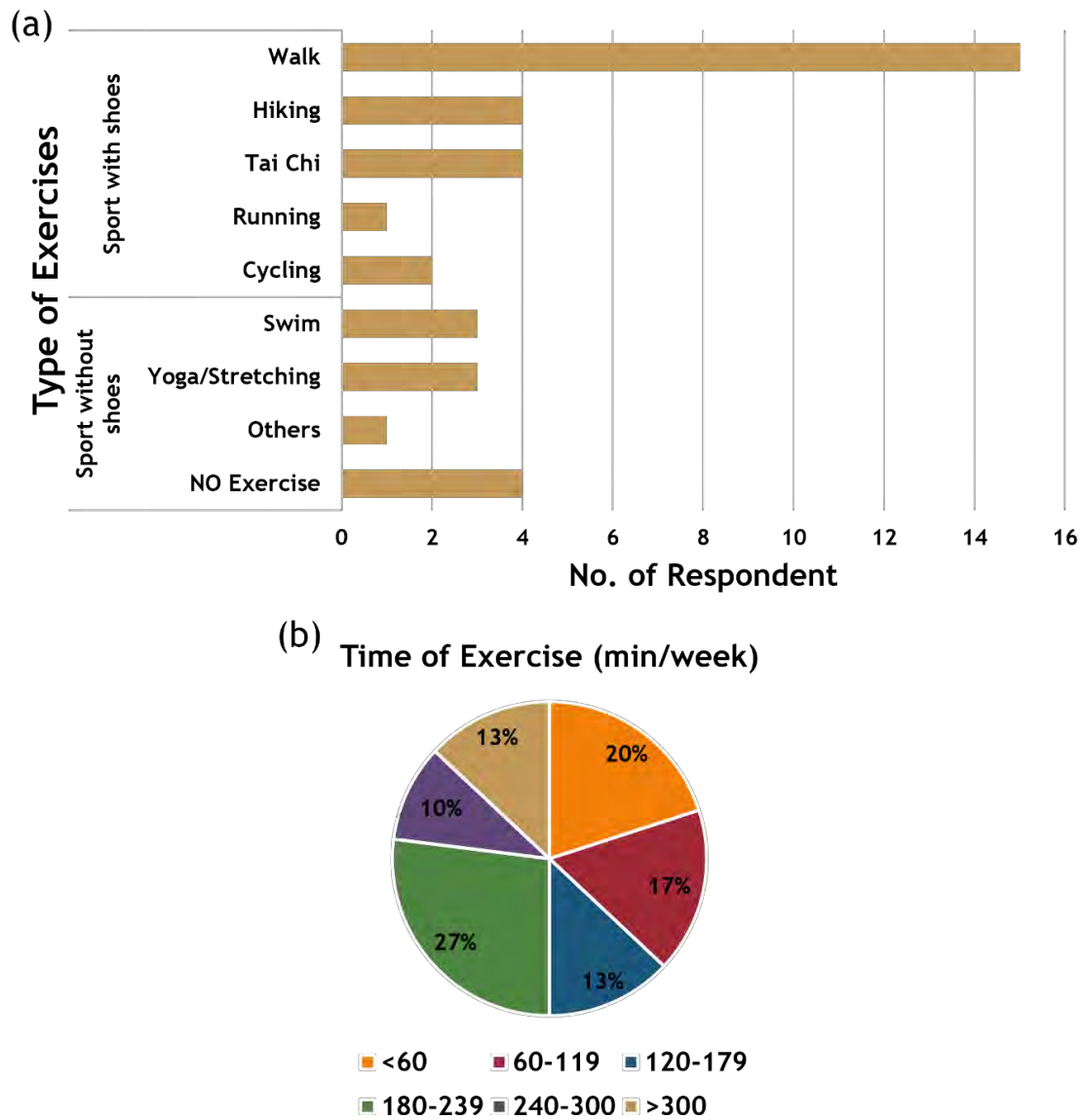


Figure 3.3 (a) the sport that the patient used to do and (b) the time they spend on the sport weekly.

By looking at the habit of the participant, it can be concluded that most of the participants have the awareness and need on having a sports activity frequently. Most of the activity increases both external and internal force on the plantar that they normally need to wear footwear. To

support the daily activity and sport of the diabetic patient, footwear with enough protection is highly preferred to avoid any occurrence of injuries and even ulcers. As the cushioning material inside the footwear, the insole plays an important role in plantar pressure reduction. Thus, the design of the insole to improve foot comfort helps the patient to maintain their daily activity level.

3.3.4 Price Preference of the Footwear Product

The price is another important concern of the patient in buying footwear or insole. To some extent, the range of price that the participants are willing to pay for their footwear could reflect their price limit in buying insole products. As nearly all the patients are wearing the original insole of their shoes, they might even not be willing to spend money on an insole. As shown in Figure. 3.4, more than half of the participants are willing to pay not more than \$500HKD for buying a pair of daily shoes and only 14% of the participants are willing to spend \$701 or higher.

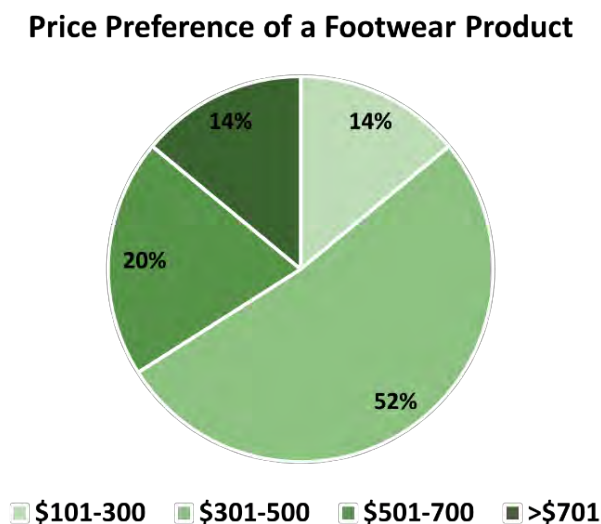


Figure 3. 4 The price the patient willing to spend on a pair of daily outdoor footwear.

Unfortunately, a pair of custom-made insoles normally cost higher than \$1000 which is even higher than their budget for the entire shoes. With the considering of the price, the patient might not consider buying a customized diabetic insole with adequate function. Not to mention, the customized insole even needs to be replaced frequently to keep the optimal function. Thus, the design of a prefabricated insole with satisfactory function is needed for the patient to purchase at an acceptable price.

3.3.5 Summary

To sum up, the common problems and needs of diabetes elderly were investigated in this study. Due to improper footwear, foot pain is generally reported at heel, forefoot, and medial side of the foot. Flat-shaped insole, arch support, and cushioning pads are commonly used for pain relief and reduction of high-pressure regions. Apart from traditional insole foam materials, textile materials are commonly used as the contact surface of the insole to the plantar.

Chapter 4 Analysis of the In-shoes Microclimate under Different Insole Materials to Enhance Orthotic Shoes Design in Thermal Comfort

4.1 Introduction

Orthotic insoles for patients with diabetes are conventionally made of foam materials and composites in a two- or three-layered construction to provide adequate cushioning and support with respect to specific needs, activity profiles and foot conditions. Since foam sheets for insoles are available in a wide range of hardness, thickness, and density, the choice of foam materials for insole fabrication is crucial. Nevertheless, the influence of insole material on the in-shoes thermal environment has been largely neglected in previous studies. It is noteworthy that materials with poor air-permeability and water vapor transmission will inevitably hamper the free flow of heat and humidity, affecting the thermal regulation performance. Also, there is very little work that examines the thermal properties of the insole materials and even rarely conducts a human trial. The performance of the insole materials in maintaining the in-shoes thermal environment remains unknown.

In this chapter, the potential use of 3D printing technology and the 3D spacer knitted structure for footwear insole in relation to foot skin temperature and humidity during treadmill walking are analysed through a wear trial. The result can act as a reference for the material selection for the design and development of diabetic foot orthoses in the later stage of study. These help to enhance the comfort of wear and maintain an appropriate skin condition to avoid skin deformation caused by excessive heat and moisture.

4.2 Methods

This study adopts a within-subject repeated-measures design. Participants were instructed to use four types of insoles made with different materials during the wear trials in March 2021. The foot skin temperature and humidity were measured during a session that involved 30 min of walking on a treadmill. Subjectively perceived comfort towards heat and moisture, and the thermal comfort of the insoles were measured after the walking trials.

4.2.1 Participants

A total of 21 female participants took part in the study (age: 25.5 ± 4.5 years old, 161.5 ± 6.5 cm, and 52.5 ± 12.5 kg). Their shoe size ranges from EU36 to 40, which was measured by using a foot-measuring device (Brannock Device®). The exclusion criteria are any foot disease, such as open wounds, foot eczema, abnormal foot morphology, or a lower limb injury. Before the experiment took place (24 hrs), all of the participants were required to avoid any intense exercise or sporting activities, and alcohol or caffeine intake. The experiment was approved by the Human Subjects Ethics Sub-Committee of the Hong Kong Polytechnic University (reference number: HSEARS20200128001) and conducted in accordance with the Declaration of Helsinki. A brief overview of the study was given to each participant who signed a written consent form prior to the start of the experiment.

4.2.2 Insole Sample

The insole samples in this study are presented in Figure. 4.1, which include a: (a) PU insole (PORON®); (b) TPU (3D-printed); (c) textile-fabricated insole made of knitted spacer fabric with silicon tubes inlay, and (d) leather insole. The specifications of the insoles are listed in Table 4.1. Except for the textile-fabricated insole, the initial thickness of the insole samples is

approximately 6 mm. To simulate the compressive performance of the insoles in the full weight-bearing condition during practical use, the compressed thickness of the insole materials under a load of 130 kPa was also measured (Kwan et al., 2021; Torgutalp et al., 2021). Each participant was subsequently fitted with four pairs of insoles according to their foot size. The thermal conductivity of all the insole materials is shown in Figure. 4.2 for reference.

Table 4. 1 Material specification of the four insoles.

Insole	Material(s)	Thickness under load of 20 kPa (mm)	Percentage of compression under load of 20 kPa (%)	Thickness under load of 130 kPa (mm)	Percentage of compression under load of 130 kPa (%)	Density (g/cm ³)
PU	All PORON®	6.103	5%	4.120	55%	0.161
TPU	All TPU	5.776	4%	4.643	29%	0.151
Textile-fabricated	surface yarn: 63% Cupro 37% Polyester spacer yarn: 100% polyester monofilament Inlay materials: silicon tube in 3mm diameter	14.233	11%	3.267	390%	0.165
Leather	Surface: Leather Bottom Layer: EVA	6.689	1%	3.323	103%	0.284

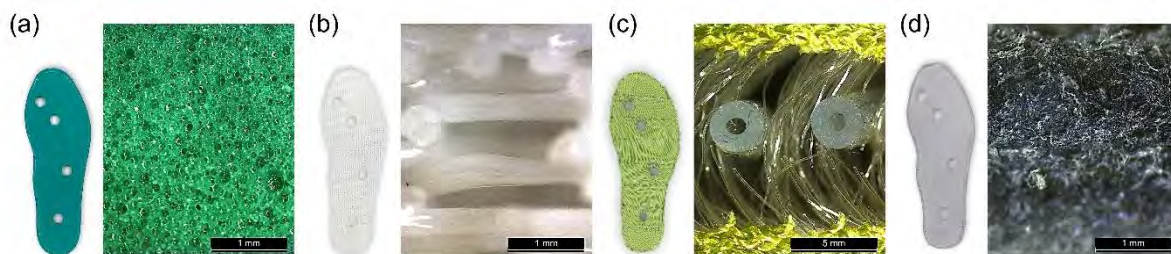


Figure 4. 1 Insole samples: (a) PU; (b) TPU; (c) textile-fabricated; (d) leather, and their microscopic longitudinal cross-sectional view.

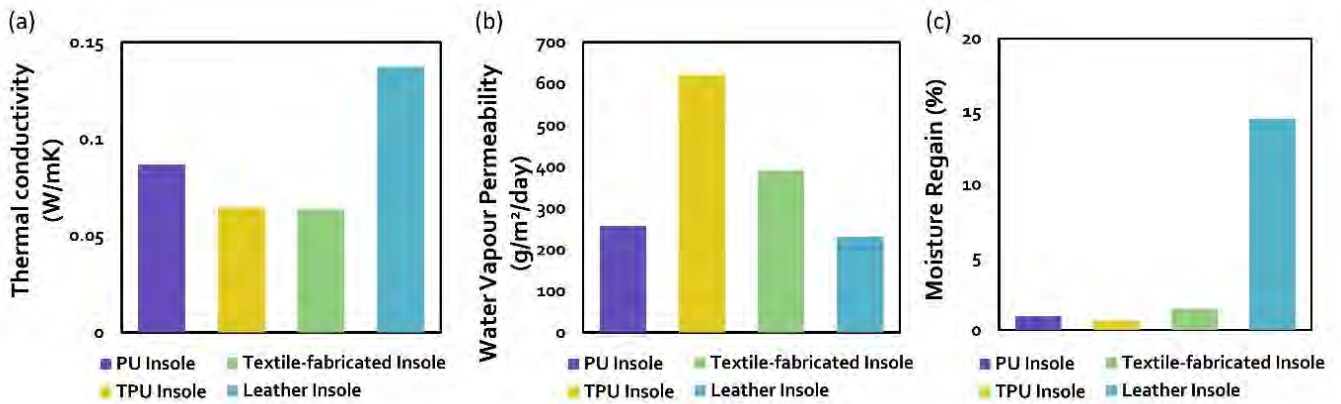


Figure 4. 2 The (a) thermal conductivity (W/mK), (b)Water Vapour Permeability (g/m²/day), and (c) moisture regain of the insole materials.

4.2.3 In-shoe Temperature and Relative Humidity

The skin temperature and humidity of five measurement points were recorded continuously by using wireless temperature sensors (Thermocrons HC, OnSolution). The temperature and RH ranged from -30°C to 85°C and from 0% to 100% respectively. The resolution of the temperature and RH is 0.0625°C and 0.04%, whilst the rate of measurement was set at intervals of every 5 seconds. The thickness and diameter of the sensor are 6 mm and 16 mm respectively. The slim profile of the sensor minimizes the negative effect on plantar comfort during walking. Five measurement points were selected including the neck of the big toe, and sole, middle sole, heel, and dorsal of the foot (Points 1, 2, 3, 4 and 5 respectively), see Figure. 4.3 (Shimazaki et al., 2016; Smith et al., 2013; Yick et al., 2019).

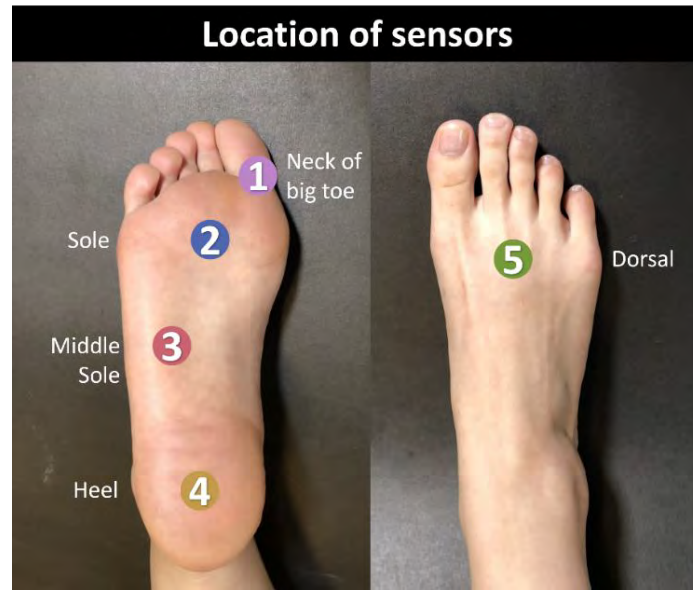


Figure 4.3 Measured locations of skin temperature and humidity on dorsal and plantar of foot.

In this study, the changes in foot skin temperature and RH are calculated by using Equations (1) and (2):

$$\Delta T = T_f - T_i \quad (1)$$

where ΔT is the change in skin temperature ($^{\circ}\text{C}$), T_f is the final measured skin temperature after 30 mins of walking, and T_i is the initial foot skin temperature

$$\Delta \text{RH} = \text{RH}_f - \text{RH}_i \quad (2)$$

where ΔRH is the change in RH (%), RH_f is final measured RH after 30 mins of walking, and RH_i is the initial RH of the foot skin.

4.2.4 Experimental Protocols

The experiment was conducted in an indoor environment at a temperature of $22 \pm 1^{\circ}\text{C}$ and RH of $70 \pm 5\%$ (Shimazaki & Murata, 2015; Yick et al., 2019). The participants were requested to wear a standard sports outfit which consists of a pair of trousers and a long-sleeve cotton T-

shirt with an insulation of about 0.3 clo (A. Yu et al., 2018). The same type of mesh shoes (Figure, 4.4) along with the four pairs of insoles were provided to the participants based on their foot size. The participants were required to walk for 30 min on a treadmill at 5 km/h for each insole condition (Shimazaki et al., 2016), and their foot skin temperature and RH were recorded. Each participant completed all four insole conditions on a single day. Prior to each insole condition, all of the participants were instructed to sit in a relaxed position in their bare feet for around 30 mins of recovery to cool down their body temperature and reduce any fatigue which could be carried over to the next test condition (Shimazaki et al., 2016; Yick et al., 2019). Their plantar temperature was monitored with an infrared camera (FLIR-T62101) as shown in Figure. 4.4(b).

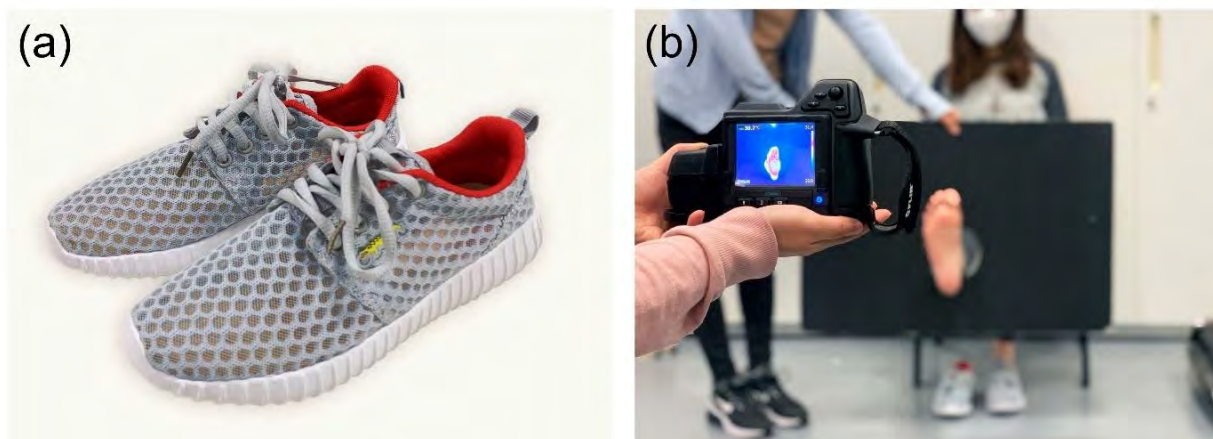


Figure 4. 4 (a) Mesh shoes used in wear trial, and (b) checking foot temperature with FLIR camera.

4.2.5 Subjective Sensation Rating

The subjective sensation of the participants for each of the four insoles was subsequently assessed. After each walking session, they were instructed to rate the level of heat and moisture sensations, and thermal comfort respectively (West, Schönfish, et al., 2019; Yick et al., 2019).

The perceived heat and moisture sensations of the insoles were rated by using a 7-point Likert-like scale, whilst the overall thermal comfort of the insoles was assessed by using an 11-point Likert-like rating scale (Figuer. 4.5).

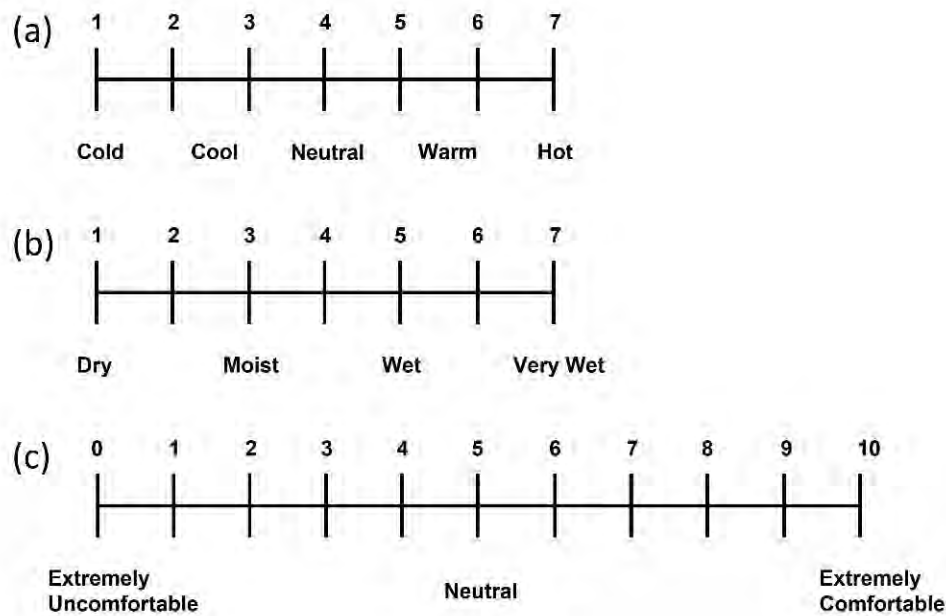


Figure 4.5 Perceived (a) heat sensation; (b) wetness; and (c) thermal comfort scales.

4.2.6 Statistical Analysis

The statistical analysis was processed by using the Statistical Package for the Social Sciences program (SPSS®21, IBM® Corporation, New York, USA). One repeated-measures analysis of variance (ANOVA) was conducted to evaluate the effect of the insole conditions for each measurement point in terms of the changes in skin temperature and RH. The repeated-measures ANOVA was also adopted to investigate the differences in the mean foot skin temperature and RH amongst the 5 measurement locations.

4.3 Results

4.3.1 Changes in Foot Skin Relative Humidity

A repeated-measures ANOVA was conducted with pairwise comparisons between all of the insoles at all of the measurement points. Significant differences were found only in the pairs with the textile-fabricated insoles at Points 2 and 4 ($p < 0.05$). There is no significant difference observed among the PU, TPU, and leather insoles for all of the measurement points. Table 4.2 is a comparison between the textile-fabricated and the other 3 insole conditions in which the RH of the skin of the foot changes during the 30 mins of walking. In the pairwise comparison, the textile-fabricated insole exhibits the lowest increase in RH among all of the insole conditions at Point 2 and the largest decrease at Point 4.

An increase of 3.21% in the RH at Point 2 was observed for the textile-fabricated insole which is significantly lower ($p < 0.05$) than that of the PU, TPU, and leather insoles. Figure. 4.6(a) shows the mean RH changes of the skin of the foot at Point 2 after 30 mins of walking. Only the textile-fabricated insole shows a decrease in the RH of the foot skin while the other three insoles show an increase. The TPU insole shows the largest increase in RH after walking for 30 mins.

The highest decrease in the mean RH with the textile-fabricated insole is also found at Point 4. Figure. 4.6(b) shows the changes in the RH at Point 4 after 30 mins of walking. Compared to the PU and TPU insoles, the reduction of the skin RH with the use of the textile-fabricated insole (-24.41%) is significantly larger ($p < 0.05$). Although the difference between the textile-fabricated and leather insoles is not significant ($p > 0.05$) at Point 4, the mean RH reduction with the use of the textile-fabricated insole is larger.

Table 4.2 Comparison between textile-fabricated and other 3 insole conditions based on skin RH during 30 mins of walking.

Measurement Points	(I)Condition	Mean	(J)Condition	Mean	Mean Differences	Sig.
Point 1 (Neck of big toe)	Textile-fabricated Insole	-15.376	PU Insole	-23.081	7.705	.437
			TPU Insole	-17.101	1.725	1.000
			Leather Insole	-16.849	1.474	1.000
Point 2 (Sole)	Textile-fabricated Insole	-3.209	PU Insole	5.112	-8.321	.014*
			TPU Insole	8.469	-11.678	.003**
			Leather Insole	7.208	-10.416	.002**
Point 3 (Middle Sole)	Textile-fabricated Insole	-19.393	PU Insole	11.979	.756	1.000
			TPU Insole	14.589	-.241	1.000
			Leather Insole	13.113	-4.583	1.000
Point 4 (Heel)	Textile-fabricated Insole	-24.411	PU Insole	-13.988	-10.423	.007**
			TPU Insole	-15.837	-8.575	.037*
			Leather Insole	-19.471	-4.940	.503
Point 5 (Dorsal)	Textile-fabricated Insole	22.949	PU Insole	21.282	1.668	1.000
			TPU Insole	22.979	-.030	1.000
			Leather Insole	21.121	1.828	1.000

Note: * $p < 0.05$, ** $p < 0.01$

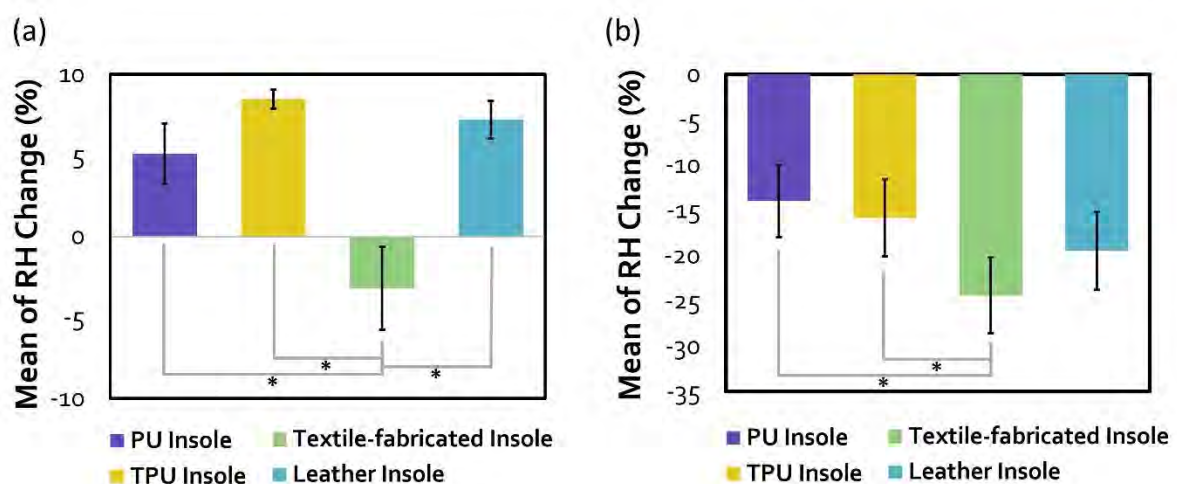


Figure 4.6 Change in mean RH after 30 mins of walking at (a) Point 2, and (b) Point 4. Error bars show the standard error.

Figure. 4.7 shows the RH during 30 mins of walking at Points (a) 1 (neck of big toes); (b) 2 (sole); (c) 3 (middle sole); (d) 4 (heel); and (e) 5 (dorsal). At Points 1 to 4, all of the insole conditions show a slight increase in the RH in the first 50 seconds followed by a continuous gradual decrease at Points 1, 3, and 4, and an increase at Point 5. The initial increment could be due to the sweating and the following decrement could be due to the absorption of sweat and the friction between the plantar and insole which further wicks away the skin moisture. Also, among all of the measurement points on the plantar (Points 1-4), only Point 2 shows an increase in the RH after 30 mins of walking. This increase is more rapid in the first 800 seconds followed by a slower increase (PU, TPU, and leather insoles) or a decrease (textile insole). For the other measurement points on the plantar, the RH of all of the insole conditions decreases continuously and the slopes of the plotted change for the 30 mins of walking are similar. Apart from the plantar, the effect of the insole on the dorsal of the foot is not obvious. As the shoe upper does not frequently come into contact with the dorsal of the foot, the sweat remained on the skin of the dorsal.

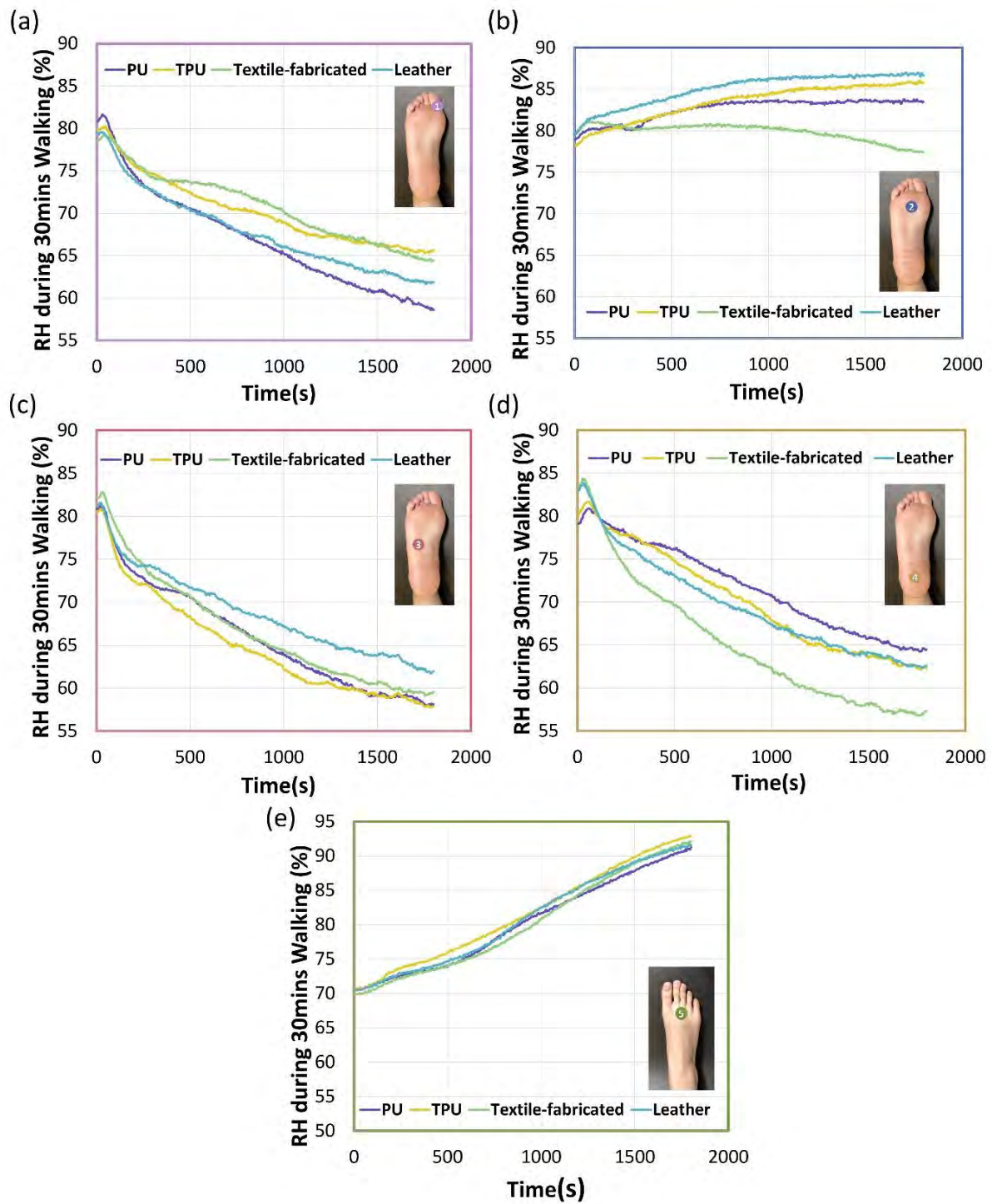


Figure 4. 7 The skin RH during 30 mins of walking at Points (a) 1 (neck of big toes); (b) 2 (sole); (c) 3 (middle sole); (d) 4 (heel); and (e) 5 (dorsal).

4.3.2 Change in Foot Skin Temperature

There is no significant difference among the insole conditions for the changes in foot skin temperature at all of the measurement points. The trend of increase in temperature for all of the measurement points is similar. Figure. 4.8 shows the foot skin temperature during the 30 mins of walking at Points (a) 1 (neck of big toes); (b) 2 (sole); (c) 3 (middle sole); (d) 4 (heel); and (e) 5 (dorsal). Although the textile-fabricated insole exhibits a slightly higher mean foot skin temperature increase than the other insole conditions, the difference is insignificant.

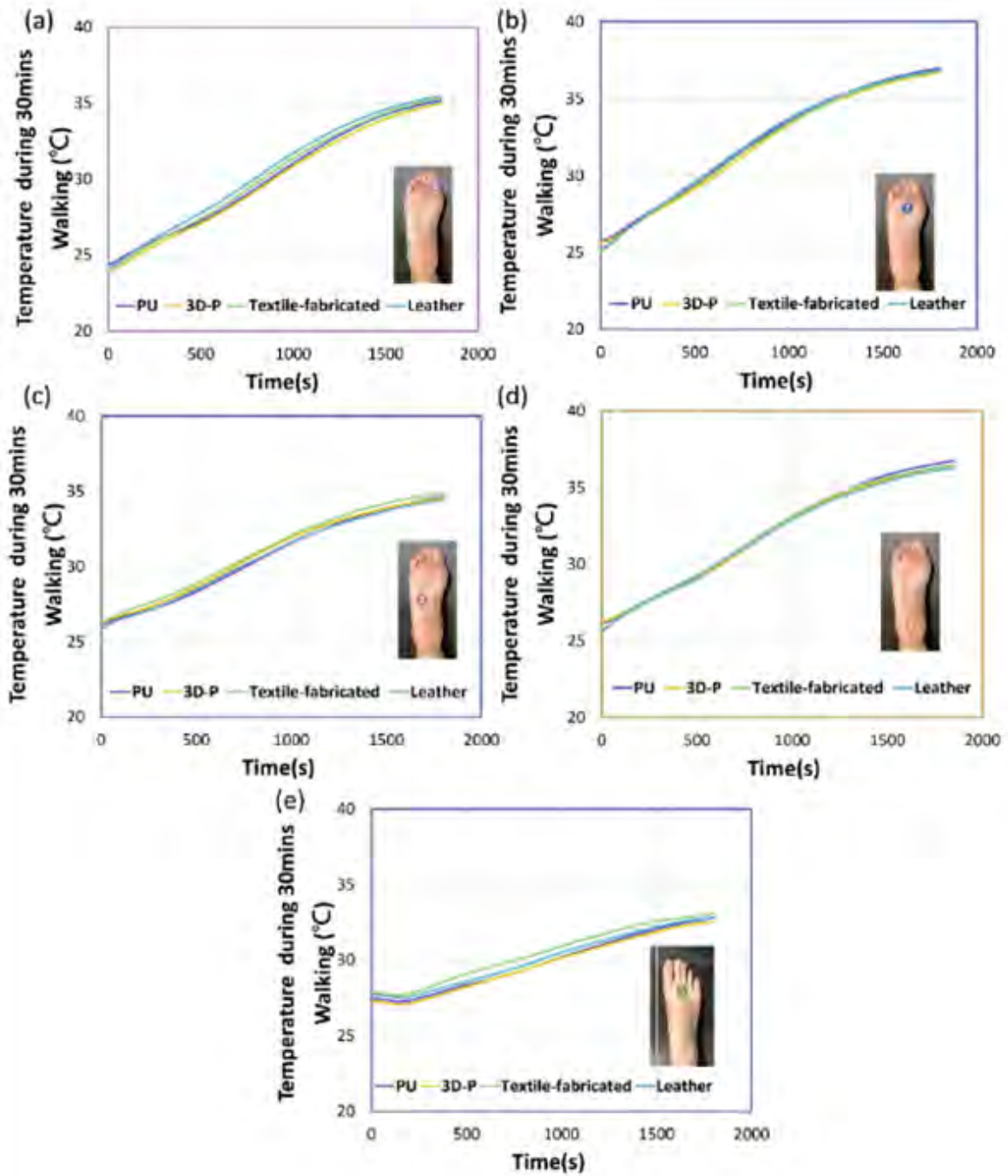


Figure 4.8 Foot skin temperature during 30 mins of walking at Points (a) 1 (neck of big toes); (b) 2 (sole); (c) 3 (middle sole); (d) 4 (heel); and (e) 5 (dorsal).

4.3.3 Distribution of Foot Skin Relative Humidity and Temperature

A significant difference was found between the measurement points for both the RH and temperature. This shows that different foot regions have different responses to heat and sweating.

Figure. 4.9(a) shows the mean change of the skin RH at the 5 measurement points. In the pairwise comparison, significant differences were found between all of the pairs with Point 2 and all of the pairs with Point 5 ($p < 0.05$). No significant difference was found among Points 1, 3, and 4 with a similar mean decrease of the RH of around 18%. Point 5 shows the highest increase in RH followed by Point 2. As mentioned, Point 2 is the only measurement point along the plantar that shows an increase in the RH.

A decrease in the RH was observed at Points 1, 3, and 4. Point 5 is the only point in the dorsal and it shows an increase in RH which is significantly higher than all of the points in the plantar. Indeed, the dorsal was reported to have a higher sweat rate than all of the plantar regions which explains for the highest RH increment in the dorsal (Smith et al., 2013).

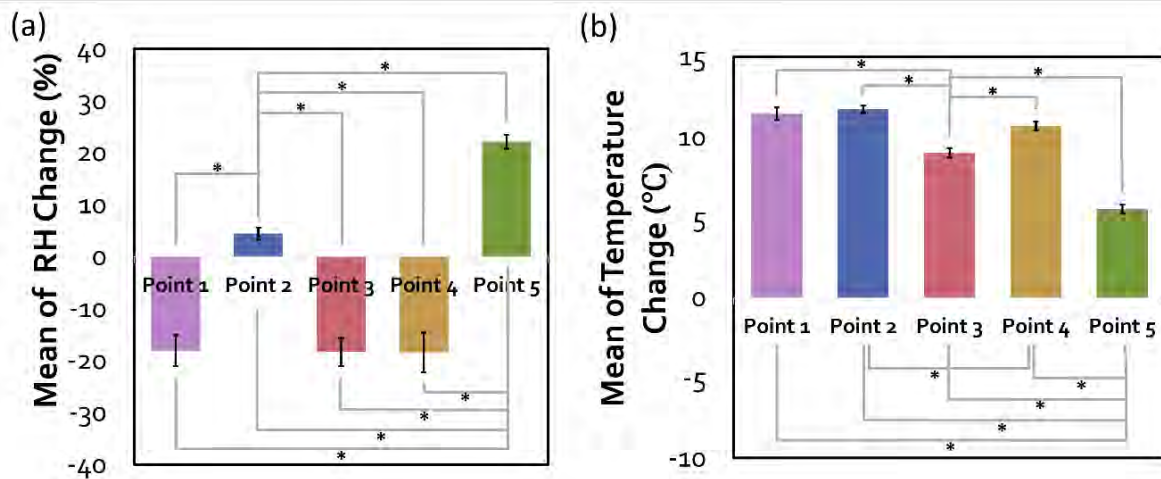


Figure 4.9 Mean of change in (a) RH and (b) temperature of all the measurement points. Error bars show the standard deviation.

The skin temperature for all the foot regions was found to increase during walking. The mean change in the skin temperature of the 5 measurement points is plotted in Figure. 4.9(b). Significant differences can be found in the pairwise comparison between all of the pairs with Point 3 and all of the pairs with Point 5 ($p < 0.05$). The difference between Points 1 and 2, and Points 1 and 4, is not significant with a mean increase in skin temperature of around $11.2 \pm 0.6^\circ\text{C}$. The highest increase in skin temperature was found at Point 2 followed by Points 1, 4, 3 and finally 5. Point 5 is the only measurement in the dorsal with the smallest temperature increase. As the pressure on the dorsal region is lower, there is less abrasion force between the dorsal to the shoe upper compared to the abrasion between the plantar and insole. Indeed, Point 3 experiences the least pressure among all of the measurement points in the plantar. Thus, the skin temperature increases at Point 3 are lower than those at Points 1, 2, and 4.

4.3.4 Subjective Sensation Rating

Figure. 4.10 is a plot of the insole conditions based on the subjective ratings of heat and moisture sensations, and thermal comfort. Although the differences between each insole

condition are not statistically significant, the result shows a trend where the textile-fabricated insole has a higher perceived comfort. For the heat sensation, the textile-fabricated insole has the least perceived heat while the leather insole has the highest perceived heat. Also, the textile-fabricated insole is perceived to have the least moisture while the remaining three insoles have similar ratings. Simultaneously, the textile-fabricated insole has the highest perceived thermal comfort while the other insole conditions have a similar rating.

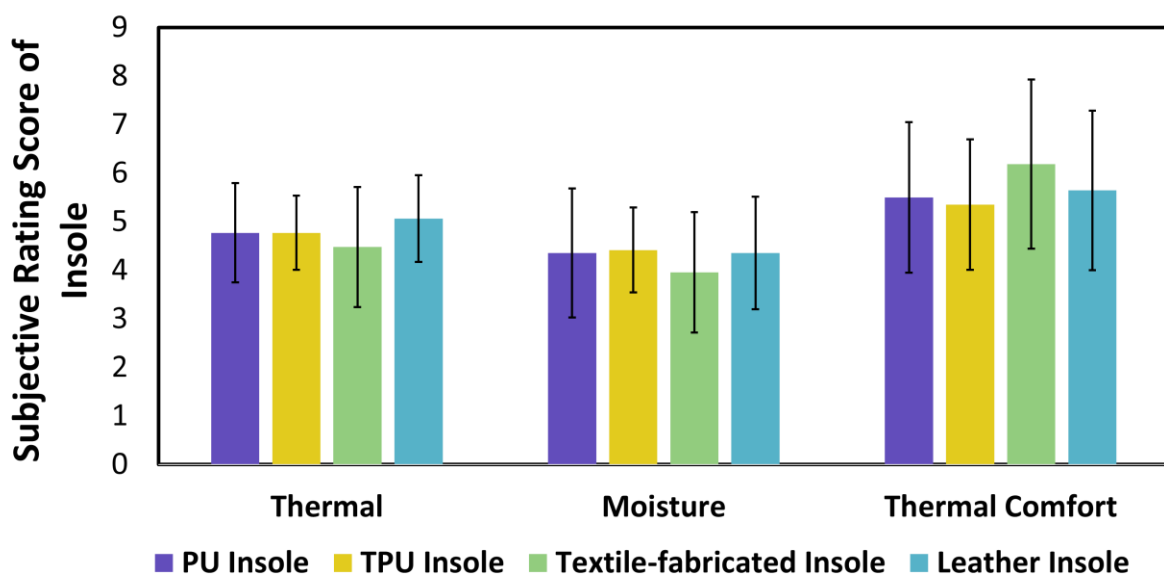


Figure 4.10 Subjective rating of heat and moisture sensations, and thermal comfort of insole conditions. Error bars show the standard deviation.

4.4 Discussion

Over the past decades, much of the work on footwear insoles has aimed to reduce the stress that acts on the feet for force reduction and cushioning, particularly in clinical practices. Nevertheless, studying the in-shoe microenvironment is paramount which not only enhances the foot thermal comfort of the wearers but is also associated with the increase in foot temperature and moisture level, thus resulting in bacteria growth on the feet and wound

infection of patients with diabetes (Irzmańska, 2016; Shimazaki et al., 2016). With the recent development of advanced materials and additive manufacturing technologies, the application of 3D textile-fabricated structures not only can resist the pressure induced by body weight, but also act as a buffer to prevent moisture build-up in the in-shoe microclimate surrounding the skin during intermittent perspiration (Rajan et al., 2016). Nevertheless, the practical use of 3D printed and textile-fabricated insoles and their impacts on foot skin temperature and humidity have not been fully investigated. The study, therefore, places wireless sensors at different foot locations so that the immediate changes in foot skin temperature and humidity in different insole conditions and foot regions during treadmill walking can be recorded and compared. Our findings are in line with our hypothesis that as opposed to traditional insole materials, there is a considerable reduction of skin humidity when textile-fabricated insoles are worn. However, there is no significant difference in the foot skin temperature across the four experimental insole conditions.

4.4.1 Foot Skin Moisture

The influence of the insole on the RH of the skin of the foot during walking is statistically significant at sole and heel while not obvious at the neck of big toes, middle sole, and dorsal. The higher pressure borne by the sole and heel contributes to significant differences between the reductions in the RH. According to previous studies, higher pressure at the sole and heel is found as opposed to the neck of the big toes and midsole during walking (Bennetts et al., 2013; Bus, 2016). The higher pressure in these two points increases the surface deformation of the insole and the contact area between the skin and insole material. Therefore, the sweat absorption effect in these two points is more obvious which explains for the significant difference in the change in RH of the skin between the insole samples.

The results confirm the best performance of the textile-fabricated insole in maintaining a slower increase in foot skin RH at sole when compare with the other samples. The slope in Figure. 4.7(b) shows a more rapid trend of increase for the PU, TPU, and leather insoles than the textile-fabricated insole. After 800 seconds, the textile-fabricated insole is the only insole condition that shows a decrease in the foot skin RH with an overall negative change in the RH. This shows that the knitted textile-fabricated insole is more effective in reducing increases in the RH with continuous sweating. This phenomenal effect could be contributed to the material of the fabric. The yarn on the fabric surface consists of 63% Cupro which is a regenerated hydrophilic cellulose fiber (Çeven & Günaydın, 2021). Thus, it is favorable for absorbing sweat in the plantar.

Moreover, the porous structure of the textile-fabricated insole is conducive to air circulation in shoes. When considering the plantar area, evaporation is not the mainstay of reducing the RH of the skin. The sweat released from the plantar cannot evaporate due to condensation and lack of airflow. As a result, sweat will accumulate, thus causing an increase in the RH of the skin. Figure. 4.1(c) shows that the textile-fabricated insole has a higher porosity in comparison to the other insoles. From the results of the thermal properties test, it could be observed that the textile-fabricated insole material has a higher water vapour permeability than PU and Leather (Figure. 4.2(b)). The spacer structure allows for a freer flow of air and water vapour which reduces the RH (Yip & Ng, 2008; Yu et al., 2020a; Yu et al., 2016). During a gait cycle, the air stored in the spacer fabric is squeezed out and tends to flow into the surrounding space when the individual puts weight onto the insole. When the heel lifts off from the ground, the air flows back into the spacer fabric. The damp air in the plantar can flow out through the permeable mesh shoe uppers.

As shown in Figure. 4.1(a), the porosity of PU allows the absorption of sweat through capillary action. Likewise, leather is a hydrophilic material that is outstanding in absorbing sweat and moisture. The moisture regain of leather is also much higher than other insole materials, see Figure. 4.2(c). However, these two materials lack water vapour permeability, thus inhibiting moisture release through gas exchange (Figure 4.2(a)). As a result, the insole would be saturated with sweat within a short period of time. The sweat accumulated in the insole might even cause wet feet as the user steps on the insole, which would exacerbate the high levels of humidity in the shoe. On the other hand, although the 3D-printed TPU insole has high permeability, neither the material nor the structure can absorb sweat. It even shows the lowest moisture regain amount all the insole materials, see Figure. 4.2(c). Therefore, the TPU insole cannot maintain a dry environment on the plantar. The result demonstrates the importance of moisture absorption and air permeability for providing a comfortable skin condition.

At the heel, the importance of air circulation for reducing the RH is further proven by the exceptional performance of the textile-fabricated insole in maintaining a dry in-shoe environment. As the heel is the closest in proximity among all of the measurement points to the shoe opening, more air flow could be facilitated. Thus, the differences between the insoles in whether they can reduce the RH in the plantar by allowing air to circulate can be easily observed. On the other hand, the performance of the PU, TPU, and leather insoles in reducing the RH at the heel has no significant difference; the reduction of RH by the PU insole is slightly less than that of the TPU and leather insoles. This further validates the ability of the knitted textile-fabricated insole to reduce moisture.

4.4.2 Foot Skin Temperature

The effect of the insole material on the skin temperature at the plantar is limited. This study has shown that the foot skin temperature will rarely be affected by changing the insole materials during continuous activity. During walking, the body temperature is increased with the generation of metabolic heat by the exercising muscles. The thermal signals are received by the receptors in the deep core body (Fortney & Vroman, 1985). When the core temperature increases, the body speeds up blood circulation where heat could be transferred to the body skin and released through radiation and convection (Wendt et al., 2007). Simultaneously, the body also increases sweating to lose heat (cool down) through the evaporation of sweat. Indeed, the core body receptors play a more significant role in thermoregulation in comparison to the skin receptors (Fortney & Vroman, 1985). Therefore, it would be difficult to cool down the foot externally through heat conduction of the insole materials or convection. Although the mesh shoes allow a certain degree of ventilation, the insole materials have no effect on heat release.

4.4.3 Distribution of Foot Skin Humidity and Temperature

The higher pressure borne by the sole and heel contributes to significant differences between the reductions in the RH. According to previous studies, higher pressure at the sole and heel is found as opposed to the neck of the big toes and midsole during walking (Bennetts et al., 2013; Bus, 2016). The higher pressure in these two points increases the surface deformation of the insole and the contact area between the skin and insole material. Therefore, the sweat absorption effect in these two points is more obvious which explains for the significant difference in the change in RH of the skin between the insole samples. In addition, the sole is the only point with an increasing trend in the RH among all of the points in the plantar regions,

see Figure. 4.7(a). This may indicate a higher sweat rate at the sole. Thus, more consideration on moisture management at the sole should be given during insole engineering.

The sweat distribution in the plantar area in this study differs from the results of studies done by other researchers. West, TARRIER, et al. (2019) found no significant difference among the sole, middle sole, and heel regions. Nevertheless, the toe area shows a noticeably higher rate of perspiration when compared with the other plantar regions. On the other hand, no significant differences in rate of sweating between plantar regions were found in the study done by Smith et al. (2013). Indeed, the different measurement methods might have resulted in different results in this study. Instead of directly adhering sensors to the skin, the sensors were inserted into the insoles in this study. As a result, the insole materials might possibly affect the measurements results of RH and temperature.

4.4.4 Thermal and Comfort Sensations

In terms of the perceived amount of moisture, the ratings are in agreement with the measurements. The least amount of moisture is perceived with the textile-fabricated insole. Simultaneously, the RH measurement is also the lowest. In contrast, the perceived heat sensation with the textile-fabricated insole is the lowest while the measured foot skin temperature is slightly higher than the other samples, even though the difference is not statistically significant. Note that apart from the skin temperature, there might be some other factors that affect heat sensation, for e.g., friction and moisture level (Zhang et al., 2020).

The textile-fabricated insole which has the best performance in reducing the RH received the highest rating in thermal comfort among the 4 insoles studied. This might be attributed to the high water vapour transmission rate of the spacer fabric. Its 3D structure allows wicking away of heat and moisture from the skin and thus enhancing the perceived wear comfort (Yu et al.,

2016). The result confirms that the RH differences of insoles play a significant role in perceived wear comfort.

4.5 Summary

The findings provide new information for the design of diabetic insole in this study with a particular focus on insole materials. The novel textile-fabricated insole has the best performance in moderating in-shoe RH by reducing the RH by 3.21% at the sole and 24.41% at the heel after 30 mins of walking. No significant difference can be found between the traditional PU, 3D printed TPU, and leather insole in maintaining foot skin humidity. Despite the popularity of custom-made 3D printed insoles, its performance in sweat absorption is less desirable as compared to the textile-fabricated insole. The subjective sensation results confirm the overall thermal comfort of the textile-fabricated insole, even though its performance in reducing foot skin temperature is insignificant. The findings are important reference for insole materials selection for insole design and further confirm the advantages of using textile materials.

Chapter 5 Development of Novel Weft-knitted Spacer Fabric with Foam Inlays for Diabetic Insole Design

5.1 Introduction

Traditional footwear insoles constructed with a structure of multiple cushioning materials, such as PU, EVA, and PE, offer poor breathability and heat retaining properties, which result in a high level of foot discomfort from heat and perspiration. In this study, a novel knitted spacer fabric with inlays is proposed to provide good air and moisture permeabilities with satisfactory compression properties for cushioning. The fabric consists of top and bottom layers with spacer monofilaments between them. Monofilaments connect these two outer layers to form a sandwich structure. With outstanding force reduction, energy absorption, and breathability, spacer fabric can be potentially used for protective or compressive garments. With the ability to transfer heat and moisture, the application of spacer fabrics for shoe insoles has been investigated to improve wear thermal comfort. Weft-knitted spacer fabric with inlays has a novel knitted structure with a cushioning effect. The addition of inlays enhances the durability of knitted spacer fabric with repeated compression. The inlays can also improve the effectiveness of impact force absorption and reduction of insoles.

This chapter explores the possibility of developing a new type of spacer fabric with different parameters by using currently available knitting techniques. The effects of the inlay spacer structure and knitting parameters on the thermal conductivity, evaporative resistance, compression behaviour, and impact force reduction, are analysed.

5.2 Methods

The process of designing the spacer fabric comprised two stages. Stage I aimed to identify a suitable type of yarn for the outer layer of the spacer fabric. Stage II compared different inlaid knitted structures so that the effect of different knitting parameters (inlay and spacer course densities) on the thermal conductivity, evaporative resistance, air permeability, compression stress, and impact force reduction can be systematically investigated.

5.2.1 Stage I – Material Preparation

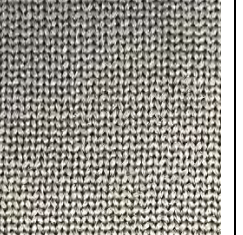
5.2.1.1 Yarn Sourcing for Outer Layer

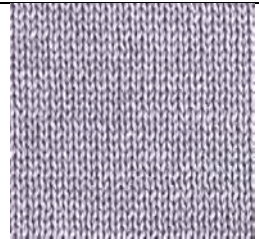
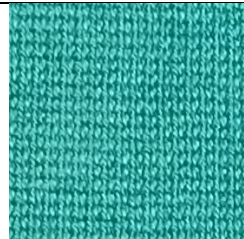
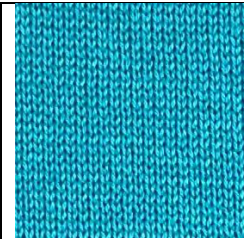
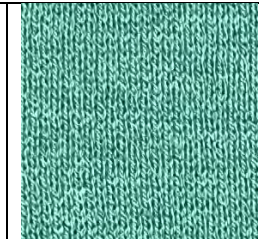
The weft-knitted spacer fabrics to be developed consist of three main components: yarn of the outer layer, spacer monofilament, and the inlaid material. The yarn used in the outer layer have an immense effect on the thermal properties of spacer fabric because it is the material that comes into direct contact with the plantar (or socks). A preliminary material test was conducted for the yarn of the outer layer of the spacer fabric to determine its thermal performance. Eight yarn samples which are said to have a good cooling performance, and can be easily dried or anti-bacterial, were sourced for evaluation. As the yarn linear density is different, they are plied into 2 to 3 ends accordingly to obtain a similar linear density for knitting. The details of yarn count, yarn linear density, and yarn content are provided included in Table 5.1. After preparation, the fabric samples were knitted by using the eight yarn samples on a 14-gauge V bed flat knitting machine (SVR123SP, Shima Seiki, Japan). The fabric samples were knitted into a single jersey structure with the same knitting tension and parameters, see Table 5.2.

Table 5.1 Yarn specifications.

Yarn code	Supplier	Yarn name	Yarn count	Yarn linear density (tex)	Resultant yarn linear density (tex)	Yarn fibre content
1	Meilun	/	300D	33.33	66.67	100% Polyester (High stretch)
2	Sawada	NATU COOL	1/27NM	37.04	74.07	63% Cupro 37% Polyester
3	Xinao	CLEAR	2/48Nm	41.67	83.33	50% Merino wool 50% Antibacterial acrylic
4	Aquafil	Dryarn	140D	15.60	62.40	100% Polypropylene
5	Biella	/	2/48Nm	41.67	83.33	45% Extrafine merino wool 55% Trevira®
6	UPW	Kepler	2/32NM	62.50	62.50	70% TENCEL 30% linen
7	UPW	Piscina	2/48NM	41.67	83.33	55% Cotton 45% Coolmax polyester
8	UPW	Jade	2/28NM	71.43	71.43	60% Cotton 40% Polyester cool jade

Table 5.2 Specifications of the knitted fabric samples.

Sample No.	F1	F2	F3	F4
Fibre Content	100% Polyester (High stretch)	63% Cupro 37% Polyester	50% Merino wool 50% Antibacterial acrylic	100% Polypropylene
Image				
Fabric structure	Single Jersey	Single Jersey	Single Jersey	Single Jersey
Sample No.	F5	F6	F7	F8
Fibre Content	100% Polyester (High stretch)	63% Cupro 37% Polyester	50% Merino wool 50% Antibacterial acrylic	100% Polypropylene

Fabric Image				
Fabric structure	Single Jersey	Single Jersey	Single Jersey	Single Jersey

The air permeability of the samples was measured by using an air permeability tester (KES-F8-AP1, KATO TECH®) for a quick and accurate assessment of the fabric breathability. The tester calculates the air resistance of the fabric (kPa·s/m) by measuring the rate of the air flow through the fabric. Smaller values refer to higher breathability and permeability.

The thermal resistance of the knitted fabric samples with different yarns was also measured in accordance with the ASTM F1868-17 Standard Test Method for Thermal and Evaporative Resistance of Clothing Materials Using a Sweating Hot Plate (Gao et al., 2022). The details of the test are the same as those described in Section 5.2.2.2. In comparing the performance of the samples, yarn (2) (NATU COOL, Sawada®) was determined to be the most suitable yarn for enhancing thermal comfort. The results are shown and elaborated in Chapter 5.3.1.

5.2.1.2 Preparation of Inlay Foam

The insertion of foam rods during the knitting process is technically difficult because of the high friction resistance between the foam surface and the yarn feeder. Also, as the foam rods are elastic, they might cause undesirable tension under high friction resistance. To avoid any issues during the knitting process, a knitting net was used to warp the foam rods (2.25 mm) so that they can smoothly pass through the yarn feeder and laid into the fabric. A multifunction fancy twister (SFM32-04, Kunsan Sun Feng Textile Co., LTD., China) was used to knit the net

with 140D 100% polypropylene yarn (DRYARN®) used to wrap the 2 ends. The warped foam rods were then manually inserted into the fabric.

Table 5.3 Materials of weft-knitted spacer fabrics.

Fabric component	Material
Outer Layer	1/27NM 63% Cupro 37% polyester (2 ends), and 107D high power Spandex (1 ends)
Spacer Monofilament	220D 100% Polyester
Inlay Material	2.25 mm silicon foam rod wrapped with 140D 100% polypropylene yarn (DRYARN®) (2 ends)

5.2.2 Stage II – Knitting and Evaluation

5.2.2.1 Knitting Parameters and Preparation

Four fabric samples with different inlay and spacer course densities were knitted by using a 14-gauge V bed flat knitting machine (SVR123SP, Shima Seiki, Japan) with a yarn feeder tip of 4.5D which would allow the insertion of materials with a diameter of 2 mm. The knitting tension and machine settings are the same for all of the samples. There are in total 6 knitting conditions with different combinations of inlay and spacer course densities. Two samples were fabricated for testing in each knitting condition. The fabric specifications are listed in Table 5.4 and the knitting patterns shown in Table 5.5.

Table 5.4 Specifications of inlaid spacer fabrics.

Fabric code	Knitted structure	Inlay density (course per cm)	Spacer course density (course per cm)
-------------	-------------------	----------------------------------	------------------------------------------

AS1	A	1.20	5
AS2	B	1.20	10
CS1	G	2.30	4
CS2	H	2.30	8
C1	C1	0	13
C2	C2	0	26

Table 5.5 Knitting notations and images of fabrics with different spacer patterns.

	Spacer Pattern AS1	Spacer Pattern AS2
Knitting notation	<p>Diagram for Spacer Pattern AS1 showing knitting notation. It includes a back needle row (1, 3, 5), a front needle row (2, 4, 6), a spacer course (2, 4, 6), and an inlay course (1, 3, 5). The inlay course is highlighted in yellow. Brackets indicate 2 courses for the back and front needle rows, and 4 courses for the spacer and inlay rows.</p>	<p>Diagram for Spacer Pattern AS2 showing knitting notation. It includes a back needle row (1, 2, 3, 4, 5, 6), a front needle row (1, 2, 3, 4, 5, 6), a spacer course (1, 2, 3, 4, 5, 6), and an inlay course (1, 2, 3, 4, 5, 6). The inlay course is highlighted in yellow. Brackets indicate 2 courses for the back and front needle rows, and 4 courses for the spacer and inlay rows.</p>

Table 5.5. (continued).

Spacer Pattern CS1	Spacer Pattern CS2
--------------------	--------------------

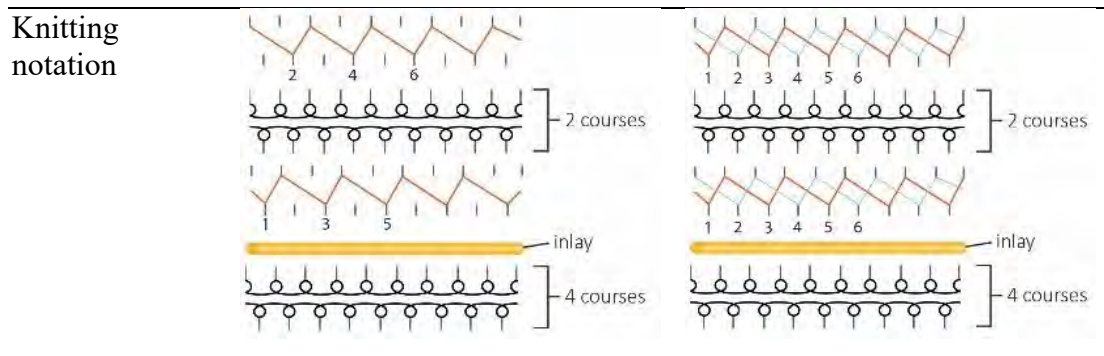
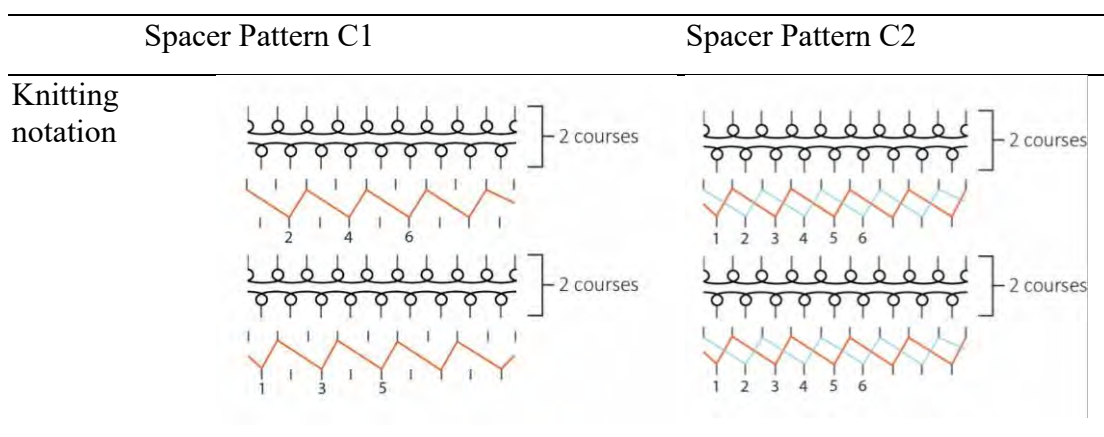


Table 5.5. (continued).



5.2.3 Evaluation of Fabric Thermal Properties

The thermal conductivity and evaporative resistance of the knitted spacer fabric samples were determined in accordance with the ASTM F1868-17 Standard Test Method for Thermal and Evaporative Resistance of Clothing Materials Using a Sweating Hot Plate. A guarded hot plate apparatus (YG(B)606G, China) was used for the testing which consists of an environmental chamber with adjustable temperature, relative humidity and air velocity, and a test plate with adjustable temperature and dampness to simulate human skin.

The thermal resistance ($\text{m}^2 \cdot \text{K}/\text{W}$) was first measured to determine the thermal conductivity (W/mK). A room temperature of 25°C and relative humidity of 65% with 1 m/s air velocity were used. The plate temperature (to simulate human skin) was maintained at 35°C . Before

measurement was carried out, the thermal resistance (R_{cbp}) was determined for reference purposes. Then the total thermal resistance (R_{ct}) was determined when the fabric was placed onto the test plate with the side normally facing the body on the test plate. Any wrinkles and air gaps between the specimen and the test plate were eliminated by smoothing the specimen. The measurements were then recorded when the fabric reached a steady-state condition. The equation to calculate the thermal resistance is as follows:

$$R_{ct} = (T_s - T_a) \times A / H_c \quad (1)$$

where R_{ct} is the total resistance to the dry heat transfer provided by the fabric and air layer ($m^2 \cdot K/W$), T_s is the surface temperature of the plate ($^{\circ}C$), T_a is the air temperature ($^{\circ}C$), A is the area of the tested section of the plate (m^2), and H_c is the power input (W).

Then, the thermal conductivity was calculated by using:

$$K = L / R_{ct} \quad (2)$$

where K is the thermal conductivity per thickness (W/mK). L is the fabric thickness (m), R_{ct} is the total resistance to dry heat transfer provided by the fabric and air layer ($m^2 \cdot K/W$).

To determine the evaporative resistance ($m^2 \cdot Pa/W$), the environmental temperature was controlled at $35^{\circ}C$ which is same as the plate temperature, at a relative humidity of 65% with a 1 m/s air velocity. There was no dry heat exchange between the samples and the test plate. First, water was fed to the surface of the test plate which was covered with a liquid barrier which to prevent the fabric sample from becoming wet. Any air bubbles and air layers inside the water layer or between the liquid barrier and the test plate were eliminated by smoothing the specimen. The evaporative resistance (R_{cbp}) of the bare plate was then measured for reference. This is followed by the measurement of the total evaporative resistance (R_{et}), by placing the sample on the test plate with the side normally facing the body on the test plate. Then, the wrinkles and air gaps between the specimen and the test plate were removed by smoothing the specimen.

Measurements were taken when the sample reached equilibrium. The equation to calculate the evaporative resistance is:

$$R_{et} = (P_s - P_a) \times A / H_E \quad (3)$$

where R_{et} is the evaporative resistance of the fabric system and air layer ($m^2 \cdot Pa / W$), P_s is the water vapour pressure at the plate surface (kPa), P_a is the water vapour pressure in the air (kPa), A is the area of the tested section of the plate (m^2), and H_H is the power input (W).

Apart from the thermal and evaporative resistances, the air permeability ($ml/s/cm^2$) of the samples was also measured under a water pressure difference of 125 Pa. An air permeability tester (SDL M021S, SDL International Textile Testing Solutions, USA) was used for the testing in accordance with the ASTM-D737 Standard Test Method for Air Permeability of Textile Fabrics.

5.2.4 Evaluation of Fabric Mechanical Properties

The performance of the spacer fabric samples with inlays when subjected to compression and impact forces was evaluated to understand their mechanical properties. In doing so, their Young's modulus and ability to withstand high compression forces can be determined. The compression properties of each fabric sample were tested by using the INSTRON 4411 tensile strength tester (Instron®, USA) following ASTM D575 Standard Test Methods for Rubber Properties in Compression. The fabric samples were compressed to 80% of their initial thickness at a controlled speed of 12 mm/min.

In addition, the impact force reduction of the samples (%) was measured with reference to a new approach in Lo et al. (2014) who modified the test in the ASTM D2632 Standard Test Method for Rubber Property - Resilience by Vertical Rebound. The measurement of the impact

force was done by using a dynamic load cell mounted onto a base plate. A fabric sample (or no fabric sample) was placed on top of the load cell. Then, a ball of 64 g in weight was vertically dropped from a height of 40 cm onto the load cell with the guidance of a plunger. The maximum impact force with and without the fabric samples was measured. The force reduction ability of the fabric sample is the percentage of the peak force that can be reduced after placing the fabric sample onto the load cell. The following equation was used to calculate the force reduction ability of the sample:

$$FR_x = (1 - F_x / F_o) \times 100\% \quad (3)$$

where FR_x is the force reduction percentage of the fabric sample (%), F_x is the peak force measured for the insole specimen (N), and F_o the peak force measured for the ground surface (N).

5.3 Results and Discussion

5.3.1 Yarn Selection for Outer Layer

The type of yarn selected for the outer layer was based on the performance of the fabric in terms of its air-permeability (kPa*s/m) and thermal conductivity (W/mK). The air-permeability and thermal resistance of the fabric formed by the different yarn samples were measured and calculated. The results are listed in Table 5.6.

Table 5.6 Thermal test results of fabric samples.

Yarn code	Fabric code	Thickness (mm)	Tightness factor (TF, %)	Air permeability, Resistance (kPa*s/m)	Thermal Conductivity (W/mK)
1	F1	1.52	12.662	0.061	0.077

2	F2	1.26	13.023	0.019	0.091
3	F3	1.44	12.875	0.054	0.034
4	F4	1.39	12.156	0.058	0.061
5	F5	1.39	13.388	0.051	0.041
6	F6	0.83	12.068	0.009	0.032
7	F7	1.31	13.098	0.054	0.046
8	F8	1.10	19.747	0.042	0.039

Figure 5.1 plots the air resistance (kPa.s/m) and thermal conductivity (W/mK) of the fabric Samples. It can be observed that Samples F2 and F6 show high air permeability when compared to the other samples with an air resistance value of 0.019 and 0.009 kPa.s/m respectively. As for the thermal conductivity, Samples F1, F2, and F4 show a significantly higher thermal conductivity (0.077, 0.091, and 0.061 W/mK, respectively) amongst all of the fabric samples. Sample F2 is the only sample that has high air permeability (or low air resistance) and high thermal conductivity. Therefore, Yarn 2, which was used to form Sample F2, was selected for the knitting of the spacer fabric in the next stage.

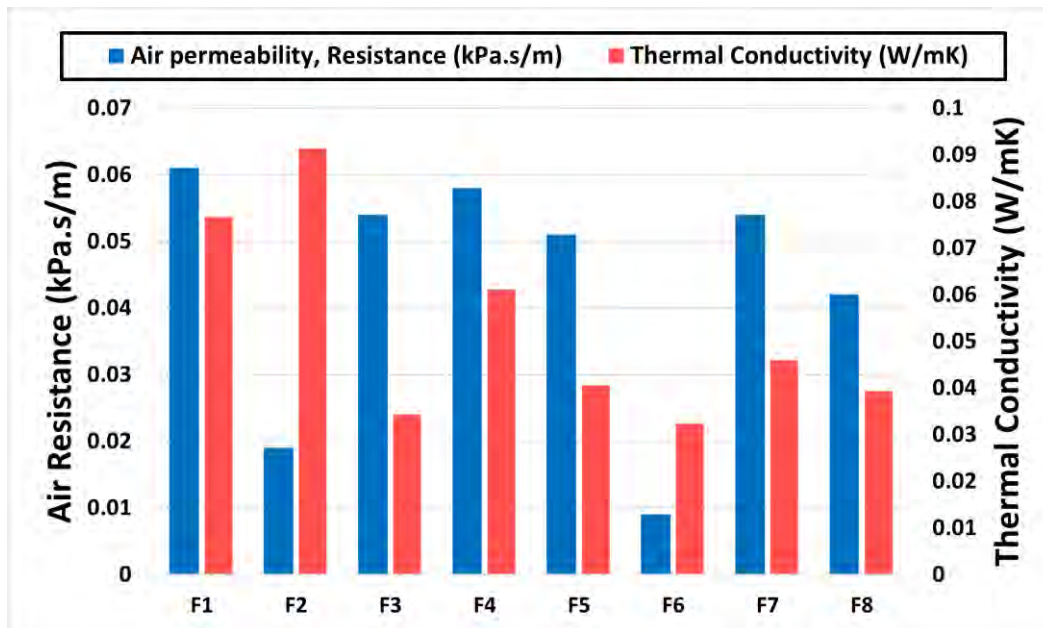


Figure 5. 1 Air resistance (kPa.s/m) and thermal conductivity (W/mK) of fabric samples.

5.3.2 Thermal Properties of Fabric Samples

The thermal properties of the samples are important for insole use because they affect the thermal comfort of the plantar of the foot and even the skin of the feet. Therefore, the sample with optimal thermal properties was selected for the spacer fabric with inlays for diabetic insoles in the later stages of the study.

5.3.2.1 Thermal Conductivity

The thermal conductivity of insole materials have an important role in transferring heat from the plantar of the foot to the footwear and surrounding environment. Depending on the purpose of the footwear, there could be different requirements for the thermal conductivity of the materials. A lower thermal conductivity can maintain warmth but harmful when the temperature of the footwear is increased, for example, during physical activities. When the temperature of the feet is higher than that of the surrounding environment, a higher thermal

conductivity of the footwear and insole materials is more favourable to reduce the foot temperature. In this study, a higher thermal conductivity is preferred to prevent excessive heat of the plantar which is regarded as a risk factor of diabetic foot ulcers.

The thermal conductivity of the spacer fabric samples was measured and is plotted in Figure 5.2. Fabrics AS1 and CS2 have a similar thermal conductivity value of around 0.071 W/mk which are the highest amongst all of the fabric samples. These are followed by Fabrics CS1, AS2, and C1 which have a similar thermal conductivity value of around 0.057 to 0.058 W/mk. Fabric C2 exhibits the lowest thermal conductivity of 0.045 W/mk. The inlay density or spacer course density does not show a dominant effect on the thermal conductivity. This indicates that the thermal conductivity of the spacer fabric tends to be affected by the interactions of multiple parameters such as fibre twist angle of the surface yarn, spacer yarn angle, and fabric thickness, porosity and density (Dehghan et al., 2022). As for use in a diabetic insole, the thermal conductivity of Fabrics AS1 and CS2 are the best options.

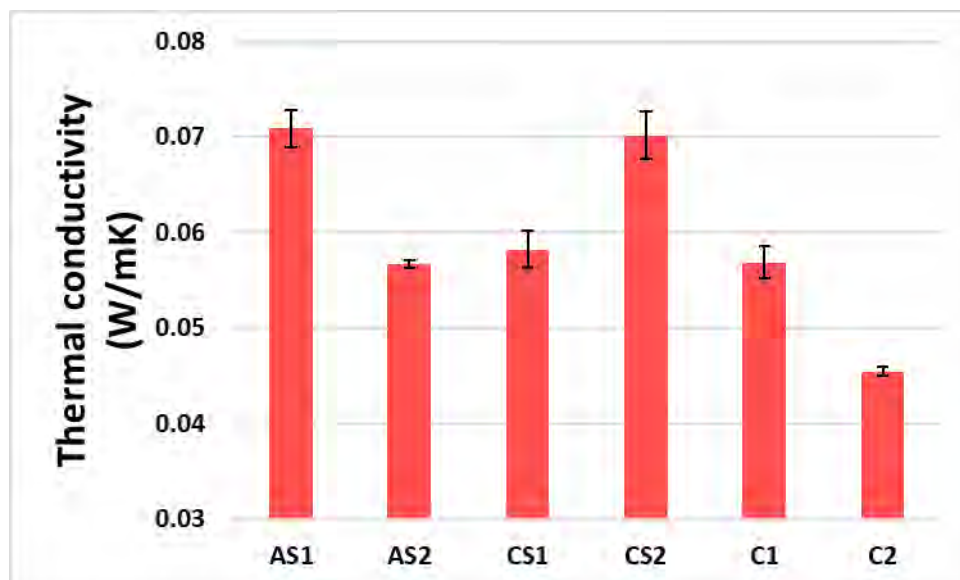


Figure 5. 2 Thermal conductivity (W/mk) of the fabric samples.

5.3.2.2 Evaporative Resistance

The evaporative resistance indicates the ability of a fabric to release moisture created by sweating from the skin through the fabric material to the surrounding environment. Normally, a lower evaporative resistance is preferred for clothing for better thermal comfort. According to Figure 5.3, Fabric CS1 shows a significantly higher evaporative resistance ($17.25 \text{ m}^2\cdot\text{Pa}/\text{W}$) than all of the other fabric samples. Fabric CS2 has the second highest evaporative resistance of $14.85 \text{ m}^2\cdot\text{Pa}/\text{W}$ which is slightly higher than Fabrics AS1, AS2, and C1 (13.85 , 13.90 , and $14.02 \text{ m}^2\cdot\text{Pa}/\text{W}$ respectively). Fabric C1 has the lowest evaporative resistance of $12.84 \text{ m}^2\cdot\text{Pa}/\text{W}$.

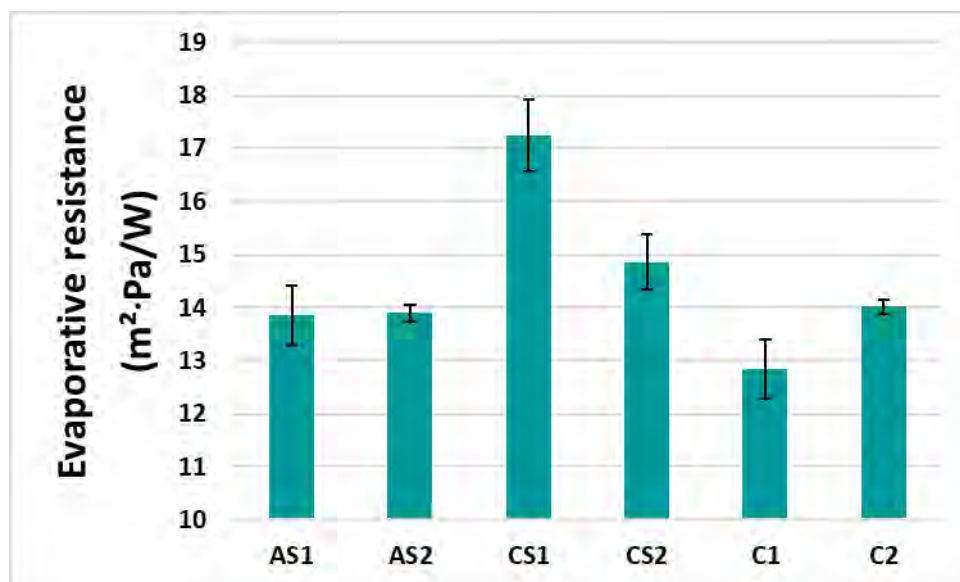


Figure 5.3 Evaporative resistance ($\text{m}^2\cdot\text{Pa}/\text{W}$) of the fabric samples.

The effect of the spacer course density is not obvious on the evaporative resistance of the spacer inlaid fabrics. No significant difference is found between the spacer fabric sample with a lower spacer course density (Fabric AS1) and higher spacer course density (Fabric AS2) with regard to the evaporative resistance.

As for the inlay density, the samples with silicon rod inlays, i.e., Fabrics CS1 and CS2 which have a higher inlay density (2.3 courses per cm) tend to have higher evaporative resistance than the samples with a lower inlay density, i.e., Fabrics AS1 and AS2 (1.2 courses per cm). Thus, increasing the use of inlay materials with an inlay density of 1.2 to 2.3 courses per cm might increase the evaporative resistance. The porosity of the fabric is therefore reduced with increased evaporative resistance which blocks the flow of air and prevents evaporation.

The fabric sample with no inlay, or Fabric C1, has the lowest spacer course and inlay densities which enable the transfer of moisture. However, Fabric C2 with no inlay shows similar results in terms of the evaporative resistance as the fabrics with inlay (i.e., Fabrics AS1 and AS2). Therefore, the spacer course density does not have a dominant effect on the evaporative resistance.

5.3.2.3 Air Permeability

The results of the air permeability tests of the spacer fabric samples are plotted in Figure 5.4. The highest air permeability value of 42.06 ml/s/cm² can be observed with Fabric AS2 followed by Fabrics C2 (38.32 ml/s/cm²) and CS2 (35.96 ml/s/cm²). These are the samples with a higher spacer course density. On the other hand, the samples with a lower spacer course density (Fabrics AS1, CS1, and C1) show lower air permeability values (19.55, 26.61, and 12.80 ml/s/cm²). This reveals that, with the same density of inlay materials (inlay density), the fabric with a higher density of spacer monofilaments (spacer course density) tends to have significantly higher air permeability.

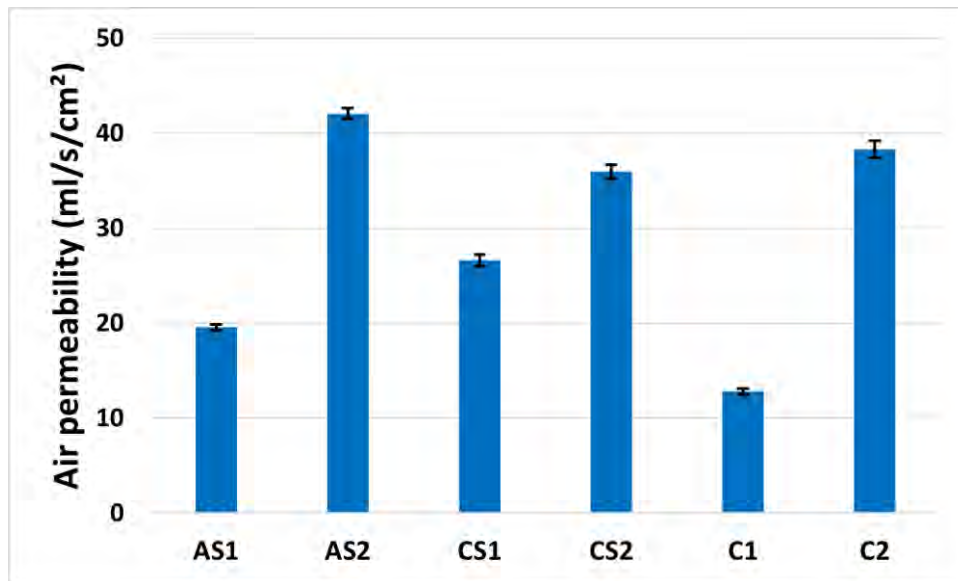


Figure 5.4 Air permeability (ml/s/cm²) of spacer fabric samples.

With reference to Table 5.7, the fabric samples with a higher density of spacer monofilaments and the same density of inlay materials have a lower weight (g/m²), are slightly thicker (mm), and have a lower stitch density (loop/cm²). The higher density of monofilaments increases the space between the two surface layers of the spacer fabric. Thus, allows the free flow of air through the fabric. Indeed, the role of the spacer monofilaments is to keep the upper and bottom layers of the spacer fabric structure apart and create space between them (Hamedi et al., 2020). When there are more spacer monofilament courses between the outer layers of the fabric, there is increased space in the fabric compared with fabric that has fewer spacer monofilament courses. Thus, the fabric can be thicker with increased porosity. Therefore, increasing the amount of inserted spacer monofilaments in a knitted structure helps to reduce the fabric density and increases the air permeability of the fabric.

5.3.3 Mechanical Properties of Fabric Samples

The physical properties of the spacer fabric samples were determined for reference purposes (Table 5.7).

Table 5.7 Physical properties of the inlaid spacer fabric samples.

Fabric Code	Weight (g/m ²)		Thickness (mm)		Stitch density (loop/ cm ²)		Hardness (Shore A)	
	Mean	SD	Mean	SD	Mean	SD	Mean	SD
AS1	1483.32	6.12	4.30	0.03	93.33	4.04	83.17	1.33
AS2	1417.25	0.46	4.31	0.03	91.00	0.00	86.17	1.72
CS1	1759.97	17.31	4.35	0.04	88.83	3.75	88.67	1.21
CS2	1689.88	17.47	4.39	0.03	86.33	4.04	88.83	0.41
C1	1094.38	5.65	3.51	0.05	108.00	4.00	88.67	1.37
C2	1068.20	16.54	3.75	0.14	106.67	4.62	89.00	0.63

5.3.3.1 Compression Deformation

The maximum compressive stress of the spacer fabric samples when compressed to 80% of their initial thickness is plotted in Figure 5.5. Fabrics CS2 and CS1 show significantly higher compressive stress than the other fabric samples (367.25 and 323.43 kPa, respectively). Lower compressive stress can be observed for Fabrics C1 and C2 (48.83 and 95.37 kPa, respectively).

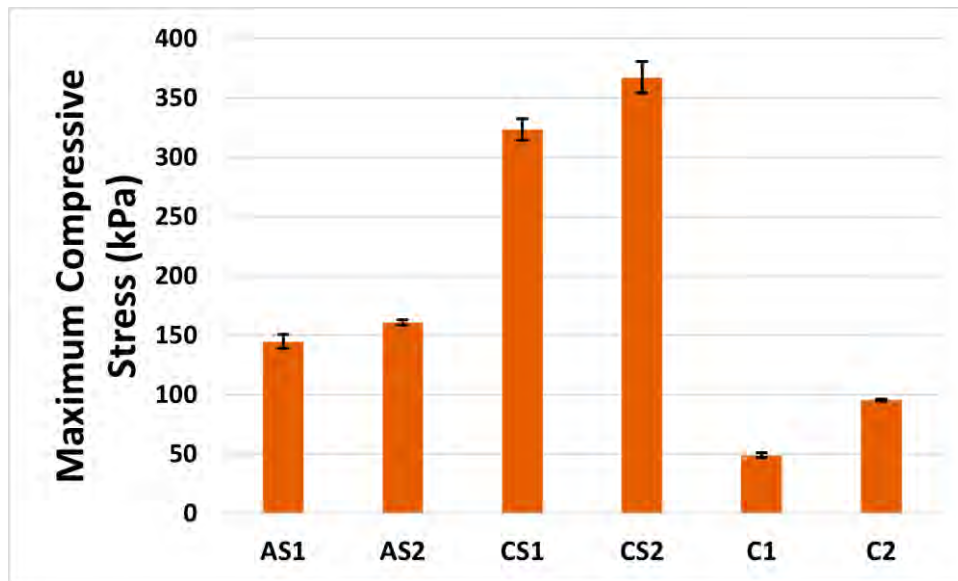


Figure 5.5 Maximum compressive stress (kPa) of spacer fabric samples.

By examining the inlay density of the spacer fabric samples, the samples with a higher inlay density (Fabrics CS1 and CS2) show a higher maximum compressive stress than those with a lower inlay density (Fabrics AS1 and AS2) regardless of their spacer course density. Also, the fabric with no inlay, i.e., Fabrics C1 and C2, exhibit the lowest maximum compressive stress. This confirms that the inlaid silicon rods have a dominant effect against compression load which is in agreement with the findings in Yu et al. (2020b) and Li et al. (2022) in that the inlaid materials enhance the compression resistance of the spacer fabrics. Thus, a higher inlay density means a higher maximum compressive stress. Apart from the inlay density, it can be observed that with the same inlay density, the maximum compressive stress (kPa) increases with spacer course density (course per cm) (see Figure 5.6). This result is also in agreement with that in Zhao et al. (2018) who found that spacer fabrics with a high density of monofilament show higher compression resistance.

5.3.3.2 Force Reduction

The force reduction ability of insole materials helps to reduce the plantar pressure during gait and protect the foot from unexpected shocks (Lo et al., 2014). Therefore, the sample with a higher percentage of force reduction might be considered to be more suitable for insole use. The force reduction (%) of the fabric samples ranged from 56.68 to 70.07% (Figure 5.6). Fabrics CS1 and CS2 have the highest force reduction (69.44 and 70.07 %) amongst the six fabric samples. The force reduction performance of Fabrics AS1 and AS2 is slightly lower than CS1 and CS2 (67.06 and 67.32%). Fabrics C1 and C2 have the lowest force reduction ability of 56.68 and 59.38% respectively.

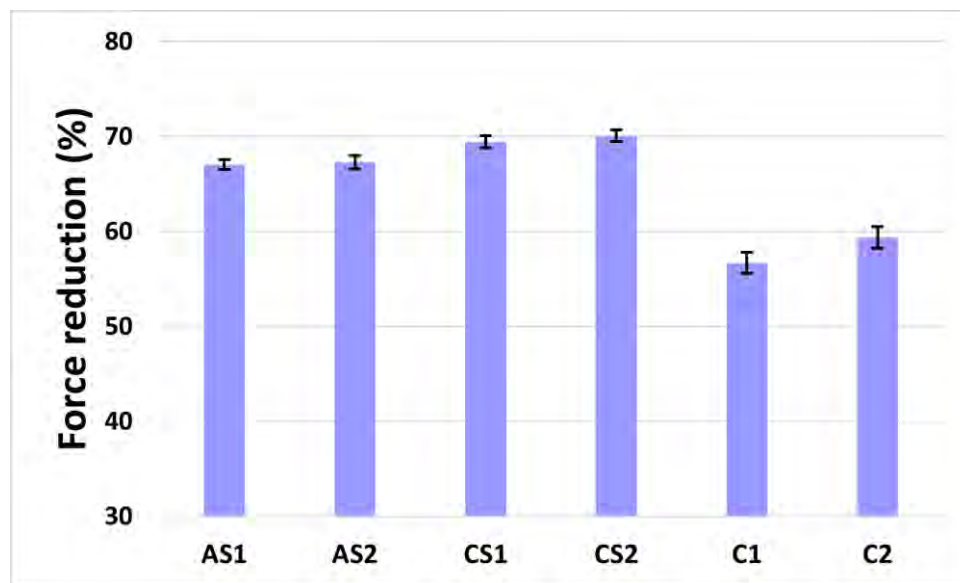


Figure 5. 6 Force reduction (%) of spacer fabric samples.

In line with the results of compression deformation, the fabrics with a higher inlay density showed a higher force reduction while the fabric with no inlay material the lowest. The difference is that the effect of the inlay density of the fabric on force reduction is smaller than that on the maximum compression stress. In contrast, whether the spacer fabric has inlaid

silicon rods is a dominant parameter that affects its force reduction ability. This explains why the fabrics inlaid with silicon rods (Fabrics AS1, AS2, CS1, and CS2) can significantly reduce a greater degree of impact force (percentage) as opposed to those without inlay (Fabrics C1 and C2). Also, the samples with the same inlay density but different spacer course density were compared (i.e., Fabrics AS1 and AS2; CS1 and CS2; and C1 and C2). It was observed that the sample with a higher spacer course density slightly reduces more of the impact forces. This shows that regardless of the inlay density, spacer course density contributes to the performance of the fabric in terms of force reduction. As indicated by Zhao et al. (2018), spacer fabrics with a high monofilament density can better absorb energy.

5.3.4 Fabric Selection for Diabetic Insole Design

The performances of the spacer fabric samples in terms of their evaporative resistance, thermal conductivity, air permeability, compressive stress, and force reduction were subsequently compared. A score of 1 to 5 was given for the performance of each fabric sample (Table 5.8). The overall performance of the six spacer fabric samples is illustrated in Figure 5.7. According to Figure 5.8, Fabric CS2 has the highest performance score for thermal conductivity, compressive stress, and force reduction, and the second highest performance for air permeability. Although its evaporative resistance performance is not the best, Fabric CS2 still has the overall best performance in comparison to the other fabric samples. Thus, Fabric CS2 is considered as the most suitable material amongst all of the spacer fabric samples studied.

Table 5.8 Performance score of fabric samples.

Fabric Code	Thermal conductivity (W/mK)	Score	Evaporative resistance (m ² ·Pa/W)	Score	Air permeability (ml/s/cm ²)	Score	Compressive Stress (kPa)	Score	Force reduction (%)	Score
AS1	0.071	5	13.85	4	19.55	2	144.77	2	67.06	3
AS2	0.057	3	13.90	4	42.06	5	160.71	2	67.32	3

CS1	0.058	3	17.25	1	26.61	3	323.43	4	69.44	4
CS2	0.070	5	14.85	3	35.96	4	367.25	5	70.07	5
C1	0.057	3	12.83	5	12.80	1	48.83	1	56.69	1
C2	0.045	2	14.02	4	38.32	4	95.37	1	59.38	2

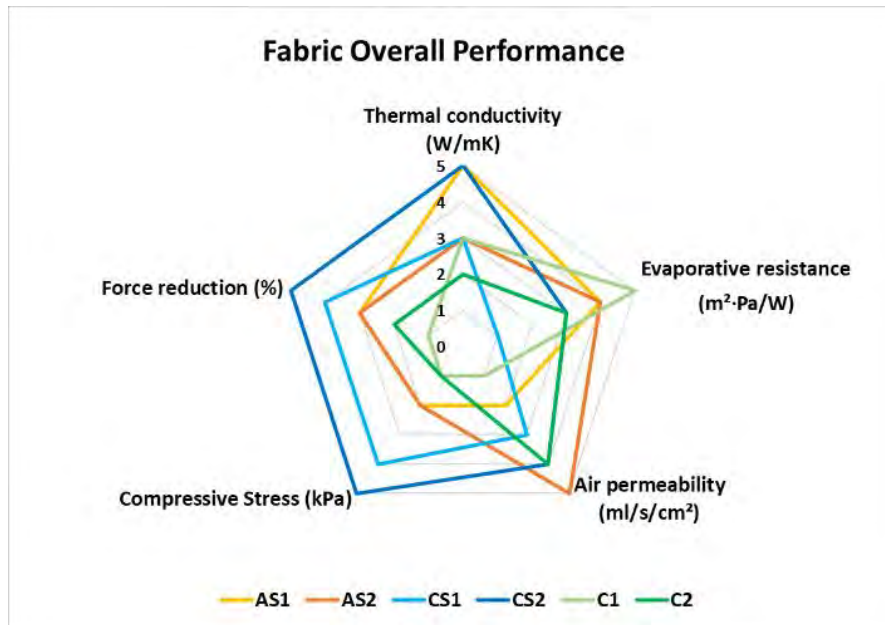


Figure 5.7 Overall performance of spacer fabric samples.

5.4 Summary

In this chapter, spacer fabric samples with different inlay and spacer course densities are designed and evaluated regarding their thermal conductivity, evaporative resistance, compression behaviour, and impact force reduction. Prior to the knitting process, eight types of yarns are examined, and the yarn that consists of 63% Cupro and 37% polyester (i.e., NATU COOL, Sawada®) exhibits the highest thermal conductivity, and the second lowest air resistance, and is subsequently selected for use as the outer layers of the insole.

This study provides useful information on the structural design of spacer fabric for applications of cushioning wearables. It is found that an increase in the inlay density and/or spacer density can increase force reduction and the maximum compressive stress of the fabric. However, for

insole applications, thermal properties should also be considered to facilitate a dry and comfortable in-shoe environment. In terms of the thermal properties of the spacer fabric, the same inlay density and higher density of spacer monofilaments increase the free flow of air. Also, the same spacer course density and higher inlay density result in higher evaporative resistance. Thus, to determine the knitting parameters of the weft-knitted spacer fabric with inlays for insole applications, a balance between the thermal properties and mechanical properties should be considered.

As for the diabetic insole design and development, Fabric CS2 shows the most satisfactory overall performance among all of the samples with superior performance in most of the tests. Fabric CS2 shows the best overall performance in thermal conductivity (0.071 W/mk), maximum compressive stress (323.43 kPa), force reduction (70.07%,) and air permeability (35.96 ml/s/cm²). This fabric is therefore applied as the first layer of the diabetic insole design in a later stage of the project to provide good support and improve the thermal comfort.

Chapter 6 Design and Development of Insole with Novel Weft-knitted Spacer Fabric and 3D Printed Arch and Heel Pad

6.1 Introduction

An insole fabricated with a novel weft-knitted spacer fabric and 3D printed arch and heel pad is developed to improve the thermal comfort of insoles along with optimal plantar pressure distribution to reduce the likelihood of foot ulcers. Unlike traditional diabetic insoles where the focus is only on the mechanical properties of the insole materials, the thermal properties will also be considered in this study. Chapter 5 outlines the development of a novel spacer knitted fabric used for the upper layer of an orthotic insole with enhanced thermal properties in comparison to traditional insole materials. To effectively redistribute the plantar pressure to the low pressure foot regions, a 3D-printed half insole with 3D arch support and a heel pad design with a novel auxetic structure is proposed as the bottom supportive layer to enhance fit, reduce the impact force, and allow moisture permeability.

In this chapter, auxetic 3D printed materials with a porous structure that uses different soft materials are explored for the heel pad which would best absorb the impact forces to the heel. Insole prototypes are made by using 3D spacer knitting techniques and 3D printing technologies which would improve the in-shoe environment, plantar pressure distribution, and wear comfort. The offloading performance of the proposed insole design will be evaluated by using the Pedar X system.

6.2 Methods

In this study, the half insole is first designed and developed by using 3D printing technology. The insole prototypes are then laminated with a layer of weft-knitted spacer fabric. A laboratory wear trial is subsequently conducted to determine the offloading performance of the prototypes. Subjective perception towards the proposed new insole design is also collected.

6.2.1 Stage I – Development of Auxetic Heel Pad

In Stage I of the study, the effect of different 3D printing parameters on the mechanical properties of 3D printed materials with an auxetic structure was investigated. The mechanical properties that were evaluated included force absorption, hysteresis energy loss during compression, water vapour transmission, and moisture regain. The evaluation was done to identify suitable materials for the auxetic structure of the 3D printed insole to be used as a heel pad for force reduction.

6.2.1.1 Materials and Structure

A total of eight 3D printed components with different 3D structures (auxetic and non-auxetic) were fabricated by using four different types of soft materials. To select the most suitable material for the 3D printed heel pad, the same 3D auxetic re-entrant structure was printed by using four different soft materials at the same scale. Also, 3D auxetic and non-auxetic structural models with the same volume were printed with two types of beam thicknesses (and total thickness) and the same materials for comparison purposes.

To better understand the performance of the 3D printed components on the insole, 3 commercially available insole materials, including double-layered EVA foam (Inocep®) from

a diabetic insole available on the market, EVA foam (nora® Lunalastik), and PU (Poron®) were sourced for comparison purposes. The material specifications and the specimens are listed and shown in Table 6.1 and Figure 6.1, respectively. The effect of the materials, beam size, and whether structure on the mechanical properties of the 3D re-entrant structural component was investigated.

Table 6.1 Material specifications.

Sample	Material	3D Printing Method	Auxetic or Non-auxetic	Beam Size (mm)	Density (g/cm³)	Thickness (mm)
A	Resin (Flexible 80A)	SLA	Auxetic	1.3	0.206	8.86
B	Resin (Elastic 50A)	SLA	Auxetic	1.3	0.227	8.6
C	TPU (Flexa Bright)	SLS	Auxetic	1.3	0.125	8.96
D	TPU (FS 1092A)	SLS	Auxetic	1.3	0.178	9.52
E	TPU (FS 1092A)	SLS	Non-auxetic	1.4	0.152	8.76
F	TPU (FS 1092A)	SLS	Auxetic	2	0.301	10.02
G	TPU (FS 1092A)	SLS	Non-auxetic	2.2	0.295	10.22
H	Double-layered EVA foam (commercially available diabetic insole - Inocep®)	/	/	/	0.127	8.56
I	EVA foam (nora® Lunalastik)	/	/	/	0.189	9.36
J	PU (Poron®)	/	/	/	0.532	9.42

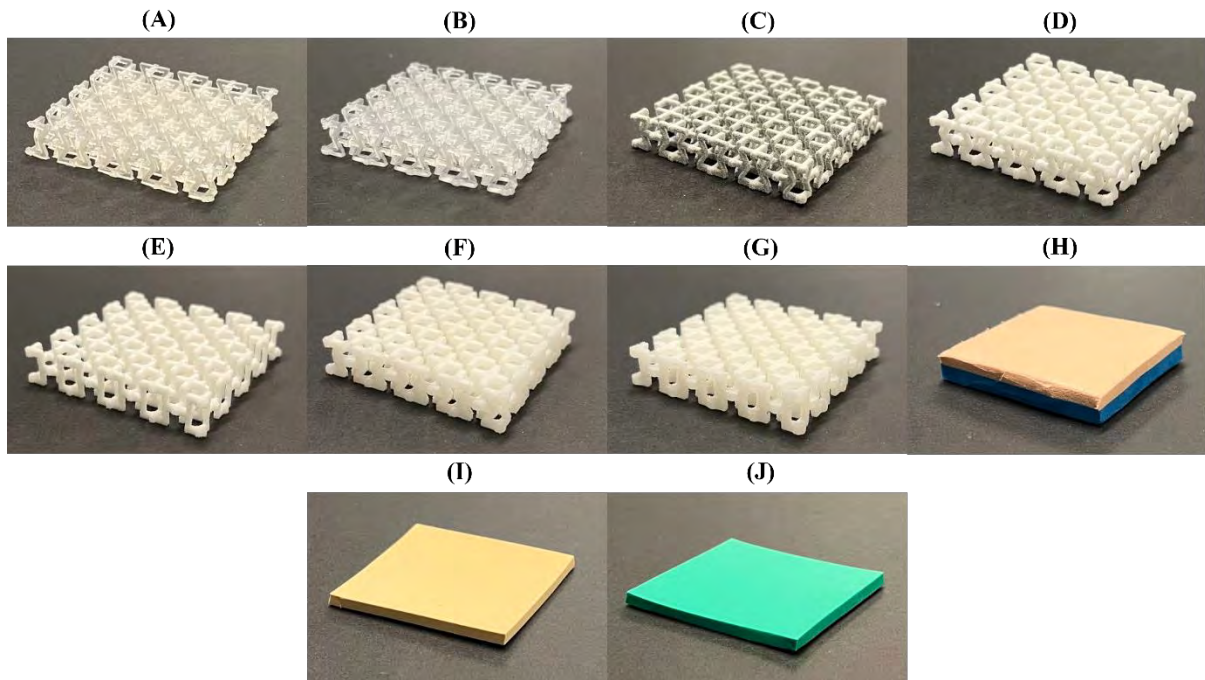


Figure 6. 1 3D view of material samples: (A) Resin (Flexible 80A), (B) Resin (Elastic 50A), (C) TPU (Flexa Bright), (D) TPU (FS 1092A), (E) TPU (FS 1092A) (Non-auxetic), (F) TPU (FS 1092A) (large beam size), (G) TPU (FS 1092A) (Non-auxetic) (large beam size), (H) Double-layered EVA foam (Inocep®), (I) EVA foam (nora® Lunalastik), and (J) PU (Poron®).

6.2.1.2 Force Absorption Test

As discussed in Section 5.2.4.1, a force absorption test was conducted in accordance with the method in Lo et al. (2014) in which the test in ASTM D2632 Standard Test Method for Rubber Property - Resilience by Vertical Rebound was modified. The force reduction (%) of the tested 3D printed materials was calculated as follows:

$$FR_x = (1 - F_x / F_o) \times 100\% \quad (1)$$

where FR_x is the force reduction percentage of the fabric samples (%), F_x is the peak force measured for the specimen (N), and F_o the peak force measured for the ground surface (N).

6.2.1.3 Compression Test - hysteresis energy loss

Hysteresis loss is measured in accordance with ASTM D3574 X6 Foam Hysteresis Energy Loss Testing which is defined as the difference between the loading and unloading energies expressed as a percentage of the loading energy. The hysteresis energy loss shows the deformation properties of a material during unloading after axial compression with a certain amount of compression force. The hysteresis energy loss of the insole materials shows their tendency to impart a reaction force onto the plantar of the foot between mid-stance and toe-off during the gait cycle. The specimens were compressed under a load of 800 N (around 81 kg) and the energy lost during unloading was calculated by using:

$$\text{Hysteresis Loss (\%)} = [(\text{loading energy} - \text{unloading energy}) \times 100] / \text{loading energy} \quad (2)$$

6.2.1.4 Water Vapour Permeability

The water vapour permeability of the materials was tested by following the international standard ASTM E96 Standard Test Method for Water Vapour Transmission of Materials (Upright cup method). This method is used to determine the ability of the materials to transfer water vapor. The specimens were covered on the mouth of the cup (90 mm in diameter) filled with 20 g of distilled water. They were then placed in a conditioning room for 24 hours at a temperature of $21 \pm 2^\circ\text{C}$ and relative humidity of $65 \pm 5\%$. The weight loss of the water was then measured, and the water vapour permeability was calculated by using:

$$\text{WVP} = (24 \times M) / At \quad (3)$$

where WVP is the water vapour permeability of the specimen ($\text{g}/\text{m}^2/\text{day}$), M is the difference in weight of the cup with the specimen after 24 hours (g), A is the tested area of the specimen (0.0054 m^2), and t is the duration of the testing (hours).

6.2.1.5 Moisture Regain

Moisture regain (R) is defined as the amount of water in mass that can be absorbed by a drying material at a specified equilibrium condition of temperature and humidity over the mass of the drying material. The test specimens were dried in an oven at a temperature of 105°C for 2 hours so that the moisture content of the materials could be entirely evaporated. The mass of the test specimens was measured right after drying in the oven. The materials were then placed in a conditioning room at a standard temperature of 21 ± 2°C and relative humidity of 65 ± 5% for 24 hours to reach equilibrium moisture content. The mass of the test specimens was then measured again. The moisture regain of the specimens was then calculated by using:

$$R = 100 \times (B - D) / D \quad (4)$$

where R is the moisture regain of the specimen (%), B is the specimen mass with resorbed moisture at moisture equilibrium (g), and D is the mass of the dried specimen (g).

6.2.1.6 Wear Trial

Two materials with good performance in the material testing were selected for further comparison with 2 commercially available insole materials to investigate their offloading performance.

Traditional EVA insoles (nora® Lunalastik) (material sample I) of 9 mm in thickness were prepared where the heel pads with different material structures are inserted as shown in Figure 6.2(a). The thickness is nearly the same as that of the 4 heel pad specimens. A pair of sports shoes was then prepared, and the original insole was removed to insert the samples during the experiment. For each participant, the heel pad sample was inserted into the shoe of their dominant foot. For the other foot, the same material was inserted. The plantar pressure of the dominant foot was subsequently evaluated and compared.

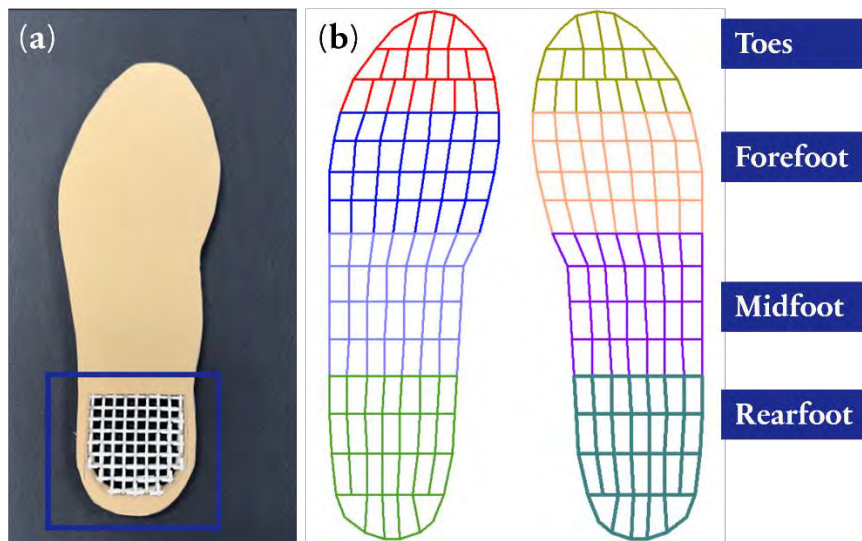


Figure 6. 2 (a) Insertion method of specimens onto EVA insole, and (b) the 4 regions for comparison of MPP.

A total of 8 female participants (age: 24 ± 2 years old; height: 161.8 ± 7.8 cm, and weight: 56 ± 9 kg) with a shoe size of EU 38-39 were invited to take part in the study. Each participant was supposed to wear sports shoes along with the 4 heel pads inserted onto the EVA insole during the experiment. The experiment included plantar pressure measurement during standing and walking on the Pedar®-x system which is a pressure system to obtain the plantar pressure distribution. The participants were instructed to put on the shoes after inserting the pressure sensor into the mesh shoes on top of the insoles with the heel pad specimen. To measure the plantar pressure during standing, the participants were to stand straight and drop their arms to their side, and look to the front with their feet separated at a shoulder's width for 20 s. In terms of walking, the participants were instructed to walk 10 times on a walkway of 8 m in length at a self-selected speed to measure their mean walking speed (Shi et al., 2022). They were then required to walk 3 times on the walkway while wearing each heel pad specimen at a speed of $\pm 10\%$ of the mean of their self-selected walking speed to minimise the effect of speed variation on the plantar pressure.

The measurement of the plantar peak pressure was divided into four regions of the foot: the toes, forefoot, midfoot, and rearfoot. The calculation of the mean peak pressure (MPP) of the plantar was also divided into four regions: the toes, forefoot, midfoot, and rearfoot (Mazur et al., 2019; Shi et al., 2022), see Figure 6.2(b). The plantar pressure in the rearfoot is the main focus and used for a performance comparison of the pressure reduction. The pressure on the toes, forefoot, and midfoot are also considered to act as a reference for comparison purposes. For standing, the MPP during the 30s of standing on each plantar region is calculated and evaluated. For walking, the MPP of each plantar region during the walking cycles is calculated and evaluated.

6.2.2 Stage II – Insole Prototyping and Pilot Trial

An insole prototype made of 3D spacer knitting techniques and 3D printing technologies in auxetic structure was proposed. A preliminary wear trial was conducted to observe possible trends in the performance differences between the proposed insole and the commercial diabetic insole. If the off-loading performance of the proposed insole is not satisfactory, further modifications may be necessary.

6.2.2.1 Development of 3D printed half-insole

A half-insole that consists of a heel pad and arch pad was designed for application as the bottom layer of the diabetic insole. The role of this half-insole is to provide a suitable insole geometry to enhance the insole fit and offer a cushioning effect for the heel.

The 3D model of the half-insole was developed by using AutoCAD 3D modelling software (Autodesk®). Figure 6.3(a) shows the top, Figure 6.3(b) the medial side, Figure 6.3(c) the front, and Figure 6.3(d) a 3D view of the 3D half-insole model. The 3D printed materials with the

most satisfactory performance during the wear trial of Stage I were identified and applied to the heel region of the insole as the heel pad. With reference to a commercially available diabetic insole, an arch pad (with a height of 1.86 mm) was added which is an important approach for plantar pressure redistribution (Bus et al., 2004; Cavanagh & Bus, 2011). A porous structure was utilized to enhance the permeability of air and moisture.

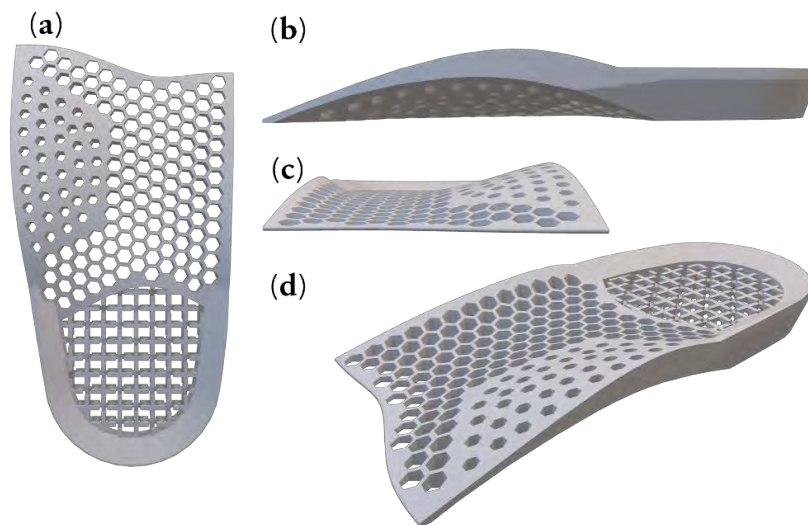


Figure 6.3 (a) Top, (b) medial side, (c) front, and (d) 3D view of the 3D half-insole model.

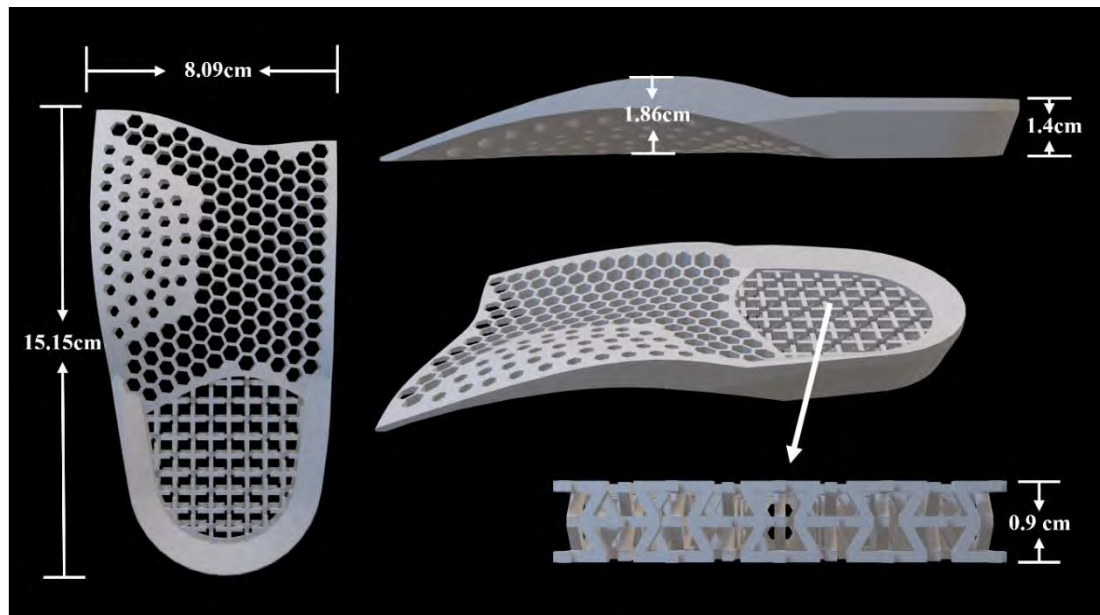


Figure 6. 4 Scale of the 3D model of the half-insole for foot size 38-40.

6.2.2.2 Development of Diabetic Insole Prototype

The diabetic insole prototype was developed by combining the novel spacer weft-knitted fabric with inlays as discussed in Chapter 5 and the 3D printed half-insole. The spacer fabric is the first layer of the insole. The fabric has outstanding thermal properties to maintain a suitable foot skin and in-shoe environment. Also, a layer of PU was added under the layer of spacer fabric to enhance the stability and resist deformation. The PU layer covered the entire forefoot and the top of the arch pad of the 3D-printed half-insole (Figure 6.5(a)). An MTH pad fabricated from PU was also included because (Yi et al., 2022) indicated that this can reduce the plantar pressure on the metatarsal area. Indeed, as the heel pad of the 3D printed half-insole (9 mm) is much thicker than the spacer fabric (4.39 mm), an increase in thickness of the insole forefoot is reasonable to ensure balance during gait.

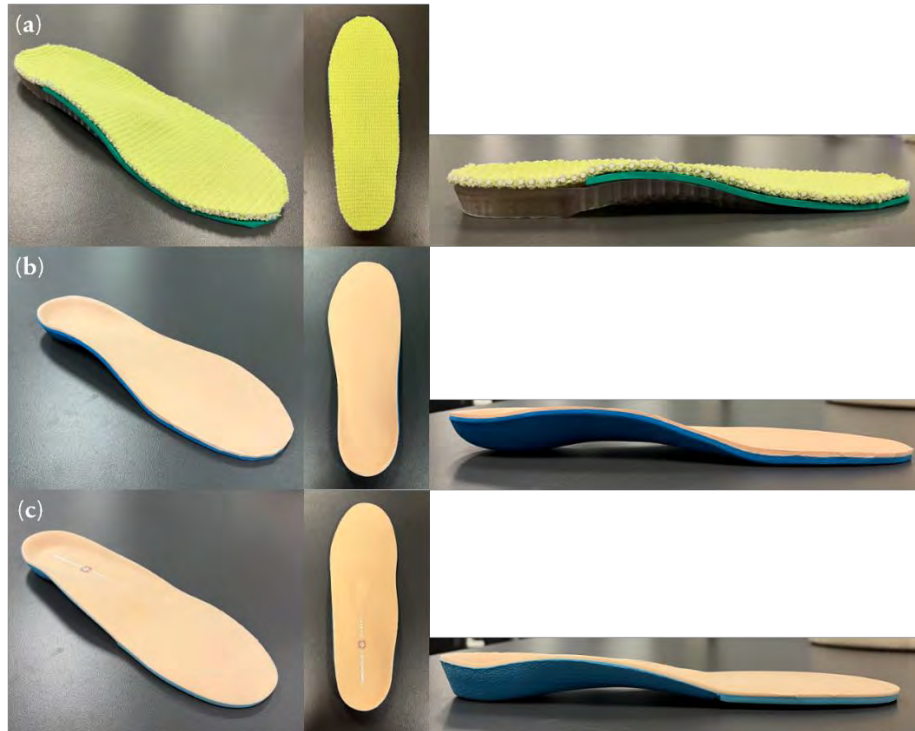


Figure 6. 5 The 3D, top, and medial side views of (a) 3D knitted and printed insole prototype (Insole X), and (b) commercially available diabetic insole with a heel cup and arch pad (Insole Y), and (c) commercially available diabetic insole (Insole Z) with a heel cup, arch pad, and MTH pad.

6.2.2.3 Wear Trial

Two different brands of commercially available diabetic insole samples were sourced from the market which have different design features for comparison purposes. The proposed orthosis insole prototype was labelled Insole X. The commercially available diabetic insoles included: Insole Y (Inocep®) and Insole Z (SpencoMedics®), see Figures 6.5(b) and 6.5(c). The material specifications of the insole samples are listed in Table 6.2. During the wear trial, the insole sample was inserted into a pair of sport shoes which was also used in Stage I to record the plantar pressure during standing and walking.

Table 6.2 Material specifications of insole samples.

Sample	Material			MTH	Arch	Heel	Heel
	1 st Layer	2 nd Layer	3 rd Layer	Pad	Pad	Cup	Pad
Insole X	spacer fabric with silicon rod inlaid	PU (Poron®): forefoot and arch	3D-printed half insole	✓	✓ (2 mm)	✓ (5 mm)	✓
Insole Y	EVA	EVA	✗	✗	✓ (2.3 mm)	✓ (~10 mm)	✗
Insole Z	PE (Plastazote®)	PVC	PU: forefoot and heel	✓	✓ (2 mm)	✓ (~13 mm)	✓

The same female participants who took part in the wear trial in Stage I also participated in this wear trial. The experimental process is the same as that in Stage I, but the insole samples are different. For more details on the experimental protocols, refer to *Section 6.2.1.6*. The participants were required to score the perceived wear comfort for five regions of the foot after wearing each insole, including the toes, forefoot, medial and lateral midfoot, and rearfoot (Figure 6.6). The perceived wear comfort scale in Figure 6.7 is used in the wear trial.

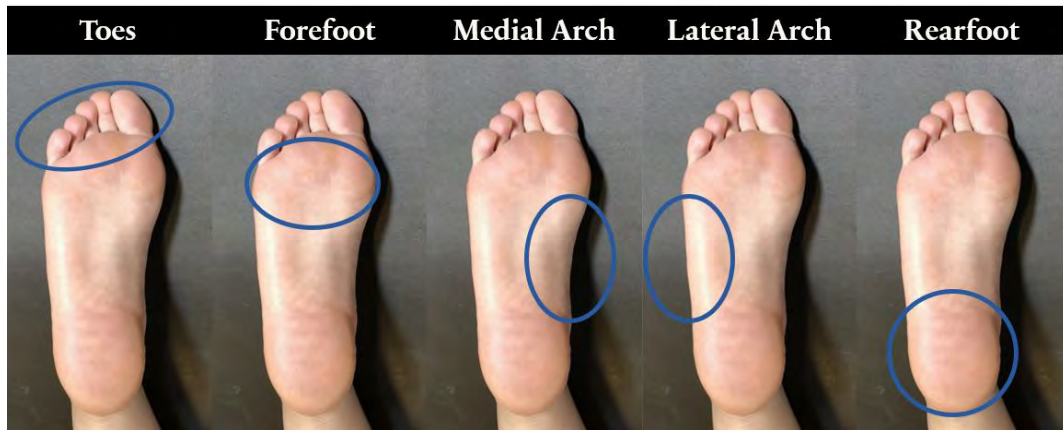


Figure 6. 6 The foot region for comfort perception.

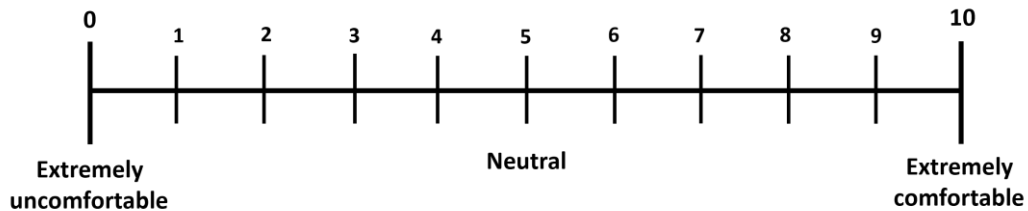


Figure 6. 7 Perceived scale of wear comfort.

6.2.2.4 Statistical Analysis

The statistical analysis was processed by using the Statistical Package for the Social Sciences program (SPSS®21, IBM® Corporation, New York, USA). The Friedman test was conducted to identify any statistically significant differences among all the MPP conditions in 4 different foot regions during standing and standing. A post hoc test - Wilcoxon signed-rank test, was also adopted to investigate the statistically significant differences between each pair of conditions.

6.2.3 Stage III – Evaluation of Insole Prototype

The plantar off-loading effect of the insole prototype on diabetic patients during walking has been verified by wear trials with elderly diabetic patients.

6.2.3.1 Wear Trial

A total of 23 elderly diabetic patients (21 females and 2 males with age: 66.3 ± 5.9 years old; height: 157.5 ± 4.3 cm, and weight: 58.5 ± 5.2 kg) with a shoe size of EU 38-39 were invited to take part in the wear trial. The inclusion criteria were as follows: (a) age between 50 and 70 years old, (b) a diagnosis of diabetes (Type 1 or 2), (c) no balance impairment (static and dynamic balance abilities were assessed using the Berg Balance Scale⁴⁰ by a therapist), (d) no high risk of falls, (e) the ability to walk along a 10-meter walkway at least five times without assistance, and (f) no current or previous history of foot ulcers.

The experimental process adopted in Stage II above has been repeated. A commercially available diabetic insole (Insole Y) (Figure 6.5b) used in Stage II was compared with the proposed insole prototype (Insole X). Their plantar MPP and the percentage reduction of plantar MPP during walking were compared with no insole condition. The changes in contact area with the plantar were also analysed. The reduction of mean peak pressure and change of contact area using the insole conditions were calculated by using Equations (1) and (2) below:

$$RMPP = MPP_i - MPP_N \quad (1)$$

where RMPP is the reduction of MPP (%), MPP_i is the mean peak pressure using the insole condition, and MPP_N is the mean peak pressure without the insole.

$$\Delta CoA = CoA_i - CoA_N \quad (2)$$

where ΔCoA is the change in the contact area between insole and plantar (%), CoA_i is the contact area using the insole condition, and CoA_N is the contact area without the insole.

Participants were invited to assess the perceived wear comfort of the foot at five regions (Figure 6.6) under different insole conditions by using the scale in Figure 6.7.

6.2.3.2 Statistical Analysis

The statistical analysis was processed by using the Statistical Package for the Social Sciences program (SPSS®21, IBM® Corporation, New York, USA). The repeated-measures analysis of variance (ANOVA) was conducted to evaluate the effect of the insole conditions for each measurement point in terms of the actual value and reduction of plantar MPP, actual value, and change of contact area with plantar.

6.3 Results and Discussion

6.3.1 Stage I – Development of Auxetic Heel Pad

The mechanical and thermal properties of the 3D printed materials and commercially available insole materials are compared in Stage I of this study, including the force absorption, compression properties (hysteresis energy loss), water vapour permeability (WVP), moisture regain and offloading performance. The effect of the auxetic properties and printing materials on the properties of the 3D printed materials is discussed in the following sections.

6.3.1.1 Force Absorption Test

The force reduction performance was measured first, and the results are plotted in Figure 6.8. Sample B offers the highest reduction of force (86.90%) followed by Samples D (86.65%) and E (84.33%) which can all absorb more force than any of the commercially available insole materials (i.e., Samples H, I, and J).

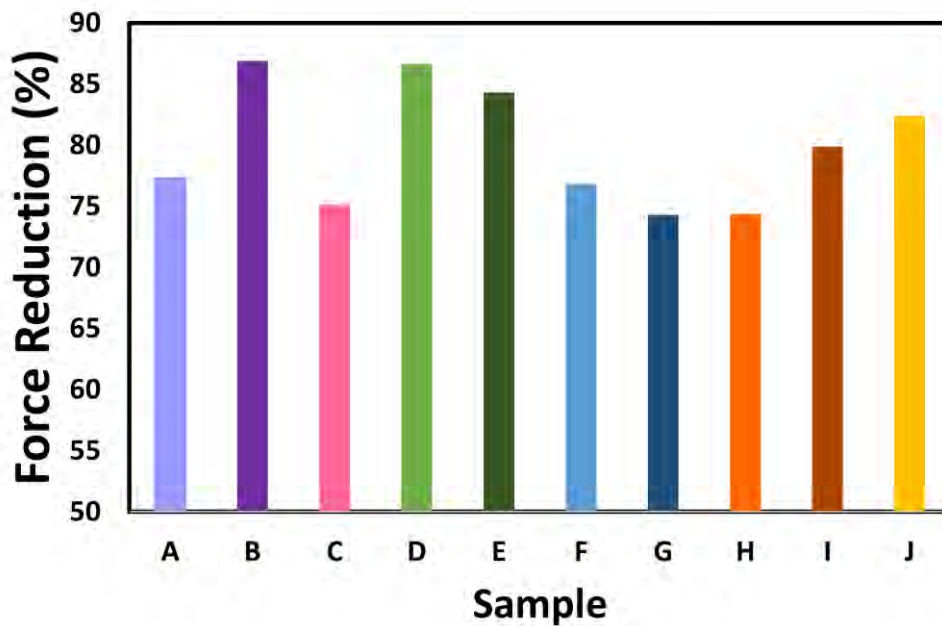


Figure 6. 8 Impact force reduction of the 3D printed materials (A to G) and commercially available insole materials (H to J).

The plotted force-time curves of the 3D printed and commercially available insole materials during the drop test are shown in Figure 6.9. It can be observed that the force-time curve of the samples can be mainly compared by using two characteristics: the height of the peak force and the length of the reaction time. Samples A, F, G, and H have a comparatively sharper peak force and shorter reaction time. Sample C has a noticeably sharp and high peak force together with a long reaction time. Sample B has a flat peak curve with a long reaction time. On the other hand, Samples D, and E have flat peak curves with a long reaction time. The materials that show a longer reaction time can better offset the load (Lo et al., 2014). This is favourable for the diabetic insole in that the force from unexpected shocks and gait termination can be buffered accordingly.

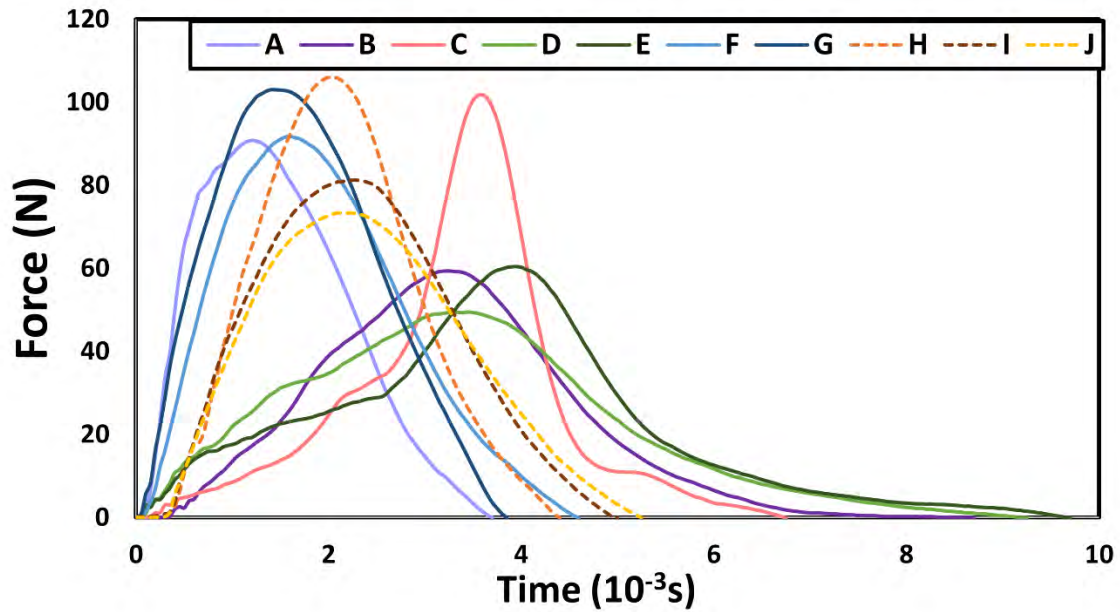


Figure 6.9 Force-time curves of the 3D printed materials (A to G) and commercially available insole materials (H to J).

The results showed that the 3D printed auxetic structures demonstrate a higher capability of reducing the impact force than the non-auxetic materials (Sample D vs E, and F vs G). With reference to the force-time curves, the auxetic structure shows a lower peak force and longer reaction time which is favourable for better foot protection against impact forces (Lo et al., 2014). In contrast, the non-auxetic structure shows a higher peak force and shorter reaction time for better foot protection against impact force.

6.3.1.2 Compression Properties and Hysteresis Energy Loss

The 3D printed and commercially available insole materials were subjected to compression with 800 N of force, and their hysteresis energy loss was calculated, and is plotted in Figure 6.10. Sample A exhibits the most significant loss of hysteresis during the compression test (73.50%) followed by Samples D (59.42%), C (56.97%), and E (56.64%). These 3D printed

samples show a more significant loss of hysteresis than the commercially available insole materials (i.e., Samples H, I, and J). Sample B demonstrates the lowest hysteresis loss (17.99%) which is less than the commercially available insole materials. Also, Sample H exhibits the highest loss of hysteresis amongst all of the commercially available insole's materials.

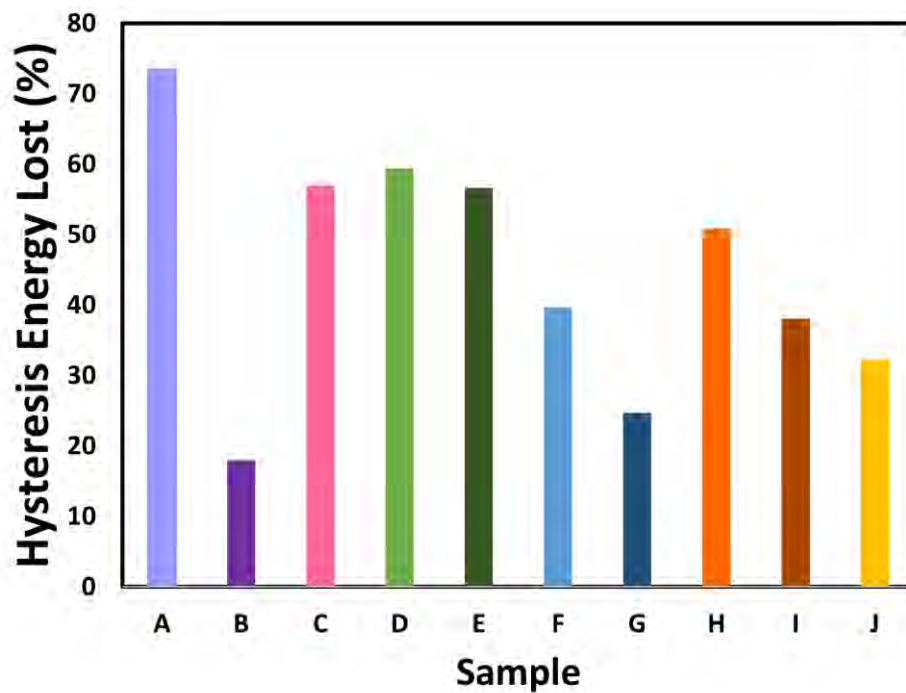


Figure 6. 10 Hysteresis energy loss of the 3D printed materials (A to G) and commercially available insole materials (H to J) during compression with 800N of force.

The stress-strain curves of the 3D printed and commercially available insole materials during compression with 800 N of force are plotted in Figure 6.11. An interesting effect of the auxetic properties can be observed in Sample A. The auxetic materials 3D printed materials exhibited a longer plastic region while the non-auxetic (commercially available insole) materials have almost no plastic region and enter the densification region very soon after the yield point. Sample A even shows a slight decrease in stress on its plastic region which is different from

the continuous increase of stress in the non-auxetic commercial insole materials. Also, the slope of the curve of force removal is different from the force application for the auxetic materials. In contrast, the non-auxetic materials showed a similar slope of the curve during both force application and removal. This different can also be observed between sample F (auxetic) and G (non-auxetic) with the almost same density.

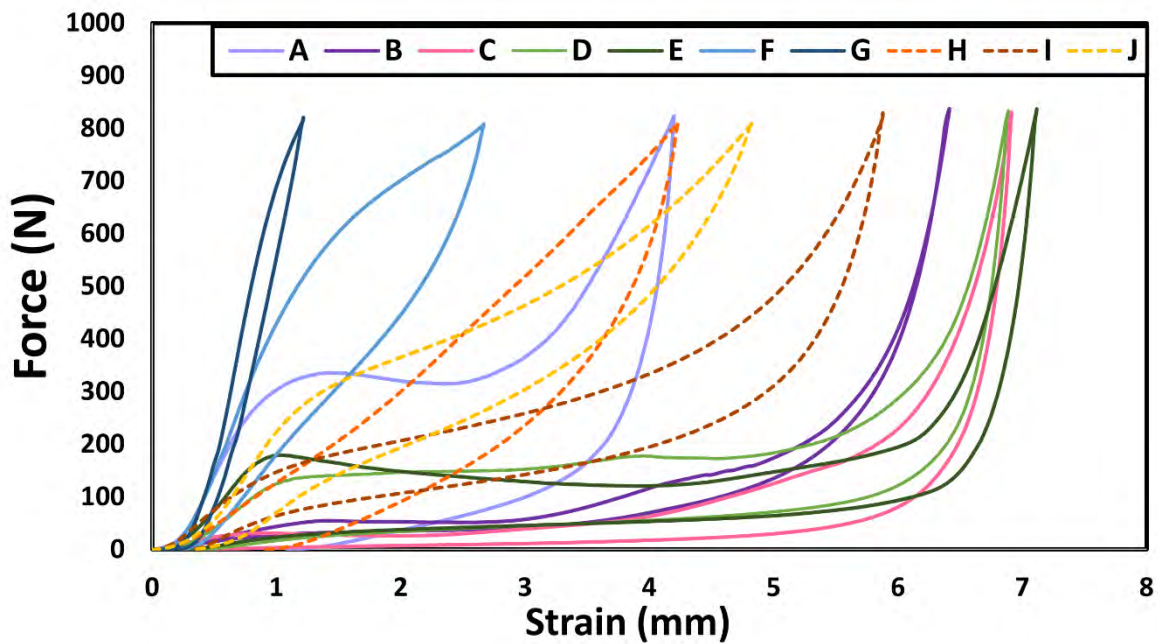


Figure 6. 11 Stress-strain curves the 3D printed materials (A to G) and commercially available insole materials (H to J) during compression with 800N of force.

In this study, the auxetic structure of the TPU material shows a higher loss of hysteresis than the material with a non-auxetic structure. Samples D (auxetic) and E (non-auxetic) are printed with the same materials and the two different models have almost the same volume. Due to the printing deviations, the density of Sample E is lower than that of Sample D even though the volume of the two 3D models is almost the same. Although there is a difference in volume, Sample D shows a 2.45% higher loss in hysteresis than Sample E. The higher loss of hysteresis with an auxetic structure can also be found when comparing Samples F (auxetic) and G (non-

auxetic). These two samples are printed with the same material and have almost the same density but Sample F shows a significantly higher loss of hysteresis in comparison to Sample G. Thus, it can be considered that materials with an auxetic structure tend to have higher loss of hysteresis during compression.

It should also be noted that Sample A which is made of flexible resin exhibited the highest loss of hysteresis during the compression test while Sample B which is made of elastic resin has the lowest loss of hysteresis. The type of resin material is critical because it affects the energy loss upon compression.

6.3.1.3 Water Vapour Permeability

The WVP of the 3D printed and commercially available insole materials is plotted in Figure 6.12. All of the 3D-printed samples are more water vapour permeable than the commercially available insole materials. The highest WVP value is observed for Samples C and E followed by Sample D at 844, 830, and 765 g/m²/day respectively. Samples A and B have a similar WVP value of 736 and 721 g/m²/day, respectively. Sample F has the lowest WVP value amongst the 3D printed samples of 691 g/m²/day. As for the commercially available insole materials, Sample J has a significantly higher WVP value of 296 g/m²/day in comparison to Samples H and I of 54.3 and 64.2 g/m²/day, respectively.

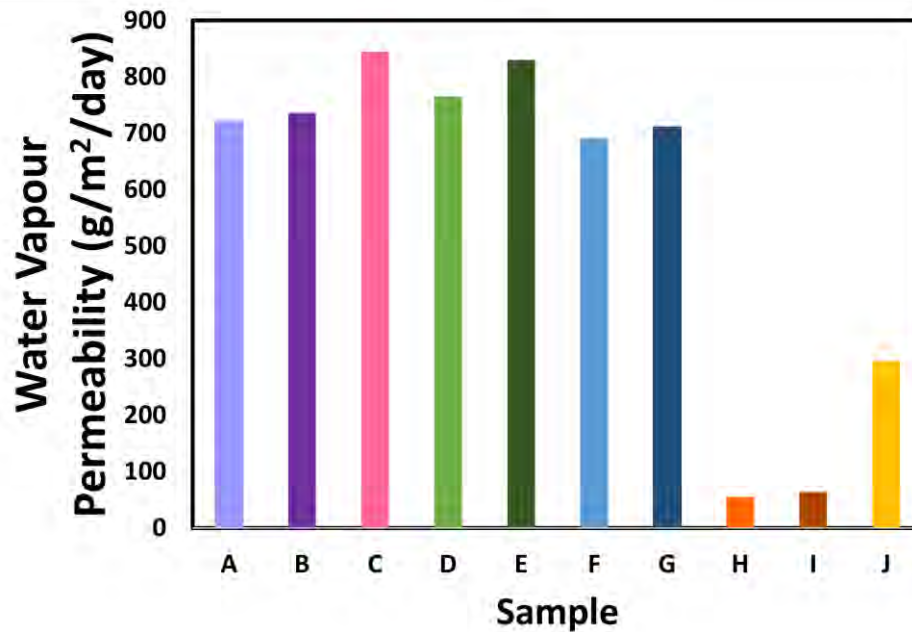


Figure 6. 12 Water vapour permeability of the 3D printed materials (A to G) and commercially available insole materials (H to J).

The difference in performance between the 3D printed and commercially available insole materials can be mainly explained by their porosity. The highly porous structure of the 3D printed materials allows air and water vapour to pass through them. In contrast, the porosity of the commercially available materials is lower than that of the 3D printed materials as both EVA (Samples H and I) and PU (Sample J) are foam materials with a closed cell structure. Furthermore, the porous 3D printed samples that were printed with a larger beam thickness (Samples F and G) have higher water vapour resistance than the other 3D printed samples. Thus, the 3D printed materials allow free flow of air and moisture which is a desirable property for the insole of concern.

With the same porous structure, the type of 3D-printed material might also affect the WVP. With reference to the results, it was found that Samples A and B formed by using different

types of resin have a slightly lower WVP value than the samples formed by different types of TPU (Samples C, D, and F). Samples C, D, and E are 3D printed by using selective laser sintering (SLS) where TPU powder was laser sintered and fused to form a specific shape. On the other hand, Samples A and B are formed by the laser polymerisation of liquid resin.

6.2.1.5 Moisture Regain

The moisture regain of the samples is plotted in Figure 6.13. The moisture regain of both the 3D printed and commercially available insole materials is relatively low (0.8-2%). As all of the materials, resin, TPU, EVA, and PU are almost not water-absorbable, it is reasonable to have a small difference amongst these materials. Sample B has the highest moisture regain of 1.98% followed by Sample A (1.19%) while most of the other samples are around 0.8-0.9%. Sample J also has a 1.51% moisture regain which is the second highest value. The 3D printed materials which contain resin (Samples A and B) have a higher moisture regain than the TPU materials (Samples C, D, E, F, and G).

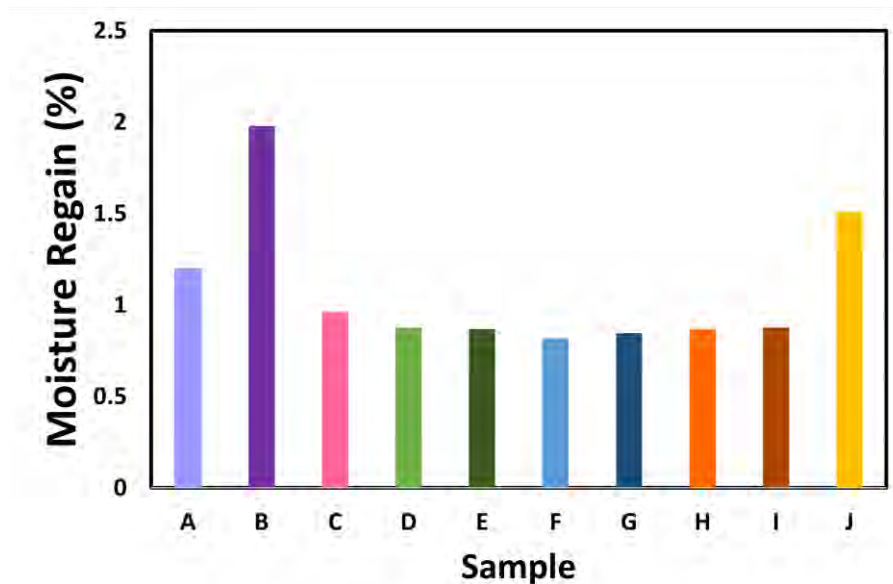


Figure 6. 13 Moisture regain of the 3D printed materials (A to G) and commercially available insole materials (H to J).

Amongst the 3 commercially available insole materials, Sample J has the best performance in terms of both the WVP and moisture regain. This shows that PU foam tends to have better thermal properties than EVA foams and is more suitable for cushioning garments for which the thermal properties are important.

A table that summarises the material properties of the samples is provided; see Table 6.3. Sample A (Flexible 80A Resin) which has the highest loss of hysteresis but second highest moisture regain ability amongst the 3D printed samples was selected for further evaluation in a wear trial. Sample D (TPU FS 1092A) was also selected because it has the best performance in force reduction. As for the commercially available insole materials, Sample H (double-layered EVA) with the highest loss of hysteresis and Sample J (PU) with the highest force reduction, water vapour permeability, and moisture regain amongst the commercially available insole materials were selected for further evaluation in a wear trial.

The heel pad samples inserted in the heel of the EVA insole are labelled according to the selected materials as follows: Heel Pads (1) 3DP-A (Resin Flexible 80A), (2) 3DP-D (TPU), (3) C-H (EVA foam), and (4) C-J (PU).

Table 6.3 Material properties of the insole samples.

Sample	Force reduction (%)	Hysteresis Energy Loss (%)	Water Vapour Permeability (g/m ² /day)	Moisture Regain (%)
A	77.32	73.50	720.99	1.20
B	86.90	17.99	735.80	1.98
C	75.17	56.97	844.44	0.96

D	86.65	59.42	765.43	0.88
E	84.33	56.64	829.63	0.87
F	76.83	39.69	691.36	0.82
G	74.29	24.70	711.11	0.85
H	74.35	50.87	54.32	0.87
I	79.88	38.07	64.20	0.88
J	82.38	32.27	296.30	1.51

Note: the bolded number denote the highest value of the respective parameter amongst the 3D printed or commercially available insole materials

6.3.1.5 Offloading performance of heel pads

The MPP of the plantar of the foot in the various heel pad conditions during standing and walking was measured and the pressure at the toes, forefoot, midfoot, and heel was compared respectively. As shown in Figure 6.14, Heel Pad C-H has the highest MPP of 77.6 kPa at the rearfoot amongst all 4 heel pads studied during standing. Heel Pads 3DP-A and C-J have a similar MMP of 69.3 kPa and 67.0 kPa respectively. Heel Pad 3DP-D has the lowest MPP at the rearfoot of 63.3 kPa.

It can be observed that Heel Pad 3DP-A has the lowest MPP at the toes (16.5 kPa) and forefoot (29.7 kPa). Also, the 3D printed heel pads have a higher MPP at the midfoot as opposed to the commercially available insole materials. This might be due to the difference in the centre of pressure during standing so that the MPP with the use of Heel Pad 3DP-A tends to be concentrated in the rearfoot.

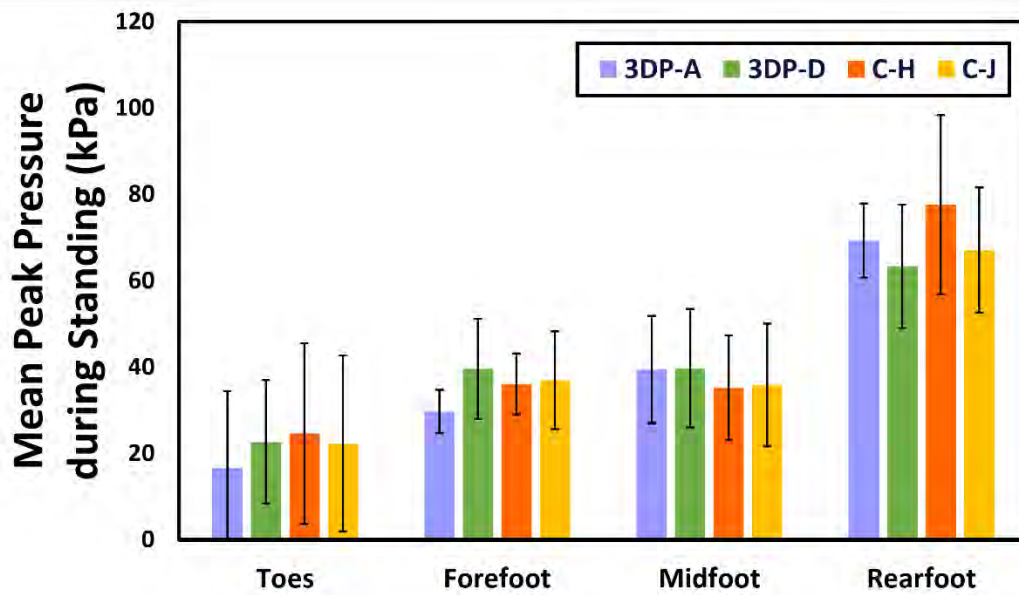


Figure 6. 14 Mean peak pressure during standing with heel pad samples.

The MPP values during walking with the different heel pad samples are plotted in Figure 6.15. The lowest MPP during walking is at the rearfoot with the use of Heel Pad 3DP-A (161 kPa) which is slightly higher than that of Heel Pad 3DP-D (164 kPa). Heel Pads C-H and C-J exhibit a comparatively higher MPP (176 and 172 kPa respectively) at the rearfoot during walking. This reveals that 3D printed auxetic materials such as the heel pad (Heel Pads 3DP-A and 3DP-D) have a better performance than the commercially available insole materials (Heel Pads C-H and C-J) in reducing the peak pressure at the rearfoot. In contrast, for the toes, forefoot, and midfoot, Heel Pads 3DP-A and 3DP-D have a higher MPP than the other regions of the feet. This might also be caused by the pressure shifting from the heel to the other foot regions.

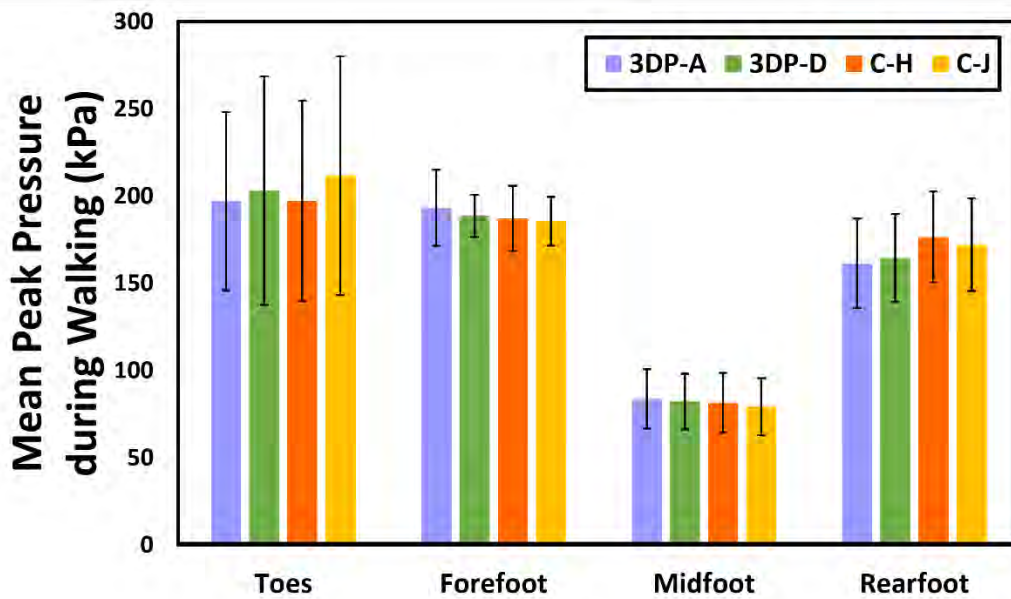


Figure 6. 15 Mean peak pressure during walking with heel pad samples.

To investigate the performance of the heel pad on reducing the peak pressure, the plantar pressure without the use of the insole was also measured to calculate the percentage of peak pressure reduced at the rearfoot. The mean peak pressure change (%) at the rearfoot during standing and walking is plotted in Figure 6.16. During standing, Heel Pad 3DP-D has the highest reduction of MPP at the rearfoot of 24.5%. The MPP with the use of Heel Pad 3DP-A (17.4%) is slightly lower than that of Heel Pad C-J (20.0%) but higher than that of Heel Pad C-H (12.3%). The results also indicated that Heel Pad 3DP-A has the highest reduction of the MPP at the rearfoot (12.7%) followed by Heel Pad 3DP-D (11.1%) during walking. The pressure reduction by Heel Pads C-H and C-J is lower than that by Heel Pads 3DP-A and 3DP-D (5.0% and 7.1 % respectively). This further proves that the performance of 3D printed auxetic materials shows a more satisfactory offloading performance than the commercially available insole materials as a heel pad.

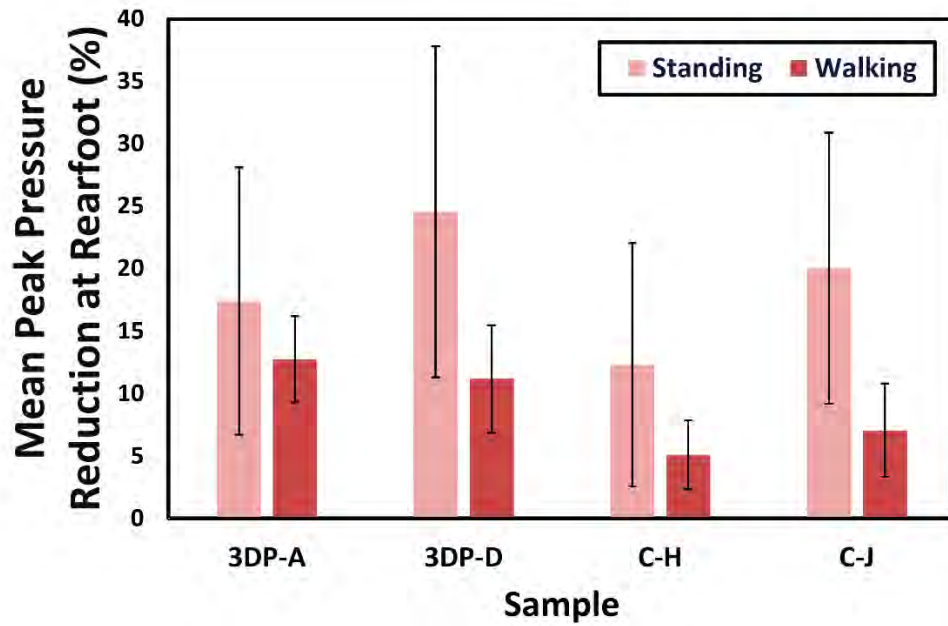


Figure 6. 16 Mean peak pressure changes (%) at the rearfoot during standing and walking.

6.3.1.5 Summary

To sum up, Sample A (3D printed auxetic material, resin) has optimal mechanical and thermal test results, and also shows a good performance in the wear trial when used as a heel pad (Heel Pad 3DP-A) in terms of reducing the plantar peak pressure during walking. On the other hand, Sample D (3D printed auxetic material, TPU FS 1092A) also shows the highest reduction in MPP at the rearfoot during standing (Heel Pad 3DP-D). In comparison to Samples H (Heel Pad C-H (double-layered EVA) and J (Heel Pad C-J; PU), the 3D printed auxetic materials show a superior performance in reducing the peak pressure at the rearfoot. For the development of the diabetic insole prototype, Sample A with the highest reduction of the MPP during walking was used and evaluated in Stage II.

6.3.2 Stage II – Insole Prototyping and Pilot Trial

Insole prototypes made of 3D spacer fabric with an auxetic structure were subsequently prepared for Stage II of the study. The 3D printing was based on the process in Stage I, in which the 3D auxetic re-entrant structure was printed by using Resin 80A with the SLA method which is the most preferred method for heel pad application with a satisfactory performance in both mechanical testing and a wear trial (Sample A). The 3D-printed half-insole is shown in Figure 6.17. During the wear trial, the MPP at the toes, forefoot, midfoot, and heel regions, during standing and walking in different insole conditions, was measured and compared to no insole worn.

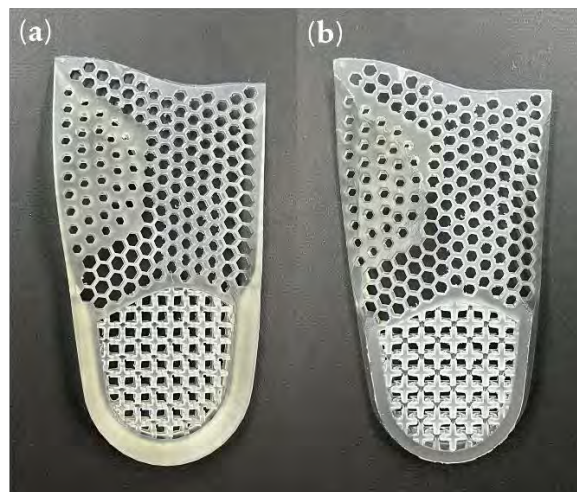


Figure 6.17 (a) Top, and (b) bottom views of the 3D half-insole model printed with resin.

6.3.2.1 Pilot trial with young subjects

6.3.2.1.1 PLANTAR PEAK PRESSURE

The MPP during standing with no insole and the use of the insole samples for all of the participants was calculated and is plotted in Figure 6.18. The highest MPP during standing is

found at the rearfoot for all of the conditions which is followed by the forefoot, midfoot, and toes in that order. This is in agreement with the findings of (Kwan et al., 2021)).

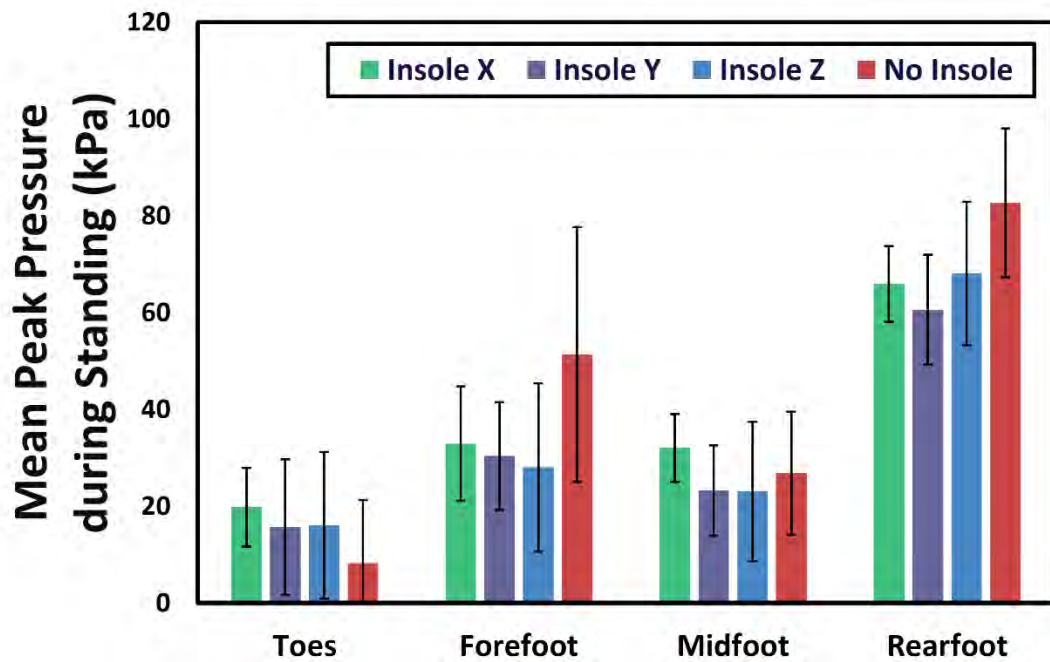


Figure 6. 18 Mean peak pressure during standing with use of insole samples and without insole.

With reference to Figure 6.18, it can be observed that the MPP during standing with no insole at the forefoot and rearfoot is significantly reduced after using the diabetic insole samples. Wilcoxon signed-rank tests were then conducted with pairwise comparisons made among all the conditions for all of the foot regions. The MPP during standing with Insole Z is significantly lower than standing with no insole ($Z = -2.521$, $p = 0.012$). Insoles X and Y also show a trend of MPP reduction at the forefoot as opposed to no insole worn even though the difference is not statistically significant. Also, the MPP at the rearfoot during standing with no insole is significantly higher than with the use of Insoles X ($Z = -2.521$, $p = 0.012$), Y ($z=-2.38$, $p=0.17$), and Z ($Z = -2.1$, $p = 0.036$). These reveal that the MPP at the forefoot and rearfoot can be significantly reduced by using Insole X.

In addition, the use of diabetic insoles (Insoles X, Y and Z) reduces the uneven distribution of pressure at the forefoot and midfoot. When no insole is used, the MPP at the forefoot is noticeably higher than that at the midfoot. In contrast, when using the diabetic insole samples during walking, the MPP at the forefoot is only slightly higher than that at the midfoot. Also, the pressure at the toes is somewhat higher with the use of any of the three insole samples compared to no insole. This shows that the plantar pressure is distributed more evenly when using a diabetic insole.

As for the difference amongst the insole samples, the results of the Friedman test indicated that there is no significant difference between the insoles for all four regions of the foot in terms of the MPP during standing. In comparison to the commercially available Insoles Y and Z, a slightly higher MPP was observed for Insole X at the toes, forefoot, and midfoot during standing (at around 4 – 8 kPa) even though the difference is not statistically significant. Also, the MPP at the rearfoot with the use of Insole X is higher than that of Insole Y at 5.34 kPa but slightly lower than Insole Z at 2.14 kPa. The highest MPP at the midfoot with Insole X might be caused by the difference in the fit of the arch pad between Insole X and the other insoles. The geometry of the arch pad on each insole is different which might cause a difference in fit. As the arch pad on Insole X has multiple layers, it is bulkier than the arch pad on the other two insoles which results in a slightly higher MPP at the midfoot. The plantar pressure is low during standing and does not need to be considered as a risk of excessive plantar pressure.

The MPP during walking for all the participants without an insole used and using the insole samples was calculated and is plotted in Figure 6.19. The MPP without the use of an insole at the forefoot is significantly higher than that at the other plantar regions (the rearfoot, toes, and midfoot respectively). This was also observed in Yamamoto et al. (2020) and Kwan et al.

(2021). After using a diabetic insole, the MPP is the highest at the toes followed by the forefoot, rearfoot, and midfoot which is in agreement with the findings in Zwaferink et al. (2020).

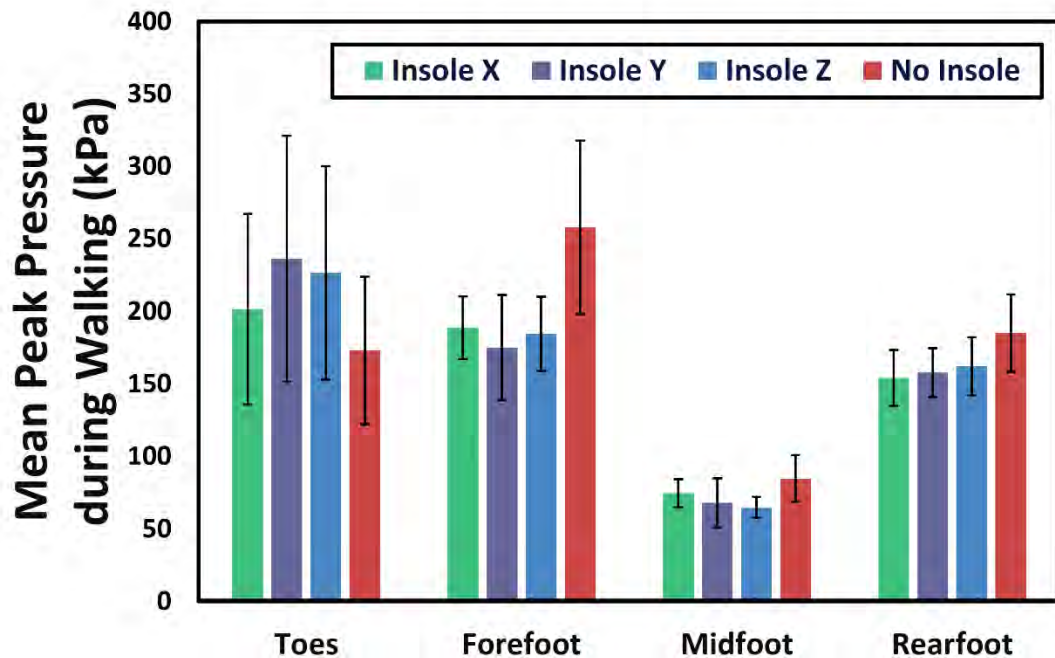


Figure 6. 19 Mean peak pressure during walking with insole samples.

Significant differences were only found between no insole worn and diabetic insoles at the forefoot, midfoot, and rearfoot ($p < 0.05$). For the MPP at the toes, the statistical results indicate that there is no significant difference amongst all of the conditions (with or without an insole) ($p > 0.05$). This might be due to the relatively larger standard deviation of the pressure at the toes during walking which is also observed in other studies (Martinez-Santos et al., 2019; Shi et al., 2022; Yamamoto et al., 2020).

Besides, a significant difference in the MPP was found at the forefoot when comparing the condition without an insole to that with the use of Insoles X ($Z = -2.521$, $p = 0.012$), Y ($Z = -2.521$, $p = 0.012$), and Z ($Z = -2.521$, $p = 0.012$). It can be observed from Figure 6.19 that the

MPP is significantly reduced after using Insole X. This shows the ability of Insole X to reduce the pressure at the forefoot region and the insole might even shift the pressure from the forefoot to other plantar regions. Thus, the plantar pressure can be more evenly distributed and the MPP reduced. Insole X is therefore effective in preventing pressure ulcers in diabetic feet caused by excessive plantar pressure on the plantar skin tissue.

As for the midfoot, the results of the Wilcoxon signed-rank tests showed a significantly higher MPP when walking without an insole as opposed to the use of Insoles X ($Z = -1.965$, $p = 0.049$), Y ($Z = -2.392$, $p = 0.017$), and Z ($Z = -2.521$, $p = 0.012$). As well, there is a significantly lower MPP at the rearfoot with the use of Insoles X ($Z = -2.24$, $p = 0.025$), Y ($Z = -2.521$, $p = 0.012$), and Z ($Z = -2.240$, $p = 0.025$) as opposed to no insole worn. This shows the reduction of MPP with the use of the insoles.

Although Insole X shows no statistically significant difference with the other two commercially available diabetic insoles, the mean values of MPP show a tendency for better performance by Insole X. For example, Insole X has the lowest MPP at the toes (201 kPa) as opposed to Insole Y (236 kPa) and Z (227 kPa). As for the midfoot, similar to standing, the MPP with Insole X (74.5 kPa) is higher than that of Insoles Y (68.0 kPa) and Z (64.7 kPa) during walking. The bulkier geometry of the heel pad of Insole X provides more support to bear the pressure created during walking. This could also explain the lowest MPP of Insole X (154 kPa) at the rearfoot region as opposed to Insoles Y (158 kPa) and Z (162 kPa) even though the difference is not statistically significant. The pressure at the heel could have shifted to the midfoot. This further enhances the even distribution of the plantar pressure. As mentioned in the literature review in Chapter 2, diabetic insoles should be able to achieve a <200 kPa plantar peak pressure (van

Netten et al., 2018; Waaijman et al., 2014). Amongst the three insole samples, Insole X almost meets this criterion.

In terms of the insole design features, even commercially available diabetic insoles with different design features still have performance limitations in terms of the reduction of plantar peak pressure. The insoles with an MTH pad (Insoles X and Z) show a higher plantar pressure than the insole without an MTH pad (Insole Y). Although Yi et al. (2022) indicated that an MTH pad can reduce the pressure on the metatarsal area, the indication is regardless of the location and geometry of the MTH pad. Thus, the shape and location of the MTH pad on the insole prototype can be further optimised to enhance the performance of reducing the pressure on the MTH. Although all the insoles have an arch pad, as mentioned, the geometry of the arch pad could also affect the plantar pressure at the midfoot and even the rearfoot. Besides, the higher heel cup does not help to reduce the pressure at the heel. According to Table 6.2, Insole Z has the highest heel cup, followed by Insoles Y and X. However, the MPP at the heel of Insole Z is also the highest during both standing and walking.

In summary, even though the MPP at the forefoot, midfoot, and rearfoot has been significantly reduced with the use of diabetic insoles, the MPP at the toes is much higher than 200 kPa with the use of Insoles Y and Z. However, Insole X (the novel diabetic insole) shows the most evenly distributed plantar pressure in all of the regions of <202 kPa in comparison to Insoles Y and Z with a lower MPP at the toes and rearfoot, and a slightly higher MPP at the forefoot and midfoot.

6.3.2.1.2 SUBJECTIVE PERCEPTION OF WEAR COMFORT

Figure 6.20 is a plot of the insole conditions based on the subjective ratings of wear comfort on the different foot regions including: the toes, forefoot, medial midfoot, lateral midfoot, and

rearfoot. The results show a similar trend of ratings for all of the foot regions. The figure shows that Insole X has the highest perceived comfort in all the foot regions followed by Insoles Y and Z. This might be caused by the difference in the contact material. The contact material of Insole X is the weft-knitted spacer fabric with inlays while Insoles Y and Z are traditional insole materials EVA and PE respectively. Insole X has a comparatively soft surface and offers a cushioning effect from the spacer monofilaments and inlaid silicon rods which enhance the subjectively perceived wear comfort of the insole. Also, the largest difference in the wear comfort score can be observed between Insole X and Insoles Y and Z at the toe region. This can be explained by the lowest MPP observed from Insole X in comparison to Insoles Y and Z. However, although Insole X has a slightly higher MPP at the forefoot and midfoot, it is still perceived to have a higher wear comfort in those regions. Thus, the small difference in MPP might not affect the perceived comfort.

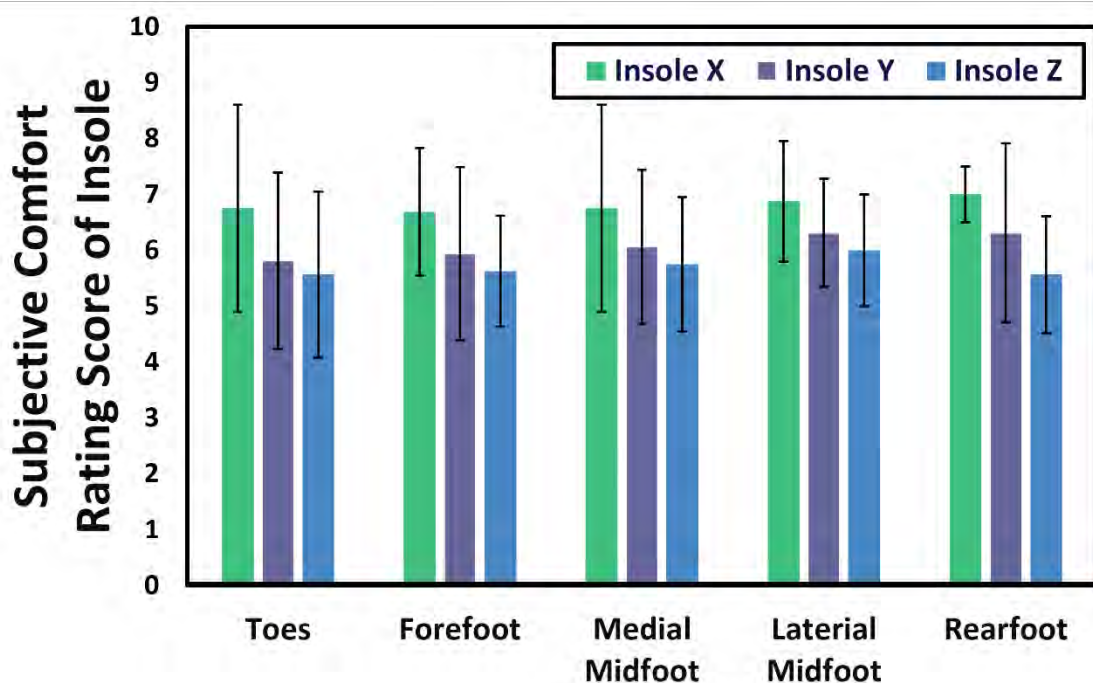


Figure 6. 20 Subjective rating of perceived comfort with the insoles at the toes, forefoot, medial midfoot, lateral midfoot, and rearfoot.

6.3.3 Stage III – Evaluation of Insole Prototypes

6.3.3.1 Plantar Peak Pressure

The results of repeated-measures analysis of variance (ANOVA) indicated that there are significant differences in plantar MPP between Insole X, Insole Y, and No Insole ($p < 0.05$) during walking at various plantar regions (toes, forefoot, midfoot, and rearfoot), except the pairs of Insole Y – No Insole at the toes and Insole X – No Insole at the midfoot.

The MPP values during walking with the different insole conditions are plotted in Figure 6.21. At the toes, a plantar MPP lower than 201 kPa has been observed from Insole X which is significantly lower than that of Insole Y (233 kPa) and the No insole conditions (264 kPa). The MPP of Insole Y is lower than the No insole condition, but the difference was not statistically significant ($p > 0.05$). Besides, Insole X shows the lowest plantar MPP at the forefoot and the rearfoot (145 kPa and 129 kPa) which is significantly lower than Insole Y (159 kPa and 141 kPa) and without insole (215 kPa and 180 kPa). As for the midfoot, the lowest MPP has been observed from Insole Y (61 kPa) followed by Insole X (64 kPa) and without insole (75 kPa). However, the difference between using Insole X and without insole was not significant ($p > 0.05$).

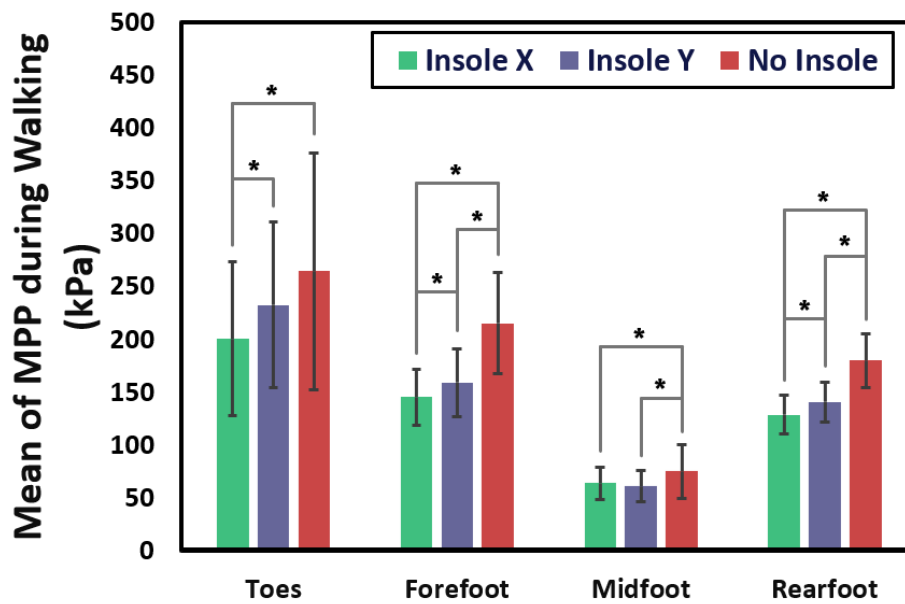


Figure 6. 21 Mean peak pressure during walking with use of insole samples and without insole (diabetic elderly participants). Error bars show the standard error.

From the results, it can be observed that using diabetic insoles (Insoles X and Y) can significantly reduce the plantar MPP during walking. There are significantly lower plantar MPP observed from both insole conditions as compared to no insole ($p < 0.05$) at the forefoot and rearfoot. At the toes, the use of Insole X shows significantly lower MPP than not using an insole. Although the lower MPP obtained from Insole Y is not statistically significant, the mean values show a trend of MPP reduction at the toes when wearing Insole Y. As for the midfoot, the use of Insole Y shows a significantly lower value MPP than without insole. Although the use of Insole X did not show a significantly lower MPP than not using insole on the midfoot, the higher MPP brings by the height of the arch pad of Insole X is favourable for reducing the MPP at other foot regions. Thus, the lower reduction of MPP on the midfoot does not represent a poor performance for the overall MPP reduction.

Besides, the plantar MPP during walking without using an insole is much higher than 200 kPa (the ideal upper limit of MPP) at the toes and the forefoot (Waijman et al., 2014). The use of insoles is effective to reduce MPP during walking. Even though the MPP at the toes under insoles is still higher than 200 kPa, Insole X shows the ability to maintain an MPP lower than 201 kPa which is 32 kPa lower than Insole Y.

Compared to the results obtained from young participants at stage II, the absence of insole resulted in higher MPP at the toes amongst the diabetic patients. The elderly diabetic patients have lower MPP at the forefoot compared to the young healthy participants. As compared to Insole Y, Insole X showed satisfactory offloading performance in the forefoot. Amongst the diabetic elderly, the MPP differences between the conditions of Insole X, Insole Y, and no insole well-aligned with the results obtained from the young participants.

The offloading performance of Insole X and Insole Y was also compared. The percentage reduction of MPP at all the foot regions using Insole X and Insole Y was plotted in Figure 6.22. The repeated-measures analysis of variance (ANOVA) indicated a significantly higher reduction of MPP by using Insole X at the toes, forefoot, and rearfoot, when compared to Insole Y. An MPP reduction of 19.4 % at the toes has been observed from Insole X, which is higher than Insole Y (6.08%). At the forefoot, Insole X is capable to reduce 30.7% of MPP, while the MPP reduction of Insole Y is 24.6%. The MPP reduction at the rearfoot using Insole X (27.2%) is higher than that of Insole Y (20.7%).

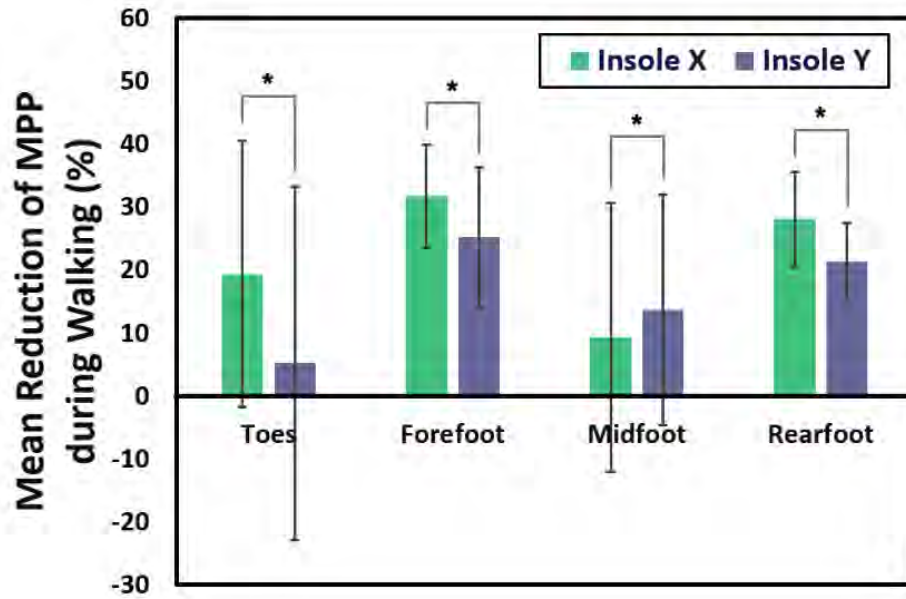


Figure 6. 22 Mean reduction of peak pressure during walking with use of insole samples (diabetic elderly participants). Error bars show the standard error.

On the other hand, the reduction of MPP observed from Insole X is lower than that of Insole Y at the midfoot. This might be the result of a higher contact area between Insole X and the midfoot in comparison to the contact area between Insole Y and the midfoot (Figure 6.23). The increased contact area between the insole and the plantar helps to redistribute the plantar pressure from the high-pressure area to the low-pressure area (Bus et al., 2004; van Netten et al., 2018). Thus, the pressure from other plantar regions shifted to the midfoot which results in a relatively lower MPP reduction at the midfoot. The results confirm that the proposed insole prototype provides effective reduction of plantar pressure during walking.

6.3.3.2 Contact Area Between Insole and Plantar

The contact area between the insole and plantar during walking at the toes, forefoot, midfoot, and rearfoot was plotted in Figure 6.23. In the pairwise comparison at the forefoot, significant

differences were found between Insole X and No insole, and between Insole Y and No insole ($p < 0.05$). Significant differences have been found between all pairs among the three conditions at the midfoot. There is no significant difference observed among Insole X, Insole Y, and No insole conditions at the toes and rearfoot.

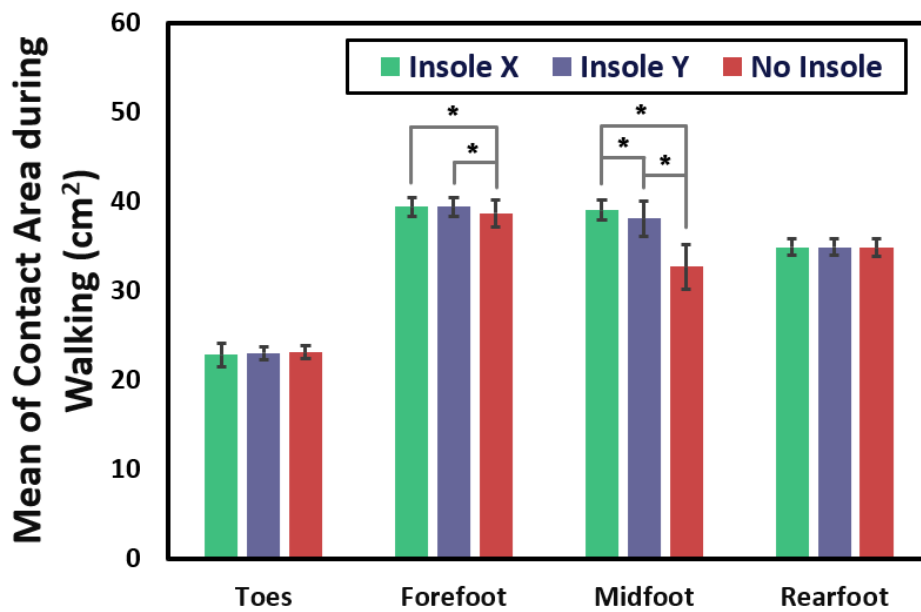


Figure 6.23 Mean contact area during walking with use of insole samples and without insole (diabetic elderly participants). Error bars show the standard error.

The results indicated that the use of insoles had a slightly larger contact area at the forefoot than the no insole condition. This might be associated with the 3D geometry of the insole at the forefoot that conforming to the plantar shape of the midfoot.

The use of insoles also resulted in significant increase in contact area at the midfoot. The arch pad in Insole X and Insole Y increases the contact area with the midfoot which helps to bear the load on the plantar to reduce the MPP at other foot regions.

Figure 6.24 shows the mean change of contact area during walking with the use of insole samples on diabetic elderly participants. The contact area with the midfoot has been increased

by 19.7% by using Insole X which significantly larger increase than using Insole Y (16.7%) ($p < 0.05$). This might be caused by their difference in the arch pad geometry and material compression properties. Apart from the midfoot, their difference in other foot regions is not significant. This shows the critical role of arch pad geometry on the contact area.

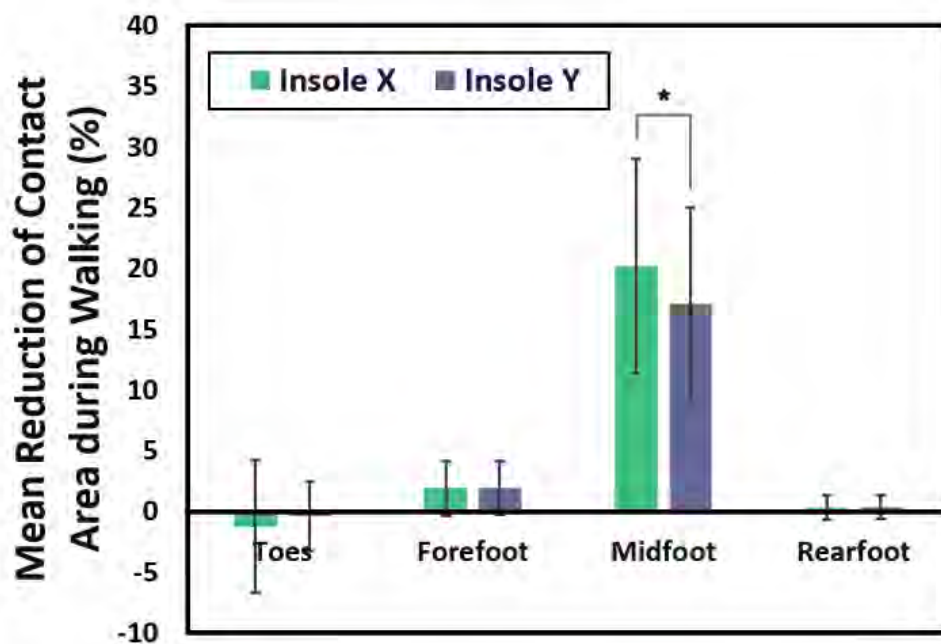


Figure 6. 24 Mean change of contact area during walking with use of insole samples (diabetic elderly participants). Error bars show the standard error.

6.3.3.3 Subjective Perception of Wear Comfort

Figure 6.25 is a plot of the insole conditions based on the subjective ratings of comfort at the toes, forefoot, medial midfoot, lateral midfoot, and rearfoot. The result shows a trend of higher perceived comfort on Insole X than Insole Y in all the foot regions. This could be explained by the lower planter peak pressure during walking when using Insole X presented in Figure 6.21. As mentioned in section 4.4.4, the contact materials affect the comfort perceptions. The softer contact surface and cushioning structure of Insole X might also result in a better subjective perception of comfort. Besides, as indicated in section 4.3.4, the thermal properties of the contact layer of the insole play a significant role in perceived wear comfort. The spacer fabric

used on top of the Insole X with the best performance in reducing the RH contributed to a higher perceived comfort than EVA material. As the material of Insole Y is also EVA, it tends to have lower perceived comfort than Insole X.

Furthermore, the differences were larger on the forefoot and the medial midfoot. This might also be related to the larger contact area on the forefoot and the midfoot using Insole X than Insole Y with better fitting with the foot geometry. However, the above difference in mean score is not significant from the results of the statistical analysis ($p > 0.05$).

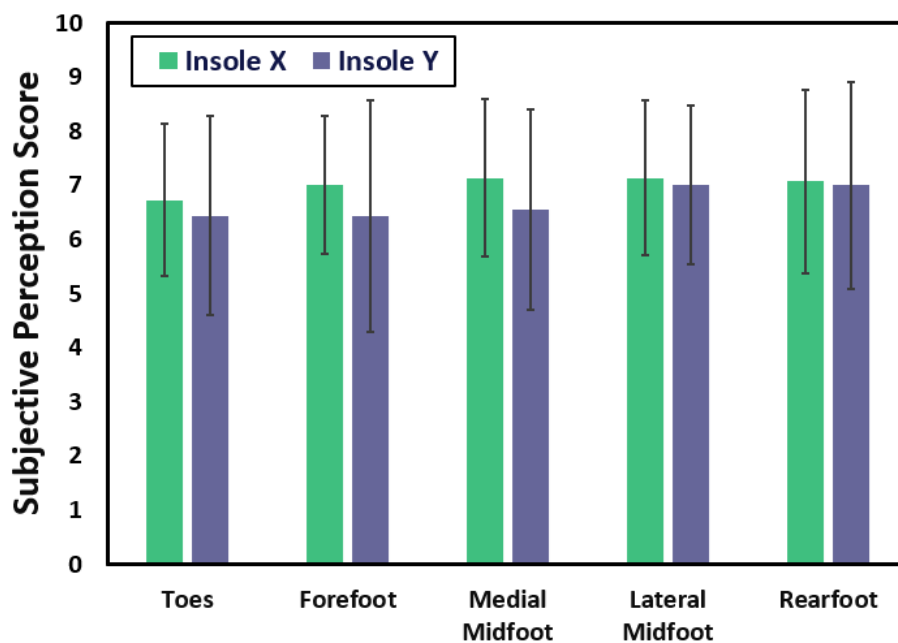


Figure 6. 25 Subjective rating of perceived comfort with the insoles at the toes, forefoot, medial midfoot, lateral midfoot, and rearfoot samples (diabetic ealderly participants).

6.4 Summary

In this chapter, a novel diabetic insole prototype has been developed by combining 3D knitted and 3D printed materials. In Stage I, eight 3D printed components with different 3D structures (auxetic and non-auxetic) are fabricated by using four different types of soft materials and then

evaluated. In considering the properties required for insoles, the materials are subsequently evaluated through material tests and a wear trial to determine their performance as a heel pad. The results show that the auxetic structure of the 3D printed material increases the impact force reduction which is an important property of an insole. Also, the 3D printed materials with an auxetic structure facilitates a rapid reduction of the compression forces when the force is absorbed by the materials. This helps to reduce the forces exerted onto the plantar of the foot when the foot is lifted during gait. Furthermore, an appropriate degree of material hardness is very important because this property can entirely affect the ability of the material to withstand the compression force. Besides, the 3D printed materials are more water vapor permeable in comparison to the traditional insole materials. In comparison to walking without an insole, the 3D printed auxetic material that uses resin (Flexible 80A) exhibits an average of 12.7% pressure reduction at the rearfoot. This material is then subsequently selected for the development of the diabetic insole prototype.

In Stage II, the diabetic insole prototype was developed and preliminarily evaluated through a wear trial. It is found that the overall peak pressure is reduced with the use of the prototype which reduces the MPP on the plantar at the forefoot and rearfoot during both standing and walking. For walking, the novel insole prototype shows a slightly higher MPP than the commercially available diabetic insoles for up to 8 kPa. However, compared to the commercially available diabetic insoles, the insole developed in this study has a lower MPP at the toes and rearfoot which can also most evenly distribute the plantar pressure in all of the regions <202 kPa. The prototype is also rated as having the highest wear comfort in all of the foot regions.

In Stage III, the superior performance of the insole prototype has been verified by a wear trial with elderly diabetic patients. The results confirm that the proposed insole prototype facilitates the reduction of plantar peak pressure in all foot regions. With increased plantar contact area on the midfoot (19.7%), the insole prototype is capable of controlling the plantar peak pressure at the threshold MPP of 201 kPa or below. The insole prototype also exhibits a higher rating on the perceived comfort in all the foot regions. The results confirm the effectiveness and practical use of the proposed insole design in plantar pressure redistribution for elderly diabetic patients.

Chapter 7 Conclusions and Suggestions for Future

Research

7.1 Conclusions

The primary goal of the research was to design and develop a diabetic insole orthosis with the use of both a novel knitted textile and 3D printed materials to optimise the wear comfort in terms of the in-shoe environment and even distribution of plantar pressure with reference to experimental analysis.

The project objectives, which are discussed in detail in Section 1.3 of Chapter 1 of the study have been realized and the achievements of the research are summarized as follows:

1. In order to understand the foot conditions and footwear needs of diabetic patients, a literature review and a foot care program are conducted with a questionnaire for diabetic elderly including 30 participants. The questionnaire survey is mainly to a) examine the common foot problem or discomfort, and daily use of orthotic footwear and/or insoles of diabetic patients, and b) understand their preferences of footwear and insole. The foot pain of the diabetic patient is reported mainly at the heel, forefoot, and medial side of the foot. Textile materials are commonly used as the insole-foot contact layer for improved comfort. The cushioning pad at the high-pressure region and 3D arch pad support are also preferred insole features for diabetic patients.
2. To examine the properties of footwear materials and investigate the thermal performance of 3D spacer knitting techniques and 3D printing technologies in footwear applications, a wear trial has been conducted regarding the effect of the insole materials on the change of foot skin temperature and humidity during fast walking. A total of 4 insole materials

including traditional insole material: PU insole and leather insole; and novel insole materials: TPU (3D-printed) insole and textile-fabricated insole. The results reveal that the novel textile-fabricated insole has the best performance maintaining a low foot skin relative humidity by reducing the RH by 3.21% at the sole and 24.41% at the heel after 30 mins of walking. Despite the air permeability of 3D printed insoles, their performance in sweat absorption is less desirable as compared to the textile-fabricated insole. The subjective sensation results confirm the overall thermal comfort of the textile-fabricated insole. As compared to traditional materials with poor air-permeability and water vapour transmission that hampering the in-shoe thermal comfort, suitable 3D spacer knitted structures not only able to reduce plantar pressures, but also enhance the comfort of wear and maintain an appropriate skin condition.

3. To design and develop an insole prototype that can effectively enhance the in-shoe micro-climate and reliably alleviate plantar pressure, a novel weft-knitted spacer fabric with foam inlays and a 3D printed insole with arch pad and auxetic heel pad was developed. The effect of inlay density and spacer course densities on the performance of weft-knitted spacer fabrics regarding their thermal conductivity, evaporative resistance, compression behaviour, and impact force reduction was investigated. It was found that fabric with higher inlay density and /or spacer density tends to perform better in force reduction and compressive resistance. With the same inlay density, higher spacer density reduces air permeability. Also, the high density of inlay materials tends to increase evaporate resistance. A fabric shows the best overall performance with thermal conductivity of 0.071W/mK, a maximum compressive stress of 323.43 kPa, and force reduction of 70.07%, and air permeability of 35.96 ml/s/cm², has been applied as the upper layer of the novel insole prototype. As for the 3D printed materials for insole application, a total of eight 3D prints with different structures using four different soft materials include: resin (Flexible

80A), resin (Elastic 50A), TPU (Flexa Bright), TPU (FS 1092A), are demonstrated and evaluated by material test and wear trial. As compared to the traditional insole materials (PU and single and double layered EVA), higher force reduction can be achieved by 3D-printed auxetic materials and outstanding water vapor permeability. It was also observed that the 3D printed materials in the auxetic structure show a rapid reduction of compression force when removing the force from the materials. The 3D printed auxetic material by Resin of 80A hardness exhibits an average of 12.7% pressure reduction at the rearfoot as a heel pad was applied on the heel of the 3D printed insole bottom. As for the 3D printed materials for insole application, a total of eight 3D prints with different structures using four different soft materials are demonstrated and evaluated by material test and wear trial. It was observed that the 3D printed materials in the auxetic structure show an excellent force reduction, a rapid reduction of compression force when removing the force from the materials, and outstanding water vapor permeability. The 3D printed auxetic material by Resin (80A hardness) exhibits an average of 12.7% pressure reduction at the rearfoot. A suitable heel pad design in auxetic structure could therefore enhance the foot protection from impact forces. The possibility of 3D spacer knitting techniques and 3D printing technologies on insole application was explored and their properties are found favourable for the enhancement of foot thermal comfort and reduce the plantar peak pressure, thus, reduce the risk of foot ulcer.

The newly designed insole orthosis prototype was developed by combining the novel spacer weft-knitted fabric with inlaid and the 3D printed half-insole was demonstrated and evaluated by laboratory wear trials. A total of 8 female participants are invited to wear the mesh shoes inserted with the insole prototype and two commercial diabetic insoles subsequently and stand for 30 seconds followed by walking at their self-selected speed where their plantar pressure was recorded by the Pedar-X pressure system. The lowest

overall peak pressure was found during the walking with the newly designed diabetic insoles with the reduced plantar MPP on the forefoot and rearfoot during both standing and walking. The reduction of overall peak pressure using diabetic insoles was observed on the forefoot and rearfoot. The insole proposed in this study exhibits a lower MPP at toes and rearfoot than the commercial diabetic insole with MPP <202 kPa and improved perceived comfort in all foot region.

The plantar off-loading effect of the insole prototype on diabetic patients during walking has been verified by wear trial with 23 elderly diabetic patients. It was found that the overall peak pressure has been reduced by using diabetic insoles with reduced plantar MPP on all the foot region during walking. Compared to the commercial diabetic insole, the insole developed in this research shows a reduction of MPP for up to 30.7% which is also able to maintain the most evenly distributed plantar pressure with all the regions <201 kPa by a 19.7% increase of contact area with the midfoot. It also has good perceived comfort in all the foot regions. The integration of spacer weft-knitted fabric with desirable thermal properties and the 3D printed insole bottom not only improve the in-shoe environment, but also reliably alleviate peak plantar pressure with improved wear comfort for daily life activities.

The weft-knitted spacer fabric with inlay and the 3D printed auxetic material structure proposed in this study provide an alternative material choice to advance the design and development of footwear insoles that improve wear comfort. The output of the study could extend to the development of customized insole orthosis to prevent the development of diabetic foot ulcers.

7.2 Limitations of the Study

Some limitations of this study are listed as follow:

1. The sample size for the experiments is relatively small while the deviation among human body is large, which may limit the generalisation of the results. As the foot of diabetic elders have different foot deformation such as the development of flat arch and Hallux Valgus, the plantar pressure distribution might be affected by these factors.
2. The shoes type might also affect the in-shoes micro-climate. Mesh sport shoes is used in the evaluation of foot condition in this study and have a relatively permeable shoes upper than other type of shoes such as leather sport shoes. Wear trials can be conducted in future study to using different type of shoes to investigate the performance of textile-fabricated insole on different footwear.
3. The wear trial regarding the in-shoe micro-climate using different insoles has been conducted in a controlled environment. No specific weather conditions in Hong Kong, such as winter with low temperatures and relative humidity, or summer with high temperatures and humidity, have been considered. However, it is necessary to further verify the most suitable material for use in different weather conditions.
4. Printing deviation in certain extend is common occurs using 3D printing machines. Two 3D model with the same volume was printed by the same 3D printer using the same material (TPU), however, difference was found on the density of the printed object. This would the material properties.
5. To investigate the properties of the 3D-printed auxetic materials for insole application, the 3D re-entrance auxetic structure was selected for evaluation. This is only one of many auxetic structures proposed for good shock absorption. In the future study, other auxetic structures can also be explored which might show different material properties.

7.3 Suggestions for Future Research

Some recommendations for the future work are proposed as follows:

1. A larger numbers of diabetic elderly subjects with different foot type can be invited to participate in a wear trial to further investigate the effect of the novel insole prototype on diabetic feet regarding plantar pressure distribution. As there is foot problem of the diabetic elderly such as the reduction of the plantar soft tissue stiffness and the foot deformation caused by aging (e.g. the development of flat arch and Hallux Valgus), the plantar pressure distribution might be different among the foot problem. Therefore, the wear trial can be conducted with diabetic elderly individuals with different foot problems, respectively, to better represent the diabetic population in Hong Kong when evaluating and further improving the design. Additionally, if there is a need to assert the insole's ability to prevent foot ulcers, conducting a larger wear trial encompassing a wider range of foot conditions would be necessary.
2. For the wear trial to evaluate the performance of insole materials on maintaining the foot skin temperature and humidity, different types of footwear can be used. Different shoes would have different porosity of the shoe upper which will affect the airflow into the footwear, thus, affecting the in-shoes environment. A pair of a very common type of mesh sports shoe with permeable shoe uppers are used in this study. The wear trial using less permeable shoes can also be conducted to investigate the performance of the insole when there is less airflow into the shoes.
3. The evaluation of the thermal performance of the insole can be further conducted under different weather conditions to simulate the weather conditions in Hong Kong more accurately. It is possible that the novel materials developed or researched in this study could demonstrate improved performance in specific weather conditions. Additionally, we can determine the most suitable material for various weather scenarios.
4. The possibility of customization of the insole prototype can be explored by alternating the dimension of the 3D model (e.g., arch pad height) of the 3D-printed insole bottom

according to the foot shape of each patient which can be obtained through 3D scanning. By having the 3D image of the foot, the foot dimension can be more accurately measured, and the geometry of the insole can be adjusted accordingly such as the height of the arch pad. This help to enhance the fitting of the insole prototype and enhance the even distribution of the plantar pressure.

5. Evaluation can also be done on the durability of the weft-knitted spacer fabric with inlaid and 3D-printed materials for repeated use as an insole. The deformation of the weft-knitted spacer fabric and 3D-printed materials can be evaluated by a repeated compression test and see the ability of recovery under repeated use.

References

- Abri, H., Aalaa, M., Sanjari, M., Amini, M. R., Mohajeri-Tehrani, M. R., & Larijani, B. (2019). Plantar pressure distribution in diverse stages of diabetic neuropathy [Article]. *Journal of Diabetes and Metabolic Disorders*, 18(1), 33-39. <https://doi.org/10.1007/s40200-019-00387-1>
- Ahmed, S., Barwick, A., Butterworth, P., & Nancarrow, S. (2020). Footwear and insole design features that reduce neuropathic plantar forefoot ulcer risk in people with diabetes: a systematic literature review. *Journal of Foot and Ankle Research*, 13(1), 30. <https://doi.org/10.1186/s13047-020-00400-4>
- Alexiadou, K., & Doupis, J. (2012). Management of diabetic foot ulcers [Review]. *Diabetes Therapy*, 3(1), 1-15, Article 4. <https://doi.org/10.1007/s13300-012-0004-9>
- Anderson, J., Williams, A. E., & Nester, C. (2020). Development and evaluation of a dual density insole for people standing for long periods of time at work [Article]. *Journal of Foot and Ankle Research*, 13(1), Article 42. <https://doi.org/10.1186/s13047-020-00402-2>
- Bagavathiappan, S., Philip, J., Jayakumar, T., Raj, B., Rao, P. N. S., Varalakshmi, M., & Mohan, V. (2010). Correlation between plantar foot temperature and diabetic neuropathy: A case study by using an infrared thermal imaging technique [Article]. *Journal of Diabetes Science and Technology*, 4(6), 1386-1392. <https://doi.org/10.1177/193229681000400613>
- Bennetts, C. J., Owings, T. M., Erdemir, A., Botek, G., & Cavanagh, P. R. (2013). Clustering and classification of regional peak plantar pressures of diabetic feet [Article]. *Journal of Biomechanics*, 46(1), 19-25. <https://doi.org/10.1016/j.jbiomech.2012.09.007>
- Bian, Y., Yang, F., Li, P., Wang, P., Li, W., & Fan, H. (2021). Energy absorption properties of macro triclinic lattice structures with twin boundaries inspired by microstructure of feldspar twinning crystals [Article]. *Composite Structures*, 271, Article 114103. <https://doi.org/10.1016/j.compstruct.2021.114103>
- Boulton, A. J. M. (2004). The diabetic foot: From art to science. The 18th Camillo Golgi lecture [Review]. *Diabetologia*, 47(8), 1343-1353. <https://doi.org/10.1007/s00125-004-1463-y>
- Bus, S. A. (2016). The role of pressure offloading on diabetic foot ulcer healing and prevention of recurrence [Article]. *Plastic and Reconstructive Surgery*, 138(3), 179S-187S. <https://doi.org/10.1097/PRS.0000000000002686>
- Bus, S. A., Haspels, R., & Busch-Westbroek, T. E. (2011). Evaluation and optimization of therapeutic footwear for neuropathic diabetic foot patients using in-shoe plantar pressure analysis [Article]. *Diabetes Care*, 34(7), 1595-1600. <https://doi.org/10.2337/dc10-2206>
- Bus, S. A., Lavery, L. A., Monteiro-Soares, M., Rasmussen, A., Rasovic, A., Sacco, I. C. N., van Netten, J. J., & on behalf of the International Working Group on the Diabetic, F. (2020). Guidelines on the prevention of foot ulcers in persons with diabetes (IWGDF 2019 update) [Article]. *Diabetes/Metabolism Research and Reviews*, 36(S1), Article e3269. <https://doi.org/10.1002/dmrr.3269>
- Bus, S. A., Ulbrecht, J. S., & Cavanagh, P. R. (2004). Pressure relief and load redistribution by custom-made insoles in diabetic patients with neuropathy and foot deformity [Article]. *Clinical Biomechanics*, 19(6), 629-638. <https://doi.org/10.1016/j.clinbiomech.2004.02.010>
- Bus, S. A., Waaijman, R., Arts, M., Haart, M. D., Busch-Westbroek, T., Van Baal, J., & Nolle, F. (2013). Effect of custom-made footwear on foot ulcer recurrence in diabetes: A multicenter randomized controlled trial [Article]. *Diabetes Care*, 36(12), 4109-4116. <https://doi.org/10.2337/dc13-0996>
- Cavanagh, P. R., & Bus, S. A. (2011). Off-loading the diabetic foot for ulcer prevention and healing [Article]. *Plastic and Reconstructive Surgery*, 127(SUPPL. 1 S), 248S-256S. <https://doi.org/10.1097/PRS.0b013e3182024864>

- Çeven, E. K., & Günaydın, G. K. (2021). Evaluation of Some Comfort and Mechanical Properties of Knitted Fabrics Made of Different Regenerated Cellulosic Fibres [Article]. *Fibers and Polymers*, 22(2), 567-577. <https://doi.org/10.1007/s12221-021-0246-0>
- Chatzistergos, P. E., Gatt, A., Formosa, C., Farrugia, K., & Chockalingam, N. (2020). Optimised cushioning in diabetic footwear can significantly enhance their capacity to reduce plantar pressure [Article]. *Gait and Posture*, 79, 244-250. <https://doi.org/10.1016/j.gaitpost.2020.05.009>
- Chatzistergos, P. E., Naemi, R., Healy, A., Gerth, P., & Chockalingam, N. (2017). Subject Specific Optimisation of the Stiffness of Footwear Material for Maximum Plantar Pressure Reduction [Article]. *Annals of Biomedical Engineering*, 45(8), 1929-1940. <https://doi.org/10.1007/s10439-017-1826-4>
- Dave, H. K., Karumuri, R. T., Prajapati, A. R., & Rajpurohit, S. R. (2022). Specific energy absorption during compression testing of ABS and FPU parts fabricated using LCD-SLA based 3D printer [Article]. *Rapid Prototyping Journal*, 28(8), 1530-1540. <https://doi.org/10.1108/RPJ-04-2021-0075>
- Dehghan, N., Payvandy, P., & Talebi, S. (2022). Introducing a novel model for predicting effective thermal conductivity of spacer fabrics based on their structural parameters [Article]. *Journal of Thermal Analysis and Calorimetry*, 147(12), 6615-6629. <https://doi.org/10.1007/s10973-021-11000-0>
- Diabetes around the world in 2021*. (2021). IDF Diabetes Atlas. <https://diabetesatlas.org/>
- Fortney, S. M., & Vroman, N. B. (1985). Exercise, Performance and Temperature Control: Temperature Regulation during Exercise and Implications for Sports Performance and Training [Review]. *Sports Medicine: An International Journal of Applied Medicine and Science in Sport and Exercise*, 2(1), 8-20. <https://doi.org/10.2165/00007256-198502010-00002>
- Gao, H., Deaton, A. S., Barker, R., Fang, X., & Watson, K. (2022). Effects of the moisture barrier and thermal liner components on the heat strain and thermal protective performance of firefighter turnout systems [Article]. *Textile Research Journal*, 92(21-22), 4163-4176. <https://doi.org/10.1177/00405175221099947>
- Gefen, A. (2003). Plantar soft tissue loading under the medial metatarsals in the standing diabetic foot [Article]. *Medical Engineering and Physics*, 25(6), 491-499. [https://doi.org/10.1016/S1350-4533\(03\)00029-8](https://doi.org/10.1016/S1350-4533(03)00029-8)
- Gefen, A., Megido-Ravid, M., Azariah, M., Itzchak, Y., & Arcan, M. (2001). Integration of plantar soft tissue stiffness measurements in routine MRI of the diabetic foot [Article]. *Clinical Biomechanics*, 16(10), 921-925. [https://doi.org/10.1016/S0268-0033\(01\)00074-2](https://doi.org/10.1016/S0268-0033(01)00074-2)
- Guiotto, A., Sawacha, Z., Guarneri, G., Cristoferi, G., Avogaro, A., & Cobelli, C. (2013). The role of foot morphology on foot function in diabetic subjects with or without neuropathy [Article]. *Gait and Posture*, 37(4), 603-610. <https://doi.org/10.1016/j.gaitpost.2012.09.024>
- Guldmond, N. A., Leffers, P., Schaper, N. C., Sanders, A. P., Nieman, F., Willems, P., & Walenkamp, G. H. I. M. (2007). The effects of insole configurations on forefoot plantar pressure and walking convenience in diabetic patients with neuropathic feet [Article]. *Clinical Biomechanics*, 22(1), 81-87. <https://doi.org/10.1016/j.clinbiomech.2006.08.004>
- Hamedi, M., Salimi, P., & Jamshidi, N. (2020). Improving cushioning properties of a 3D weft knitted spacer fabric in a novel design with NiTi monofilaments [Article]. *Journal of Industrial Textiles*, 49(10), 1389-1410. <https://doi.org/10.1177/1528083718817560>
- Healy, A., Dunning, D. N., & Chockalingam, N. (2012). Effect of insole material on lower limb kinematics and plantar pressures during treadmill walking [Article]. *Prosthetics and Orthotics International*, 36(1), 53-62. <https://doi.org/10.1177/0309364611429986>
- Hicks, C. W., Selvarajah, S., Mathioudakis, N., Sherman, R. E., Hines, K. F., Black, J. H., III, & Abularrage, C. J. (2016). Burden of Infected Diabetic Foot Ulcers on Hospital Admissions and Costs [Article]. *Annals of Vascular Surgery*, 33, 149-158. <https://doi.org/10.1016/j.avsg.2015.11.025>

- Holmes, D. W., Singh, D., Lamont, R., Daley, R., Forrestal, D. P., Slattery, P., Pickering, E., Paxton, N. C., Powell, S. K., & Woodruff, M. A. (2022). Mechanical behaviour of flexible 3D printed gyroid structures as a tuneable replacement for soft padding foam [Article]. *Additive Manufacturing*, 50, Article 102555. <https://doi.org/10.1016/j.addma.2021.102555>
- Irzmańska, E. (2015). The impact of different types of textile liners used in protective footwear on the subjective sensations of firefighters [Article]. *Applied Ergonomics*, 47, 34-42. <https://doi.org/10.1016/j.apergo.2014.08.013>
- Irzmańska, E. (2016). The microclimate in protective fire fighter footwear: Foot temperature and air temperature and relative humidity [Article]. *Autex Research Journal*, 16(2), 75-79. <https://doi.org/10.1515/aut-2015-0030>
- Irzmańska, E., Dutkiewicz, J. K., & Irzmański, R. (2014). New approach to assessing comfort of use of protective footwear with a textile liner and its impact on foot physiology [Article]. *Textile Research Journal*, 84(7), 728-738. <https://doi.org/10.1177/0040517513507362>
- Jones, P. J., Bibb, R. J., Davies, M. J., Khunti, K., McCarthy, M., Fong, D. T. P., & Webb, D. (2019). A fitting problem: Standardising shoe fit standards to reduce related diabetic foot ulcers [Review]. *Diabetes Research and Clinical Practice*, 154, 66-74. <https://doi.org/10.1016/j.diabres.2019.05.017>
- Karimi, M. T. (2018). The Evaluation of Foot Rockers on the Kinematic Parameters of Individuals With Diabetes [Article]. *Foot and Ankle Specialist*, 11(4), 322-329. <https://doi.org/10.1177/1938640017729500>
- Kaul, K., Tarr, J. M., Ahmad, S. I., Kohner, E. M., & Chibber, R. (2013). Introduction to Diabetes Mellitus. In S. I. Ahmad (Ed.), *Diabetes: An Old Disease, a New Insight* (pp. 1-11). Springer New York. https://doi.org/10.1007/978-1-4614-5441-0_1
- Kwan, M. Y., Yick, K. L., Yip, J., & Tse, C. Y. (2021). The immediate effects of hallux valgus orthoses: A comparison of orthosis designs [Article]. *Gait and Posture*, 90, 283-288. <https://doi.org/10.1016/j.gaitpost.2021.09.174>
- Leung, M. S. H., Yick, K. L., Sun, Y., Chow, L., & Ng, S. P. (2022). 3D printed auxetic heel pads for patients with diabetic mellitus [Article]. *Computers in Biology and Medicine*, 146, Article 105582. <https://doi.org/10.1016/j.combiomed.2022.105582>
- Li, N. W., Yick, K. L., & Yu, A. (2022). Novel weft-knitted spacer structure with silicone tube and foam inlays for cushioning insoles [Article]. *Journal of Industrial Textiles*, 51(4), 6463S-6483S. <https://doi.org/10.1177/15280837211073359>
- Li, T., Liu, F., & Wang, L. (2020). Enhancing indentation and impact resistance in auxetic composite materials [Article]. *Composites Part B: Engineering*, 198, Article 108229. <https://doi.org/10.1016/j.compositesb.2020.108229>
- Liu, Y., & Hu, H. (2011). Compression property and air permeability of weft-knitted spacer fabrics [Note]. *Journal of the Textile Institute*, 102(4), 366-372. <https://doi.org/10.1080/00405001003771200>
- Liu, Y., Hu, H., Zhao, L., & Long, H. (2012). Compression behavior of warp-knitted spacer fabrics for cushioning applications [Article]. *Textile Research Journal*, 82(1), 11-20. <https://doi.org/10.1177/0040517511416283>
- Lo, W. T., Wong, D. P., Yick, K. L., Ng, S. P., & Yip, J. (2016). Effects of custom-made textile insoles on plantar pressure distribution and lower limb EMG activity during turning. *Journal of Foot and Ankle Research*, 9(1), 22. <https://doi.org/10.1186/s13047-016-0154-5>
- Lo, W. T., Wong, D. P., Yick, K. L., Ng, S. P., & Yip, J. (2018). The biomechanical effects and perceived comfort of textile-fabricated insoles during straight line walking [Article]. *Prosthetics and Orthotics International*, 42(2), 153-162. <https://doi.org/10.1177/0309364617696084>
- Lo, W. T., Yick, K. L., Ng, S. P., & Yip, J. (2014). New methods for evaluating physical and thermal comfort properties of orthotic materials used in insoles for patients with diabetes [Article]. *Journal of Rehabilitation Research and Development*, 51(2), 311-324. <https://doi.org/10.1682/JRRD.2013.01.0012>

- Ma, X. L. (2013). Research on application of SLA technology in the 3D printing technology. *Applied Mechanics and Materials*,
- Ma, Z., Lin, J., Xu, X., Ma, Z., Tang, L., Sun, C., Li, D., Liu, C., Zhong, Y., & Wang, L. (2019). Design and 3D printing of adjustable modulus porous structures for customized diabetic foot insoles [Article]. *International Journal of Lightweight Materials and Manufacture*, 2(1), 57-63. <https://doi.org/10.1016/j.ijlmm.2018.10.003>
- Martinelli, A. R., Mantovani, A. M., Nozabiel, A. J. L., Ferreira, D. M. A., Barela, J. A., Camargo, M. R. D., & Fregonesi, C. E. P. T. (2013). Muscle strength and ankle mobility for the gait parameters in diabetic neuropathies [Article]. *Foot*, 23(1), 17-21. <https://doi.org/10.1016/j.foot.2012.11.001>
- Martinez-Santos, A., Preece, S., & Nester, C. J. (2019). Evaluation of orthotic insoles for people with diabetes who are at-risk of first ulceration [Article]. *Journal of Foot and Ankle Research*, 12(1), Article 35. <https://doi.org/10.1186/s13047-019-0344-z>
- Mazur, F., Swoboda, B., Carl, H. D., Lutter, C., Engelhardt, M., Hoppe, M. W., Hotfiel, T., & Grim, C. (2019). Plantar pressure changes in hindfoot relief devices of different designs [Article]. *Journal of Experimental Orthopaedics*, 6(1), Article 7. <https://doi.org/10.1186/s40634-019-0173-9>
- Melia, G., Siegkas, P., Levick, J., & Apps, C. (2021). Insoles of uniform softer material reduced plantar pressure compared to dual-material insoles during regular and loaded gait [Article]. *Applied Ergonomics*, 91, Article 103298. <https://doi.org/10.1016/j.apergo.2020.103298>
- Moulaei, K., Malek, M., & Sheikhtaheri, A. (2021). A smart wearable device for monitoring and self-management of diabetic foot: A proof of concept study [Article]. *International Journal of Medical Informatics*, 146, Article 104343. <https://doi.org/10.1016/j.ijmedinf.2020.104343>
- Muthu Kumar, N., Thilagavathi, G., & Periasamy, S. (2020). Development and characterization of warp knitted spacer fabrics for helmet comfort liner application [Article]. *Journal of Industrial Textiles*. <https://doi.org/10.1177/1528083720939215>
- Nouman, M., Dissaneewate, T., Leelasamran, W., & Chatpun, S. (2019). The insole materials influence the plantar pressure distributions in diabetic foot with neuropathy during different walking activities [Article]. *Gait and Posture*, 74, 154-161. <https://doi.org/10.1016/j.gaitpost.2019.08.023>
- Novak, N., Vesenj, M., & Ren, Z. (2016). Auxetic cellular materials - A review [Review]. *Strojniski Vestnik/Journal of Mechanical Engineering*, 62(9), 485-493. <https://doi.org/10.5545/sv-jme.2016.3656>
- Nurse, M. A., & Nigg, B. M. (2001). The effect of changes in foot sensation on plantar pressure and muscle activity [Article]. *Clinical Biomechanics*, 16(9), 719-727. [https://doi.org/10.1016/S0268-0033\(01\)00090-0](https://doi.org/10.1016/S0268-0033(01)00090-0)
- Owings, T. M., Woerner, J. L., Frampton, J. D., Cavanagh, P. R., & Botek, G. (2008). Custom therapeutic insoles based on both foot shape and plantar pressure measurement provide enhanced pressure relief [Article]. *Diabetes Care*, 31(5), 839-844. <https://doi.org/10.2337/dc07-2288>
- Pai, S., & Ledoux, W. R. (2012). The shear mechanical properties of diabetic and non-diabetic plantar soft tissue [Article]. *Journal of Biomechanics*, 45(2), 364-370. <https://doi.org/10.1016/j.jbiomech.2011.10.021>
- Papanas, N., & Maltezos, E. (2009). The diabetic foot: a global threat and a huge challenge for Greece. *Hippokratia*, 13(4), 199-204.
- Rajan, T. P., Souza, L. D., Ramakrishnan, G., & Zakriya, G. M. (2016). Comfort properties of functional warp-knitted polyester spacer fabrics for shoe insole applications [Article]. *Journal of Industrial Textiles*, 45(6), 1239-1251. <https://doi.org/10.1177/1528083714557056>
- Rao, S., Saltzman, C. L., & Yack, H. J. (2010). Relationships between segmental foot mobility and plantar loading in individuals with and without diabetes and neuropathy [Article]. *Gait and Posture*, 31(2), 251-255. <https://doi.org/10.1016/j.gaitpost.2009.10.016>

- Raspovic, A. (2013). Gait characteristics of people with diabetes-related peripheral neuropathy, with and without a history of ulceration [Article]. *Gait and Posture*, 38(4), 723-728. <https://doi.org/10.1016/j.gaitpost.2013.03.009>
- Ren, X., Das, R., Tran, P., Ngo, T. D., & Xie, Y. M. (2018). Auxetic metamaterials and structures: A review [Review]. *Smart Materials and Structures*, 27(2), Article 023001. <https://doi.org/10.1088/1361-665X/aaa61c>
- Sacco, I. C. N., Hamamoto, A. N., Tonicelli, L. M. G., Watari, R., Ortega, N. R. S., & Sartor, C. D. (2014). Abnormalities of plantar pressure distribution in early, intermediate, and late stages of diabetic neuropathy [Article]. *Gait and Posture*, 40(4), 570-574. <https://doi.org/10.1016/j.gaitpost.2014.06.018>
- Scarpa, F., Giacomini, J. A., Bezazi, A., & Bullough, W. A. (2006). Dynamic behavior and damping capacity of auxetic foam pads. Proceedings of SPIE - The International Society for Optical Engineering,
- Schaper, N. C., Van Netten, J. J., Apelqvist, J., Lipsky, B. A., & Bakker, K. (2016). Prevention and management of foot problems in diabetes: A Summary Guidance for Daily Practice 2015, based on the IWGDF Guidance Documents [Article]. *Diabetes/Metabolism Research and Reviews*, 32, 7-15. <https://doi.org/10.1002/dmrr.2695>
- Schario, M., Tomova-Simitchieva, T., Lichterfeld, A., Herfert, H., Dobos, G., Lahmann, N., Blume-Peytavi, U., & Kottner, J. (2017). Effects of two different fabrics on skin barrier function under real pressure conditions [Article]. *Journal of Tissue Viability*, 26(2), 150-155. <https://doi.org/10.1016/j.jtv.2016.10.003>
- Shen, J., Liu, K., Zeng, Q., Ge, J., Dong, Z., & Liang, J. (2021). Design and mechanical property studies of 3D re-entrant lattice auxetic structure [Article]. *Aerospace Science and Technology*, 118, Article 106998. <https://doi.org/10.1016/j.ast.2021.106998>
- Shi, Q. Q., Li, P. L., Yick, K. L., Li, N. W., & Jiao, J. (2022). Effects of contoured insoles with different materials on plantar pressure offloading in diabetic elderly during gait [Article]. *Scientific Reports*, 12(1), Article 15395. <https://doi.org/10.1038/s41598-022-19814-0>
- Shimazaki, Y., Matsutani, T., & Satsumoto, Y. (2016). Evaluation of thermal formation and air ventilation inside footwear during gait: The role of gait and fitting [Article]. *Applied Ergonomics*, 55, 234-240. <https://doi.org/10.1016/j.apergo.2015.11.002>
- Shimazaki, Y., & Murata, M. (2015). Effect of gait on formation of thermal environment inside footwear [Article]. *Applied Ergonomics*, 49, 55-62. <https://doi.org/10.1016/j.apergo.2015.01.007>
- Smith, C. J., Machado-Moreira, C. A., Plant, G., Hodder, S., Havenith, G., & Taylor, N. A. S. (2013). Design data for footwear: Sweating distribution on the human foot [Article]. *International Journal of Clothing Science and Technology*, 25(1), 43-58. <https://doi.org/10.1108/09556221311292200>
- Tarrade, T., Doucet, F., Saint-Lô, N., Llari, M., & Behr, M. (2019). Are custom-made foot orthoses of any interest on the treatment of foot pain for prolonged standing workers? *Applied Ergonomics*, 80, 130-135. <https://doi.org/https://doi.org/10.1016/j.apergo.2019.05.013>
- Torgutalp, Ş., Babayeva, N., Özkan, Ö., Yilmaz, S., Dönmez, G., & Korkusuz, F. (2021). Do Plantar Pressure and Loading Patterns Vary with Joint Hypermobility in Young Females? *J Am Podiatr Med Assoc*, 111(1). <https://doi.org/10.7547/18-146>
- Uccioli, L., Faglia, E., Monticone, G., Favales, F., Durola, L., Aldeghi, A., Quarantiello, A., Calia, P., & Menzinger, G. (1995). Manufactured shoes in the prevention of diabetic foot ulcers [Article]. *Diabetes Care*, 18(10), 1376-1378. <https://doi.org/10.2337/diacare.18.10.1376>
- van Netten, J. J., Lazzarini, P. A., Armstrong, D. G., Bus, S. A., Fitridge, R., Harding, K., Kinnear, E., Malone, M., Menz, H. B., Perrin, B. M., Postema, K., Prentice, J., Schott, K. H., & Wraight, P. R. (2018). Diabetic Foot Australia guideline on footwear for people with diabetes [Article]. *Journal of Foot and Ankle Research*, 11(1), Article 2. <https://doi.org/10.1186/s13047-017-0244-z>

- Waaajman, R., De Haart, M., Arts, M. L. J., Wever, D., Verlouw, A. J. W. E., Nollet, F., & Bus, S. A. (2014). Risk factors for plantar foot ulcer recurrence in neuropathic diabetic patients [Article]. *Diabetes Care*, 37(6), 1697-1705. <https://doi.org/10.2337/dc13-2470>
- Wang, S., Deng, C., Ojo, O., Akinrinlola, B., Kozub, J., & Wu, N. (2022). Design and modeling of a novel three dimensional auxetic reentrant honeycomb structure for energy absorption [Article]. *Composite Structures*, 280, Article 114882. <https://doi.org/10.1016/j.compstruct.2021.114882>
- Wang, T., An, J., He, H., Wen, X., & Xi, X. (2021). A novel 3D impact energy absorption structure with negative Poisson's ratio and its application in aircraft crashworthiness [Article]. *Composite Structures*, 262, Article 113663. <https://doi.org/10.1016/j.compstruct.2021.113663>
- Wendt, D., Van Loon, L. J. C., & Van Marken Lichtenbelt, W. D. (2007). Thermoregulation during exercise in the heat: Strategies for maintaining health and performance [Review]. *Sports Medicine*, 37(8), 669-682. <https://doi.org/10.2165/00007256-200737080-00002>
- West, A. M., Schönfisch, D., Picard, A., TARRIER, J., Hodder, S., & Havenith, G. (2019). Shoe microclimate: An objective characterisation and subjective evaluation [Article]. *Applied Ergonomics*, 78, 1-12. <https://doi.org/10.1016/j.apergo.2019.01.010>
- West, A. M., TARRIER, J., Hodder, S., & Havenith, G. (2019). Sweat distribution and perceived wetness across the human foot: the effect of shoes and exercise intensity [Article]. *ERGONOMICS*, 62(11), 1450-1461. <https://doi.org/10.1080/00140139.2019.1657185>
- Xiaogang, J., Lin, D., Wei, W., & Chuang, F. (2022). Study on Tensile Properties of 3D Porous Lattice Structures Based on Cube Truss Cells [Article]. *Journal of Materials Engineering and Performance*. <https://doi.org/10.1007/s11665-022-07319-w>
- Yamamoto, T., Hoshino, Y., Kanzaki, N., Nukuto, K., Yamashita, T., Ibaraki, K., Nagamune, K., Nagai, K., Araki, D., Matsushita, T., & Kuroda, R. (2020). Plantar pressure sensors indicate women to have a significantly higher peak pressure on the hallux, toes, forefoot, and medial of the foot compared to men [Article]. *Journal of Foot and Ankle Research*, 13(1), Article 40. <https://doi.org/10.1186/s13047-020-00410-2>
- Yang, C., Vora, H. D., & Chang, Y. (2018). Behavior of auxetic structures under compression and impact forces [Article]. *Smart Materials and Structures*, 27(2), Article 025012. <https://doi.org/10.1088/1361-665X/aaa3cf>
- Yi, T. I., Lee, E. C., Son, N. H., & Sohn, M. K. (2022). Comparison of the Forefoot Pressure-Relieving Effects of Foot Orthoses [Article]. *Yonsei Medical Journal*, 63(9), 864-872. <https://doi.org/10.3349/ymj.2022.63.9.864>
- Yick, K. L., Yu, A., & Li, P. L. (2019). Insights into footwear preferences and insole design to improve thermal environment of footwear [Article]. *International journal of fashion design, technology and education*, 12(3), 325-334. <https://doi.org/10.1080/17543266.2019.1629028>
- Yip, J., & Ng, S. P. (2008). Study of three-dimensional spacer fabrics: Physical and mechanical properties [Article]. *Journal of Materials Processing Technology*, 206(1-3), 359-364. <https://doi.org/10.1016/j.jimatprotec.2007.12.073>
- Yu, A., Li, P. L., Yick, K. L., Ng, S. P., & Yip, J. (2018). Investigation of microclimate in sports shoes with the integration of human subjective sensations. In *Key Engineering Materials* (Vol. 765 KEM, pp. 140-146).
- Yu, A., Sukigara, S., Yick, K. L., & Li, P. L. (2020a). Novel weft-knitted spacer structure with silicone tube inlay for enhancing mechanical behavior [Article]. *Mechanics of Advanced Materials and Structures*. <https://doi.org/10.1080/15376494.2020.1850948>
- Yu, A., Sukigara, S., Yick, K. L., & Li, P. L. (2020b). Novel weft-knitted spacer structure with silicone tube inlay for enhancing mechanical behavior [Article]. *Mechanics of Advanced Materials and Structures*, 29(14), 2053-2064. <https://doi.org/10.1080/15376494.2020.1850948>
- Yu, A., Yick, K. L., Ng, S. P., & Yip, J. (2016). Orthopaedic textile inserts for pressure treatment of hypertrophic scars [Review]. *Textile Research Journal*, 86(14), 1549-1562. <https://doi.org/10.1177/0040517515573409>

- Yu, X., Zhou, J., Liang, H., Jiang, Z., & Wu, L. (2018). Mechanical metamaterials associated with stiffness, rigidity and compressibility: A brief review [Review]. *Progress in Materials Science*, 94, 114-173. <https://doi.org/10.1016/j.pmatsci.2017.12.003>
- Zhang, Z., Tang, X., Li, J., & Yang, W. (2020). The effect of dynamic friction with wet fabrics on skin wetness perception [Article]. *International Journal of Occupational Safety and Ergonomics*, 26(2), 370-383. <https://doi.org/10.1080/10803548.2018.1453023>
- Zhao, T., Long, H., Yang, T., & Liu, Y. (2018). Cushioning properties of weft-knitted spacer fabrics [Article]. *Textile Research Journal*, 88(14), 1628-1640. <https://doi.org/10.1177/0040517517705630>
- Zwaferink, J. B. J., Custers, W., Paardekooper, I., Berendsen, H. A., & Bus, S. A. (2020). Optimizing footwear for the diabetic foot: Data-driven custom-made footwear concepts and their effect on pressure relief to prevent diabetic foot ulceration [Article]. *PLoS ONE*, 15(4), Article e0224010. <https://doi.org/10.1371/journal.pone.0224010>